UNIVERSITY OF CAPE TOWN

Department of Civil Engineering

CORROSION PROPAGATION IN CRACKED AND UNCRACKED CONCRETE

By

Mike Otieno

A Dissertation submitted to the Faculty of Engineering and The Built Environment, University of Cape Town, in partial fulfilment of the requirements for the degree of Master of Science in Engineering

September, 2008

DECLARATION

I, Mike Otieno, hereby declare that this Dissertation is my own, unaided work. I know the meaning of plagiarism and declare that all the work in this document, save for that which is properly acknowledged, is my own. It is being submitted for the degree of Master of Science in Engineering in the University of Cape Town. It has not been submitted before for any degree or examination in any other University.

Signed by candidate

Mike Benjamin Otieno

September, 2008

Dedication

To

Mum & Dad

Abstract

Durability is a major concern for reinforced concrete (RC) structures. Cracks can influence the durability of RC structures in aggressive environments by accelerating the ingress of corrosion agents (oxygen, carbon dioxide, moisture, chlorides) into the concrete to the embedded steel level. The overall effect is that cracks accelerate both initiation and propagation of corrosion. The corrosion rate during the propagation phase directly affects the service life of a RC structure. The service life of corroding RC structures may therefore be drastically reduced in the presence of cracks.

This study focuses on chloride-induced corrosion in both cracked and uncracked RC using 100 x 100 x 500 mm long beam specimens. Four concrete mixes were made using two water/binder (w/b) ratios (0.40 and 0.55) and two binder types (100% CEM I 42.5N (OPC) and 50/50 OPC/Corex slag blend). Crack widths of 0.4 mm and 0.7 mm as well as incipient cracks were introduced in the beam specimens. The beams had a constant concrete cover to reinforcing steel of 40 mm. All specimens were subjected to a cycle of 3 days wetting (with 5% NaCl solution) and 4 days drying. The cracked beam specimens were subjected to occasional three-point reloading during the study period to investigate the effect of crack self-healing. The beam specimens were monitored for corrosion rate (coulostatic technique), half-cell potential (Ag/AgCl) and concrete resistivity (Wenner probe technique).

Results indicate that corrosion rate is sensitive to crack width, concrete quality and reloading. For a given binder type and w/b ratio corrosion rate increased with increasing crack width. However, the increase in corrosion rate with increasing crack width in the Corex slag specimens (SL-40 and SL-55) was relatively lower than that in the OPC specimens (PC-40 and PC-55). Little difference was noticed between the corrosion rates for both uncracked and incipient-cracked Corex slag specimens. In addition, corrosion rates were found to be sensitive to binder type and w/b ratio, or more precisely concrete quality (penetrability). For the four different concrete mixes, corrosion rates decreased in the following order: PC-55 > PC-40 > SL-55 > SL-40. These results show the necessity of specifying crack width limits accompanied by a corresponding concrete quality, especially for RC durability design. Similar to the design for chloride threshold levels, the study proposes that the design for crack widths should be concrete-quality specific. Reloading was found to increase the corrosion rate in the cracked specimens. However, the increase in corrosion rate was higher if the specimen was actively corroding prior to the reloading than if it was passively corroding.

Concrete electrical resistivity was found to be an unreliable corrosion assessment technique for cracked concrete. This was mainly because resistivity measurements were taken at the end of the 4 days wetting period when the cracks were filled with the NaCl solution. This ensured electrical continuity across the crack. For a given binder, there was therefore no notable difference between the resistivities of both the cracked and uncracked specimens. The use of half-cell potential (HCP) measurements was more reliable than concrete electrical resistivity for both cracked and uncracked concrete. Nevertheless, HCP readings require careful interpretation as they are affected by several factors, for example oxygen concentration. Other corrosion assessment techniques such as linear polarisation resistance are essential to supplement HCP measurements.

This study provides insight into the combined effects of crack width, binder type, w/b ratio and crack re-opening on chloride-induced corrosion in RC structures. The study recommends that these factors should be taken into consideration in RC durability design.

Acknowledgements

I would like to express my sincere gratitude to my supervisor and co-supervisor Prof. Mark Gavin Alexander and Dr Hans-Dieter Beushausen respectively for their guidance, encouragement and technical support during the research period at the University of Cape Town, South Africa. It was a great privilege to study under your supervision. I enjoyed it very much.

Special thanks to my fellow postgraduate colleagues in the Concrete Materials and Structural Integrity Research Group (CSIRG) and all others who provided support in one way or another. Your effort is greatly appreciated.

Thanks are also due to the concrete laboratory and the workshop personnel who assisted me in the experimental work from time to time.

Finally, special thanks to my mum, dad, brother and sisters for their emotional, spiritual and moral support throughout my academic career, and also for their endless love, patience, encouragement and prayers.

"Where the willingness is great, the difficulties cannot be great", Niccoló Machiavelli (1469-1527)

…… God Bless You All Abundantly ……

TABLE OF CONTENTS

List of Figures

List of Tables

Abbreviations & Notations

CEM I 42.5N	Class 42.5 Normal hardening Ordinary Portland Cement (OPC)
CCI	Chloride Conductivity Index
DI	Durability Index
GGBS	Ground Granulated Blastfurnace slag
GGCS	Ground Granulated Corex slag
HCP	Half-cell potential
LPR	Linear Polarisation Resistance
OPI	Oxygen Permeability Index test
SRPC	Sulphate Resisting Portland Cement
RC	Reinforced Concrete
w/b	Water to binder ratio (by mass)
WSI	Water Sorptivity Index Test

Concrete mix labels

PC-40	Concrete made using OPC at w/b ratio of 0.40
PC-55	Concrete made using OPC at w/b ratio of 0.55
SL-40	Concrete made using 50/50 OPC/Corex slag blend at w/b ratio of 0.40
SL-55	Concrete made using 50/50 OPC/Corex slag blend at w/b ratio of 0.55

Chapter 1

1 INTRODUCTION

1.1 Background

Steel reinforced concrete (RC) has been used for decades as the construction material of choice. It is economical, versatile and can be moulded to a variety of shapes and finishes. Concrete is generally resistant to harsh environmental conditions, and hence concrete structures are designed to have a long service life (Hertlein, 1992, Broomfield, 1997, Schiessl, 1998). It is usually durable and strong, performing well during its service life. Reinforced concrete is a composite construction material based on the principle that concrete is an ideal environment for reinforcing steel.

However, corrosion of steel reinforcement has become a major problem for the durability of RC structures in view of the economic consequences with regard to assessment, maintenance and repair, especially for the increasing amount of ageing infrastructure. It has been recognised as a serious problem throughout the world (Swarup and Trikha, 1996, Kropp and Alexander, 2007), and is a topic of continued international interest particularly for existing, perhaps already partly affected, structures (Melchers and Li, 2006). In the majority of cases, reinforcement corrosion is caused by either carbonation or chloride ingress to the embedded steel level. Concrete structures such as bridges, buildings, sanitary and water facilities can be severely damaged due to corrosion of the reinforcing steel.

Corrosion of steel in concrete may cause damage and early failure of RC structures. It may also cause both the safety and performance of concrete structures to significantly deteriorate. Reinforcement corrosion may have severe implications for the mechanical properties of RC (Palsson and Mirza, 2002) including:

- loss in load-carrying capacity due to a reduced cross sectional area of reinforcing steel;
- loss in load-carrying capacity due to a loss in bond at the concrete-steel interface; and
- loss in ductility due to an uneven distribution of cross-sectional area along the length of the reinforcing bar and stress concentrations associated with the abrupt changes in geometry.

To build environmentally sustainable concrete structures, it is clear that modern construction should be driven by considerations of durability rather than strength (Alexander and Beushausen, 2007). Durability of RC is indispensable and needs to be ensured in future works from both an economic and an environmental viewpoint. Durability is *the ability of a*

material or structure to withstand its design service conditions for its design life without significant deterioration (Ballim *et al*., 2004). The American Concrete Institute (ACI) defines concrete durability as *its resistance to weathering action, chemical attack, abrasion and other degradation processes* while the British Standard (BS 8110-1:1997) defines a durable concrete as *one that is designed and constructed to protect embedded metal from corrosion and to perform satisfactorily in the working environment for the life-time of the structure.*

Durability is mainly related to the transport properties and chemical composition of concrete. Transport properties are a function of concrete penetrability and cracking. *Penetrability* may be defined as the ease with which an ion, molecule or fluid may move through the concrete (Richardson, 2002). It is a function of interconnection between the pores, the pore size distribution and its tortousity. It is a major factor responsible for the degree of protection of steel reinforcement provided by the concrete cover. It is affected by several parameters such as the water/binder (w/b) ratio and the degree of hydration of the cement paste. A reduction of penetrability and elimination of cracking or minimization of the crack width increases durability of concrete (Reinhardt, 2005).

Three aspects that have to be taken into account for durability to be achieved include the following (Alexander and Beushausen, 2007):

- *Cost*: ensured durability may require higher initial costs, although this is not inevitable. These costs should be incorporated in the tender and cost schedules, either implicitly or explicitly, or both.
- *Selection of materials*: proper selection of materials at the design stage should be done with regard to foreseen exposure conditions to which the structure will be subjected during its service life.
- *Testing*: appropriate test methods and interpretation of results are critical.

When RC structures are built in chloride laden environments such as marine environments, an important deterioration phenomenon that must be taken into account is chloride-induced corrosion of the steel reinforcement. In such environments, RC durability depends mainly on the risk of rebar corrosion due to chloride penetration (Miguel and Guitierrez, 2008). For durability to be achieved in such environments, concrete should be resistant to weathering action, chemical attack, abrasion and other degradation processes in order to protect the embedded steel reinforcement from chloride-induced corrosion.

1.2 Effect of cracking on corrosion of steel in concrete

The penetration of species that cause corrosion in RC such as chloride ions, oxygen, carbon dioxide and moisture into concrete is governed by the quality and condition of the cover

concrete (*covercrete*). The presence of cracks in the concrete cover may therefore aggravate the problem of corrosion in RC structures. Once cracks occur, they may influence the reinforcement corrosion process by accelerating the ingress of detrimental species (chlorides, sulphates, carbon dioxide) that may enhance concrete deterioration and result in further cracking. Cracks could therefore impair the durability of RC structures by creating preferential paths for the penetration of various types of potentially aggressive agents. This can result in substantial reduction in service life owing to rapid initiation and propagation of steel corrosion.

The severity of cracks in RC structures also depends on whether the cracks are dormant/inactive or active. Dormant cracks are characterised by having constant widths as opposed to active cracks whose widths are subject to change from time to time. Dormant cracks may be caused due to drying and thermal shrinkage or in cases where applied loads are constant over the time while active cracks would be expected in cases where the applied load is varying. It can also occur in situations where the exposure conditions are variable e.g. thermal cycling. Dormant cracks are therefore more amenable to self healing than active cracks but may be reactivated (opened) by the application of load (Edvardsen, 1999).

It is generally believed that the compact structure of calcium silicate hydrates (C-S-H), refined pore size distribution, and low penetrability are responsible for improved durability (Xu *et al*., 2008). In an attempt to control corrosion of steel reinforcement, mineral cement extenders such as fly ash, silica fume and slag are therefore being used extensively in the production of concrete to reduce its penetrability by densification of the microstructure, pore refinement and alteration of the pore solution chemistry.

However in the presence of cracks, the effectiveness of these mineral cement extenders in preventing the ingress of chloride ions into concrete is drastically reduced. The presence of cracks may not only shorten the time to corrosion initiation but also drastically increase the corrosion rate in the propagation stage. Despite the research that has been done on the influence of cracks on chloride-induced corrosion (Beeby, 1983, Suzuki *et al*., 1990, Arya and Wood, 1995, Arya and Ofori-Darko, 1996, Schiessl, 1998, Edvardsen, 1999, Scott, 2004), corrosion mitigation in the marine environment continues to be a problem for many steel RC structures; and its prevention still engages considerable effort and resources.

*1.3 **Service life of RC structures***

Ideally, the risk of a concrete structure failing to perform satisfactorily over its desired service life should be low. However, given the current understanding of deterioration mechanisms,

and maybe more importantly failure to implement known technology, the risk remains unacceptably high.

Service life may be defined as the time for which a structure is expected to be able to fulfil its requirements with sufficient reliability with or without periodic inspection and maintenance and without unexpected high costs of maintenance and repair (CEB 1999). The service life of a RC structure with respect to corrosion is usually described in terms of initiation and propagation phases of corrosion (Figure 1.1). Each phase contributes, in different proportions, to the overall concrete deterioration, with the propagation stage having a significant impact depending on the corrosion rate.

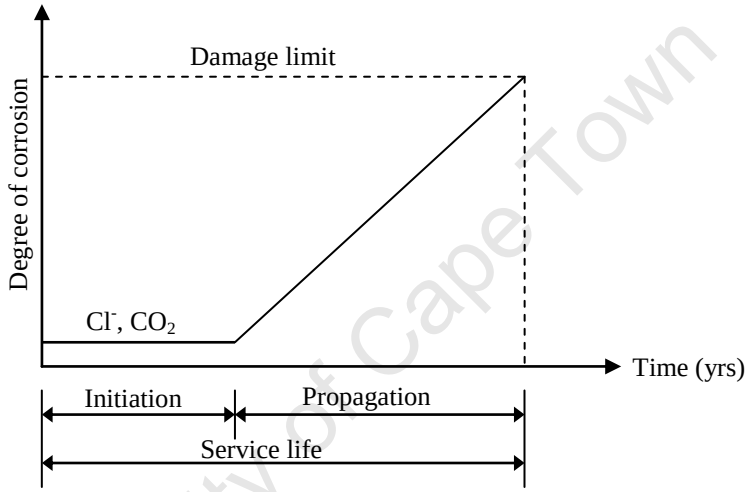

Figure 1.1: Tuutti corrosion damage model
(Tuutti, 1982)

Corrosion initiation period defines the time it takes for chlorides to penetrate from the external environment through the cover concrete and accumulate at the level of the steel in sufficient concentration to break down the passive protective layer on the steel surface and thereby cause active corrosion. If no cracks are present, the length of the initiation phase is a function of the penetrability of the concrete, the concrete cover, the binder type used, and the corrosion resistance of the bars (Ryell and Richardson, 1972). However, when cracks are present, then corrosion resistance of the bars may be the only factor that has any practical influence on the corrosion initiation phase.

The propagation stage is the period during which the corrosion rate and the accumulative amount of corrosion products gradually increase until an unacceptable level of damage has occurred. The length of this period therefore depends on the definition of *unacceptable corrosion damage* which directly depends on the rate of the corrosion process.

1.3.1 ***Service life predictions of cracked RC structures exposed to chlorides***

The development of reliable methods for predicting chloride ingress into concrete is important to prevent deterioration of new structures and to assess the condition of existing ones. Extensive research has been conducted over the past decades to study transport properties of concrete and numerous service life prediction models have been introduced. While these models may correlate well with laboratory investigations, they usually fail to accurately predict service life of real cracked RC structures. Their common disadvantage is that all predictions are carried out considering uncracked concrete (De Schutter, 2000). The fact that most RC structures have cracks is often either ignored or not explicitly accounted for.

For example, Clear (1989) proposed a relationship between corrosion rate and service life in terms of probability of corrosion damage (Table 1.1).

Table 1.1: Proposed relationship between Corrosion rate and remaining Service Life (Clear, 1989)

i_{corr} ($\mu A/cm^2$)	*Severity of Damage*
< 0.2	no corrosion damage expected
0.2-1.0	corrosion damage possible in 10 to 15 years
1.0-10	corrosion damage expected in 2 to 10 years
> 10	corrosion damage expected in 2 years or less

While such relationships may provide indications on the level of corrosion damage, they may have little or no meaning in the case of cracked concrete where corrosion initiation is almost instantaneous and progresses at a faster rate than in uncracked concrete. The expected time to corrosion damage is therefore shortened and relationships such as the one presented in Table 1.1 may not be reliably applied.

In the presence of cracks, ingress of chloride ions mainly by absorption and convection is accelerated (as will be seen in chapter two) and the initiation of corrosion is more or less instantaneous. The overall result is that cracks increase the corrosion rate and hence shorten service life of the RC structure. Relevant experimental data (and long-term experience) is needed to facilitate accurate prediction of service life due to degradation by corrosion of steel in cracked concrete (Djerbi *et al*., 2008).

The estimation of the life span of cracked reinforced concrete structures is influenced by crack characteristics such as width, length, frequency, orientation, etc., in addition to the concrete properties and environmental exposure conditions (Win *et al*., 2004). Models aimed at predicting the service life of RC structures may therefore provide an incomplete description

of the behaviour of a structure if the influence of cracking is not included. The influence of cracking on corrosion should therefore be considered in combination with environmental conditions and material proportions to obtain a rational service life prediction.

A review of the literature has revealed at least two main reasons why the influence of cracking is often omitted from service life predictions of concrete structures:

- Insufficient knowledge on the effect of cracks. Although a general consensus exists about the fact that cracks can significantly modify the transport properties of concrete, the limited research in this area has not yet allowed any accurate quantification of such effects (Gerard and Marchand, 2000).

- The introduction of cracks into the models greatly complicates the analysis. There are a number of factors that have to be taken into account when modelling transport properties of cracked concrete. Some of these are the geometry of the cracks, their distribution (which is usually non-uniform), connectivity of cracks, scatter in crack sizes and crack healing (Breysse and Gerard, 1997). The complexity of modelling transport in cracked concrete, as well as the pressing need for reliable methods of evaluation and prediction of concrete durability poses a new challenge in the field of concrete research.

1.4 Motivation and research significance

There is considerable controversy in the published literature regarding the relationship between the presence of cracks and corrosion. Nevertheless, designers often assume that RC structures will crack in service. Most codes of practice specify maximum permissible crack widths, which vary with thickness of the cover over steel reinforcement. For example, according to the ACI 318-05 (2005) and the British Standard BS 8110 (1997) design codes, the practical criterion related to concrete cracking is to limit the crack width to a prescribed level rather than to eliminate cracking completely. This leaves one with the impression that perhaps there is a relationship between crack width and reinforcement corrosion.

Increasingly, it is recognized that access for detrimental agents such as chloride ions cannot be restricted indefinitely and that there is a finite service life for any RC structure (Rostram, 2003). Within this finite service life, serious risks arise through a combination of chemical, biological and physical actions which may result in significant losses in terms of repair, maintenance and rehabilitation.

In recent years a growing awareness has evolved to address explicitly durability in the design stage of new RC structures as well as in the management stage of existing structures. As a consequence, a number of deterioration models have been developed to predict degradation

over time. The models can be grouped into two major groups: those that predict time to corrosion initiation and, those for corrosion propagation period. Models such as LIFE-365 (ACI committee 365, 2005), Duracrete (DuraCrete, 1998), Clinconc (Tang, 1996) and the South African chloride prediction model (Mackechnie, 2001) have been developed to predict time to chloride-induced corrosion initiation in marine environments. For the corrosion propagation period, there exist models to predict time to corrosion-induced cracking such as the one by Liu and Weyers (1998), while some predict time to attain a predetermined loss in steel cross-sectional area.

The majority of the deterioration models focus on the corrosion initiation stage, addressing the ingress of deleterious substances from the exposure environment into the concrete cover. This partly stems from:

(i) The prevailing opinion that initiation of reinforcement corrosion defines the end of service life, despite the fact that the propagation stage may contribute significantly to service life and;
(ii) The difficulties and uncertainties encountered in modelling steel corrosion in a concrete environment, especially for the development of empirical models.

Accurate service life prediction models for the corrosion propagation stage of corrosion-affected cracked RC structures are therefore also vital.

To develop such models, an in-depth understanding of factors that affect the corrosion process in the propagation stage is mandatory. The presence of cracks is deemed to be one such factor. In the presence of cracks, corrosion rate may increase. In this light, this study takes a step forward to improve the understanding of the relationship between crack width and corrosion rate. This relationship, together with factors such as stress level in the steel, w/b ratio and binder type, can then be quantified and incorporated in corrosion propagation service life models to estimate the remaining service life more accurately.

1.5 ***Problem statement***

Premature deterioration of RC is a serious problem at present from both a theoretical and practical point of view. Effort has been made to understand the durability of concrete in corrosive environments, yet it still remains the foremost problem facing structural concrete used today, (Mehta, 1991).

In an aggressive environment, a cracked RC is highly susceptible to reinforcement corrosion and hence its durability may be compromised. Despite the considerable research done, the impact of cracking on the corrosion of reinforcing steel remains a controversial issue. Two

schools of thought exist. On the one hand, it is believed that cracks can reduce the service life of RC structures by accelerating the onset of corrosion and by promoting active corrosion of the reinforcing steel (Bentur *et al*., 1997). On the other hand, literature suggests that, since chlorides eventually penetrate the uncracked concrete after some years and cause more widespread corrosion, the difference between service life of cracked and uncracked concrete is marginal (Pettersson and Jorgensen, 1996).

These conflicting viewpoints can be explained by the fact that the effect of cracking on the durability of concrete structures is a complex function of their type, width, length, depth, frequency and orientation with respect to reinforcement (ACI Committee 222, 1996). An attempt to understand the effects of these factors on reinforcement corrosion so that they can be quantified and incorporated in service life prediction models in the corrosion propagation stage is one of the main focuses of today's research. It is on these grounds that the following objective and aims are set for this study.

1.6 ***Objective***

This study explores the effect(s) of crack width and reactivation of cracks on the corrosion rate of reinforced concrete specimens exposed to chloride ions, in order to improve the understanding of the process and governing factors. This can lead to more accurate prediction of the service life of cracked reinforced concrete structures in the marine environment.

1.7 ***Aims***

The aims of this study are to:

- explore the effect(s) of crack width on the corrosion initiation and propagation (i.e. corrosion rates) of reinforcing steel.
- compare the rates of corrosion of steel (at specific crack widths) in concrete made using;
  - Ordinary Portland Cement (CEM I 42.5N - OPC)
  - OPC/Corex slag (50/50) blend
- explore the effect of occasional re-loading on rate of corrosion in order to reactivate existing cracks.
- investigate the effect of water/binder (w/b) ratio on rate of corrosion.
- synthesise information so as to improve the understanding and ability to model the presence of cracks i.e. to provide data that can be used in service-life modelling of cracked reinforced concretes.

1.8 ***Scope of study***

The scope of this study is limited to the following aspects:

(i) The corrosion of the steel reinforcement will be limited to that caused by chloride ions. Corrosion due to carbonation will not be investigated but will be briefly mentioned in the literature review.

(ii) Only ordinary Portland cement (OPC) and 50/50 OPC/Corex slag binders will be used in making the concrete test specimens.

(iii) Two w/b ratios of 0.40 and 0.55 will be used.

(iv) The crack widths used are: zero crack width, incipient crack*, 0.4 mm and 0.7 mm.

* Incipient crack as used in this study refers to a crack just induced by three-point loading of beam specimens and thereafter unloading.

*1.9 **Thesis outline***

This thesis is divided into five chapters as follows:

Chapter one gives a general introduction with emphasis on steel corrosion in RC structures in the marine environments. A brief overview is given on durability and service life prediction of RC structures, with a focus on cracked concrete.

Chapter two is a literature review of the corrosion fundamentals, factors affecting it and its assessment. In this chapter focus is on chloride-induced corrosion, which is the core of this study. Some of the existing service life prediction models for the corrosion initiation and propagation periods are briefly covered.

Chapter three gives the experimental details and methodology employed in this study.

Chapter four presents the experimental results of this study and the discussion thereof.

Chapter five concludes the thesis by giving the conclusions based on a critical evaluation and discussion of the experimental results of this study and recommendations for future study.

1.10 ***References***

ACI Committee 222, (1996), *Corrosion of metals in concrete*, ACI 222R-96, American Concrete Institute, Detroit, MI, pp. 30.

ACI 318-05, (2005), *Building Code Requirements for Structural Concrete and Commentary*, American Concrete Institute.

Alexander, M. G. and Beushausen H.-D., (2007), Performance-based durability design and specification in South Africa, *Proceedings of International Concrete Conference and Exhibition* (ICCX - Concrete Awareness), 14-16 February 2007, Cape Town, South Africa, pp. 12-15.

Arya, C. and Wood L., (1995), The relevance of cracking in concrete to corrosion of reinforcement, *Concrete Society Technical Report* No. 44.

Arya, C. and Ofori-Darko, F. K., (1996), Influence of crack frequency on reinforcement corrosion in concrete, *Cement and Concrete Research*, 26(3), pp. 333-353.

Ballim, Y., Grieve G. R. H. and Alexander, M. G., (2004), reinforced concrete durability design status and prospects in South Africa., *Conference proceedings on Developing Concrete to serve Practical Needs*, 13 - 14th October 2004 in Midrand, South Africa.

Beeby, A., (1983), Cracking, cover and corrosion of reinforcement, *Concrete International*, February, pp. 35-40.

Bentur, A., Diamond, S. and Berke, N,. (1997), *Steel Corrosion in Concrete*, Fundamentals and civil engineering practice, London: E & FN Spon, pp. 41-43.

British Standard BS 8110-1, (1997), *Structural use of concrete* - Part 1: Code of practice for design and construction.

Broomfield, J. P., (1997), *Corrosion of Steel in Concrete: Understanding, Investigation and Repair*, London, UK: E&FN Spon.

Breysse, D. and Gerard, B., (1997), Transport of fiuids in cracked media, *RILEM report 16 - Barriers to organic and contaminating liquids*, ed. Reinhardt H. W., published by E & FN SPON, London, pp. 123-153.

CEB, (1999), Durable Concrete Structures, *CEB Bulletin No. 183*, Chapter 6: Reinforcement, pp. 27-34.

Clear, K. C., (1989), Measuring rate of corrosion of steel in field concrete structures, *Transportation Research Record 1211*, pp. 28-37.

Djerbi, A., Bonnet, S., Khelidj, A. and Baroghel-bouny, V., (2008), Influence of traversing crack on chloride diffusion into concrete, *Cement and Concrete Research*, 38, pp. 877–883.

DuraCrete, (1998), Probabilistic performance based durability design: modelling of degradation, *DuraCrete Project Document*, BE95-1347/R4-5, The Netherlands.

Edvardsen, C., (1999), Water permeability and autogenous healing of crack in concrete, *ACI Materials Journal*, 96(4), pp. 448–454.

Gerard, B. and Marchand, J., (2000), Influence of cracking on the diffusion properties of cement-based materials, Part 1: Influence of continuous cracks on the steady-state regime, *Cement and Concrete Research*, 30(1), pp. 37-43.

Hertlein, B. H., (1992), Assessing the role of steel corrosion in the deterioration of concrete in the national infrastructure : a review of the causes of corrosion and current diagnostic techniques, *Corrosion Forms and Control for Infrastructure*, San Diego, CA, 3-4 June 1991, ASTM Publication, Race St., PA, pp. 1916.

Kropp, J. and Alexander, M. G., (2007), Transport mechanisms and reference tests, Chapter two, *RILEM TC 189-NEC: State-of-the-art Report, Non-Destructive Evaluation of the Penetrability and Thickness of the Cover*.

LIFE-365 Service life prediction model, (2005), Computer program for predicting the service life and life-cycle costs of reinforced concrete exposed to chlorides, *ACI Committee 365.*

Liu, Y. and Weyers, R. E., (1998), Modelling the time-to-corrosion cracking in chloride contaminated reinforced concrete structures, *ACI Materials Journal*, 95(6), pp. 675-681.

Mackechnie, J. R., (2001), Predictions of reinforced concrete durability in the marine environment, *Research monograph No. 1*, Department of Civil Engineering, University of Cape Town.

Mehta, P., (1991), Durability of concrete-Fifty years of progress, durability of concrete, 2nd international conference, *ACI Special Publication-126*, Montreal, pp. 1-31.

Melchers, R. and Li, C. Q., (2006), Phenomenological modelling of reinforcement corrosion in marine environments, *ACI Materials Journal*, 103(1).

Miguel, A. B. and Guitierrez, P. A., (2008), Comparative study test methods for reinforced concrete durability assessment in marine environment, *Materials and Structures* (41), pp. 527-541.

Palsson, R. and Mirza, M. S., (2002), Mechanical response of corroded steel reinforcement of abandoned concrete bridge, *ACI Structural Journal*, 99(2), March-April.

Pettersson, K. and Jorgensen, O., (1996), The effect of cracks on reinforcement corrosion in high-performance concrete in a marine environment, *Proceedings third ACI/CANMET Int. conference on the Performance of Concrete in Marine Environment*, St. Andrews by-the Sea, Canada, pp. 185-200.

Reinhardt, H. W., (2005), Concrete with enhanced durability, *Otto-Graf-Journal*, 9(16).

Richardson, M. G., (2002), *Fundamentals of Durable Concrete*, Modern concrete.

Rostram, S., (2003), Reinforced Concrete Structures - Shall concrete remain the dominating means of corrosion prevention?, *Materials and Corrosion*, 54, pp. 369-378.

Ryell, J. and Richardson, B. S., (1972), Cracks in concrete bridge decks and their contribution to corrosion of reinforcing steel and prestressed cables, *Report No. IR51, Ontario Ministry of transportation and Commission*, Ontario, Canada.

Schiessl, P. ed., (1998), *Corrosion of Steel in Concrete*, Chapman and Hall Ltd: London.

Scott, A. N., (2004), The influence of binder type and cracking on reinforcing steel corrosion in concrete, *PhD Thesis*, University of Cape town.

Swarup, J. and Trikha, D. N., (1996), Corrosion of reinforcement in concrete structure under various conditions, *Transactions of the Metals Finishers' Association of India*, 5(1), pp. 15.

Suzuki, K., Ohno, Y., Praparntanatorn, S. and Tamura, H., (1990), Mechanism of steel corrosion in cracked concrete, *Corrosion of Reinforcement in Concrete*, Ed. Page, C., Treadaway, K. and Bramforth, P., London: Society of Chemical Industry, pp. 19-28.

Tang, L., (1996), Chloride transport in concrete: measurement and prediction, *PhD Thesis*, Publication P-96:6, Department of Building Materials, Chalmers University of Technology, Gothenburg, Sweden.

Tuutti, K,. (1982), Corrosion of steel in concrete, *Swedish Cement and Concrete Research Institute*, Stockholm, Report No.CBI Research 4:82, pp. 468.

Win, P. P., Watanabe, M. and Machida, A., (2004), Penetration profile of chloride ion in cracked reinforced concrete, *Cement and Concrete Research*, 34, pp. 1073-1079.

Xu, H., Provis, J. L., Deventer, J. S. J. and Krivenko, P. V., (2008), Characterization of aged slag concretes, *ACI Materials Journal*, 105(2), pp. 131-139.

Chapter 2

2 LITERATURE REVIEW

2.1 ***Introduction***

This chapter covers the fundamentals of steel reinforcement corrosion in concrete with emphasis on chloride-induced corrosion which is the focus of this study. A brief background on the fundamental transport mechanisms in concrete is also covered. Factors affecting both initiation and propagation of corrosion together with some of the existing service life prediction models for both the corrosion initiation and propagation periods are covered. Lastly, different techniques used to assess corrosion in reinforced concrete (RC) are covered.

2.2 ***Background***

Reinforcement corrosion is one of the main durability-threatening mechanisms in RC. Much research has focused on increasing the basic understanding of both the transport mechanisms of aggressive ions (chloride ions) through concrete and the subsequent corrosion of reinforcing steel (Tuutti, 1982, Mackechnie, 1996, Schiessl, 1998).

The degradation of RC structures mainly involves three stages as shown in Figure 2.1, (Heckroodt, 2002):

(i) An initiation period before corrosion activation, during which little deterioration occurs.

(ii) A propagation period after corrosion activation that generates expansive corrosion products causing cracking of the cover concrete.

(iii) An acceleration period where corrosion increases due to easy access of oxygen, water and further aggressive agents through cracks and spalls.

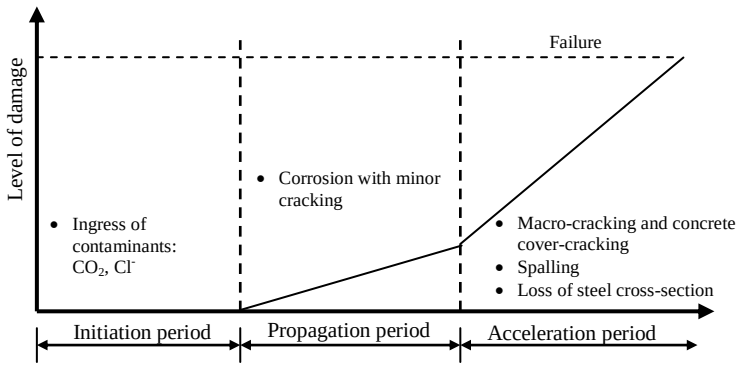

Figure 2.1: Three-stage corrosion damage model (Heckroodt, 2002)

This model is an extension of Tuutti's model (1982) presented in Chapter 1, Figure 1.1, which has only the initiation and propagation periods. The acceleration period depicts a time when visible corrosion damage is clearly evident and the penetrability of concrete cover may be insignificant in controlling corrosion rate due to extensive macro-cracking and spalling. The boundary between the propagation and acceleration stages may be dependent on factors such as tensile strength of the concrete. Before covering in detail the corrosion process of steel in RC, the following section will briefly cover the fundamental mechanisms of transport in concrete.

2.3 ***Transport mechanisms in concrete***

Transport properties of cementitious materials are a key factor for predicting their durability, since deterioration mechanisms such as corrosion, leaching or carbonation are all related to the ease with which a fluid or ion can move through the concrete microstructure. The passage of potentially aggressive species (ions or molecules in the form of liquids and gases) is primarily influenced by the penetrability of the concrete. Penetrability is broadly defined as the degree to which a material permits the transport through it of gases, liquids, or ionic species. It embraces the concepts of permeability, sorption, diffusion and migration and is quantifiable in terms of the transport parameters (Alexander and Mindess, 2005). For a durable RC structure, limiting the movement of fluids is one of the functions it has to fulfil (Stanish *et al*., 2004).

The processes involved in fluid and ion movement include the distinct mechanisms of capillary action, fluid flow under pressure and flow under a concentration gradient. These mechanisms are characterised by the material properties of sorptivity, permeability and diffusivity respectively (Richardson, 2002). The permeability of concrete will predominantly be influenced by the permeability of the cement paste, especially at the interface with aggregate particles.

Mechanisms of diffusion, migration, permeation, sorption, convection and wick action are briefly covered in the following sections.

2.3.1 ***Diffusion***

Diffusion is the movement of gases, ions and/or molecules under a concentration gradient, from an area of high concentration to one with a low concentration. Gaseous diffusion is experienced in unsaturated concrete while ionic diffusion occurs in saturated and partially saturated conditions. Molecular diffusion takes place if the pores of the medium are relatively large (Sharif *et al.*, 1999).

The modelling of gaseous and ionic diffusion in concrete is commonly done using Fick's first law of diffusion (for steady state diffusion). This law may be used to describe the rate of diffusion of a gas/ion into a uniformly permeable material (Richardson, 2002):

$$J = -D_{eff}\frac{dC}{dx} \tag{2.1}$$

where: J = mass transport rate (g/m^2s)
D_{eff} = effective diffusion coefficient (m^2/s)
dC/dx = concentration gradient (g/m^4)
C = Concentration of fluid (ion or gas)
x = distance (m)

The negative prefix denotes that the flux occurs along a negative concentration gradient. The modelling of ionic diffusion in concrete is done using Fick's second law of diffusion (for non-steady state diffusion) as will be seen in section 2.5.6. The penetration of chloride ions through concrete is best represented by a diffusion process if the concrete is assumed to be saturated (Kim and Stewart, 2000).

Diffusion acts as a predominant mechanism for concrete structures fully submerged in sea water or salt-contaminated soil. In combination with other mechanisms, diffusion contributes to chloride transport in concrete under most exposure conditions. The transport of oxygen in concrete to the steel surface is also governed mainly by a diffusion process. The rate of diffusion of oxygen is determined by the pore structure, pore size distribution and moisture content and decreases sharply with increase in moisture content (Richardson, 2002).

2.3.1.1 ***Migration***

Migration (also referred to as *accelerated diffusion*, *electro-diffusion*, or *conduction*) is the movement of ions in a solution under an electrical field. It is the transport mechanism most often used in laboratory accelerated chloride tests and is described by the Nernst-Planck equation (Andrade, 1993):

$$v = \left(D\frac{zF}{RT}\right)\left(\frac{dU}{dx}\right) \tag{2.2}$$

where: v = velocity of the ionic species
D = diffusion coefficient of the ionic species
z = electrical charge (ionic valence)
F = Faraday's constant

T = absolute temperature
U = potential difference across the sample
x = distance variable
R = universal gas constant (8.314 J/molK)

When diffusion and migration occur simultaneously, migration is usually the dominating mechanism (i.e. migration >> diffusion) and the total flux is the sum of both (Stanish *et al*., 2004).

2.3.2 ***Permeation***

Permeability of concrete is defined as the capacity of concrete to transfer fluids through its pore structure under an externally applied pressure whilst the pores are saturated with that fluid. The driving force for liquids and gases through the pore spaces or crack networks is a pressure gradient (Samaha and Hover, 1992). D'Arcy's law is used to calculate average velocity of flow ($\bar{v}$):

$$\bar{v} = \left(\frac{k}{n}\right)\left(-\frac{dh}{dx}\right) \tag{2.3}$$

where: k = permeability coefficient
n = porosity
h = hydraulic head
x = distance

Permeation plays an important role in water retaining structures where water transport through the structure is detrimental.

2.3.3 ***Sorption***

Sorption refers to uptake of liquids into a solid by capillary suction. It is measured using parameters such as bulk absorption, or sorptivity S. Sorptivity is the movement of a wetting front in a dry or partially saturated porous medium (Alexander and Mindess, 2005):

$$\mathrm{S} = \frac{\Delta M_t}{t^{1/2}}\left[\frac{d}{M_{sat} - M_o}\right] \tag{2.4}$$

where: $\Delta \mathrm{M}/t^{1/2}$ = slope of the straight line produced when the mass of water absorbed is plotted against the square root of time
d = sample thickness

M_o & M_{sat} = saturated mass and dry mass of concrete respectively

Sorptivity is influenced by the larger capillaries and their degree of continuity, and is very sensitive to hydration of the outer concrete surface, and hence curing. It is also influenced by compaction and aggregate orientation and distribution and by mix composition (Kropp and Alexander, 2007).

2.3.4 ***Convection***

Convection (or *advection*) is the process that describes the transport of a solute (e.g. chloride or sulphate ions) as a result of bulk moving water (Boddy *et al*., 1999). It is mainly influenced by the pore radius, connectivity of the pore system, permeability, and the concentration of the pore solution (Terheiden, 2008). The process is described by:

$$\frac{\partial C}{\partial t} = -\bar{v}\frac{\partial^2 C}{\partial x^2} \qquad (2.5)$$

where: C = Concentration of solute at depth x after time t

$\bar{v}$ = average velocity vector of fluid flow

From the equation, it can be deduced that to some extent, convection is concentration-driven. Convection (together with diffusion) is the main transport mechanism for chloride ingress in cracked concrete (Paulsson and Johan, 2002). It also has an important role in the movement of chloride ions when concrete is exposed to drying-wetting conditions.

2.3.5 ***Wick action***

Wick action is the transport of water and the ions it may contain through a concrete structure from a face in contact with water/salt solution to a drying face (Figure 2.2). It may also occur in concrete exposed to wetting and drying cycles. It results in a build-up of chlorides in the concrete, especially at the drying face (Buenfeld *et al*., 1997, Boddy *et al*., 1999).

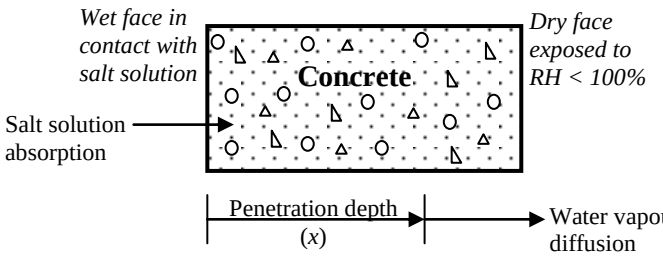

Figure 2.2: A schematic illustration of wick action in concrete (Puyate.and Lawrence, 1999)

2.3.6 ***Combined transport processes***

The selection in isolation of a single transport mechanism for the ingress of a particular substance may represent an over-simplification of the real transport process since more than one transport mechanism may be active at a given time, either in parallel or in different sections along the flow paths (Boddy *et al*., 1999, Kropp and Alexander, 2007).

To date, the quantification of the combined transport processes (also referred to as *mixed modes of transport*) has not been fully achieved. To do this, an in-depth understanding of the individual mechanisms is mandatory. Studies on transport processes should aspire to obtain models for predicting simultaneous movement of the deleterious corrosion species (chlorides, sulphates, oxygen, carbon dioxide, moisture) including the deposition and dissolution of ions (Nilssson *et al*., 1996). In line with this, development should be made in the field of testing in order to develop testing methods that can assess combined transport mechanisms.

Considering chloride penetration into concrete alone, the combined transport processes are usually physically quantified in terms of chloride profiles showing the distribution of chlorides with depth from the concrete surface at different times of exposure.

2.3.7 ***Effect of concrete aging on transport mechanisms***

Within its service life, the transport properties of concrete are most likely to be modified. This is mainly due to the ongoing hydration of the cementitious material. As a result, the porosity as well as the continuity of the capillary porosity may decrease with time. Other processes such as chloride binding also continue during this time (Gerard and Marchand, 2000). This is of considerable importance when transport parameters are assessed in laboratory experiments on young concrete specimens to provide input data for a long term assessment of structures, e.g. service life prediction.

Therefore, the transport characteristics of concrete also change with time and should be considered. One way of taking into consideration the effect of concrete aging is by using time functions (Mackechnie, 1996, Kropp and Alexander, 2007) as will be seen in section 2.5.6.

2.3.8 ***Transport properties of cracked concrete***

Knowledge of the transport properties of cracked concrete is essential for predicting its durability since the deterioration mechanisms (freeze and thaw, corrosion, leaching) depend on the flow of aggressive agents through the cracked concrete. The presence of cracks can substantially modify transport properties of concrete. Microcracks that are discrete and well distributed will influence transport in a very different manner compared to visible, connected,

localised macrocracks. Transport in a cracked concrete is therefore a coupled phenomenon between the matrix and the crack (Mohamed *et al*., 2003).

However, since the kinetics of different transport processes varies, changes resulting from cracking greatly depend on the mechanism which is predominant (Rodriguez, 2001, Weiss *et al*., 2007). Moreover, it has been shown that the main parameters for describing flow in damaged and sound material are different; for example in uncracked concrete permeability is related to its porosity, while in cracked concrete it is related to crack properties. Regardless of the transport mechanism, properties of the cracks become more important in cracked concrete than the properties of the concrete itself. Parameters such as crack width and shape, crack density/frequency and degree of connectivity, as well as crack origin, govern transport in cracked concrete (Breysse and Gerard, 1997). Therefore, no predictions on the behaviour of cracked concrete can be made based on data for uncracked concrete.

Transport processes in cracked concrete can be predicted using methods such as:

- Numerical simulation/modelling (Marsavina *et al*., 2007).
- Feedback-controlled splitting tests (Aldea *et al*., 1999).
- Imitation of various cracking mechanisms that RC structures encounter under actual service conditions.
- Creation of artificial cracks e.g. by positioning of shims in the mould prior to casting.

Therefore, either model (simulated) or artificial cracks could be successfully used in studying cracked concrete, as they are much easier to characterize and control than actual cracks. However, any models derived from experimenting with artificial cracks should always be calibrated on real concrete structures to ensure their reliability.

*2.4 **Fundamentals of steel corrosion in concrete***

Corrosion may be defined as the surface wastage that occurs when metals are exposed to corrosive environments. It is an electrochemical process in which iron enters into solution at the anode and oxygen is reduced at the cathode. It results in the flow of electrons between anodic and cathodic sites on the steel. The fundamental cause of corrosion is the inherent instability of metals in the metallic form. The tendency is for metals to revert to more stable forms, such as oxides, hydroxides or sulphides (Heckroodt, 2002).

The conventional steel grades commonly used as reinforcing steel in concrete are susceptible to corrosion when exposed to the atmosphere. However, steel embedded in concrete is naturally protected by the high alkalinity of the cement matrix (pH > 12.5) and by the barrier effect of the concrete cover. The concrete cover limits the amount of oxygen, moisture,

carbon dioxide and chlorides, which are required for active corrosion. The high alkalinity results from the presence of sodium hydroxide (*NaOH*) and potassium hydroxide (*KOH*), due to the dominant alkalis in the cement i.e. sodium oxide (Na_2O) and potassium oxide (K_2O), in a saturated calcium hydroxide solution ($Ca(OH)_2$). Without ingress of corrosive species such as carbon dioxide and chlorides into concrete during its service life, reinforcing steel passivates due to the alkaline concrete pore solution, resulting in negligible corrosion rates. The high pH suppresses steel corrosion by encouraging the formation of a very thin (1-10 nm) passive ferric oxide film (maghemite, $\gamma - Fe_2O_3$) on the steel surface (Richardson, 2002, Heckroodt, 2002).

For corrosion to occur four basic elements are required (Figure 2.3):

(i) Anode – site where corrosion occurs and from which current (electrons) flows.

(ii) Cathode – site where no corrosion occurs and to which current flows.

(iii) Electrolyte – a medium capable of conducting electric current by ionic current flow. In the case of concrete, the alkaline pore solution constitutes the electrolyte.

(iv) Metallic path – connection between the anode and cathode, which allows current return and completes the circuit. Steel serves this purpose in reinforced concrete.

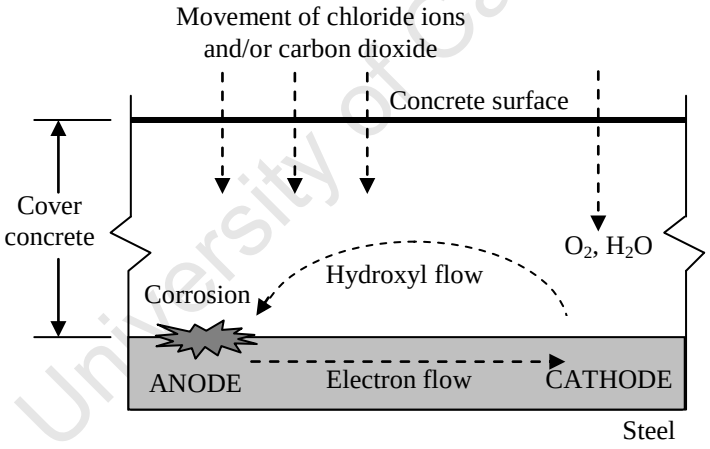

Figure 2.3: A schematic illustration of the corrosion process in concrete (Mackechnie and Alexander, 2001)

The basic anodic reaction for steel embedded in concrete is (Bockris *et al*., 1981):

$$Fe \rightarrow Fe^{2+} + 2e^{-} \qquad (2.6)$$

Electrons released at the anode are consumed at the cathode by reduction. The possible cathodic reactions depend on the availability of O_2 and on the pH in the vicinity of the steel surface. The most likely reaction is (Bockris *et al*., 1981):

$$2H_2O + O_2 + 4e^- \rightarrow 4OH^- \quad (2.7)$$

There can be either microcell or macrocell corrosion of steel in concrete. Macrocell corrosion is characterised by a small anode and a large cathode i.e. the anode and cathode are clearly separated in different areas. It frequently occurs in chloride-induced corrosion and/or in concrete with a low resistivity (high conductivity). It is characterised by very high local corrosion (pitting corrosion) and steel cross-section reduction. In microcell corrosion the anodic and cathodic sites are adjacent to each other. It is common in carbonation-induced corrosion and/or in concrete with high resistivity e.g. carbonated concrete (Bockris *et al*., 1981).

The passive layer can be disrupted by either agents of acidification e.g. carbon dioxide leading to carbonation or chloride attack. After depassivation corrosion may occur and propagate depending on the availability of corrosion agents (chlorides, carbon dioxide, moisture and oxygen).

2.4.1 ***Corrosion of steel in cracked concrete***

In cracked concrete, corrosion starts either in the crack zone or in the areas immediately adjacent to the crack. There are two different corrosion mechanisms that are theoretically possible in the region of cracks (Schiessl and Raupach, 1997):

Mechanism I: Where both the anodic and cathodic sites are in the zone of the crack. Anodic and cathodic areas are very small and located close to each other (microcell corrosion). The oxygen required for the cathodic reaction is supplied through the crack.

Mechanism II: Where the reinforcement in the crack zone acts as an anode, and the passive steel surface between the cracks forms the cathode. In this instance, oxygen penetrates mainly through the uncracked area of the concrete (macrocell corrosion). The steel surface involved in this corrosion process is larger than in the first mechanism, hence, higher corrosion rates can be expected.

2.5 ***Corrosion initiation***

Corrosion initiation is the process of continuous breakdown of the passive protective layer on the steel surface. It can be caused by several factors including ingress of chlorides, carbon dioxide, stray currents and bacterial attack. However, the main causes that will be discussed in this section are carbonation-induced and chloride-induced corrosion. Focus is placed on chloride-induced corrosion.

2.5.1 ***Initiation of carbonation-induced corrosion***

Carbonation occurs in concrete when carbonic acid (H_2CO_3) reacts with the calcium, alkaline hydroxides and cement phases to form calcium carbonate ($CaCO_3$) and compounds of silica and alumina gels. The carbonation process involves the following stages. First, the atmospheric carbon dioxide reacts with water in the concrete pores to form carbonic acid which lowers the pH of the concrete pore solution from above 12 to less than 9.

$$H_2O + CO_2 \rightarrow H_2CO_3 \tag{2.8}$$

This is followed by reaction of the carbonic acid with $Ca(OH)_2$ in the concrete as follows:

$$H_2CO_3 + Ca(OH)_2 \rightarrow CaCO_3 + 2H_2O \tag{2.9}$$

The above process leads to the depassivation of the steel in contact with the carbonated zones. The water released during the chemical reactions can sustain both the formation of carbonic acid and the carbonation process. Hence when carbonation starts, it is almost self-sustaining because of this release of water; but it soon becomes limited due to the increasing difficulty for the carbon dioxide to penetrate into the depth of the concrete (Richardson, 2002). As soon as the carbonation front reaches the steel, in the presence of water and oxygen, the corrosion process begins.

Carbonation is a diffusion process and therefore its depth (i.e. carbonation front) progresses by an exponential decrease with time. The carbonation process is generally modelled by means of the simplified expression (Richardson, 2002):

$$x = K_{co_2}\sqrt{t} \tag{2.10}$$

where: x = carbonation depth after time t

K_{co_2} = carbonation factor of the particular concrete

It does not develop if the concrete is water-saturated or in very dry conditions. This is because (a) moisture is required to form carbonic acid which attacks the $Ca(OH)_2$ and (b) CO_2 is not readily soluble in water.

Carbonation usually induces a generalized (macrocell) type of corrosion i.e. there are neither distinct anodes nor cathodes. Optimal conditions for increased carbonation rates include temperatures near 20 °C, relative humidity in the range of 50-70%, increased carbon dioxide volumes, w/b ratios at or above 0.6, and use of fly ash or slag as a cement replacement.

Pozzolanic concretes (e.g. concretes incorporating fly ash or slag) are less capable of resisting carbonation than Portland cements owing to their lower $Ca(OH)_2$ (portlandite) content (Sisomphon *et al.*, 2007). Concrete intrinsic factors tend to have the greatest impact on carbonation rates. The most important is the w/b ratio. Carbonation is often greatly reduced at w/b ratios below approximately 0.4. A reduction in carbonation depth of approximately 50% is observed when the w/b ratio is reduced from 0.6 to 0.4 (Parrott, 1987).

*2.5.2 **Initiation of chloride-induced corrosion***

When chloride ions are introduced in concrete during mixing or after exposure to the environment, they may depassivate the steel by locally breaking down the protective layer, γ-Fe_2O_3. Chlorides act as a catalyst to corrosion when they are in sufficient concentration at the steel surface. They are not consumed in the process but help to break down the passive layer and allow the corrosion process to proceed faster (Figure 2.4) (Broomfield, 1997).

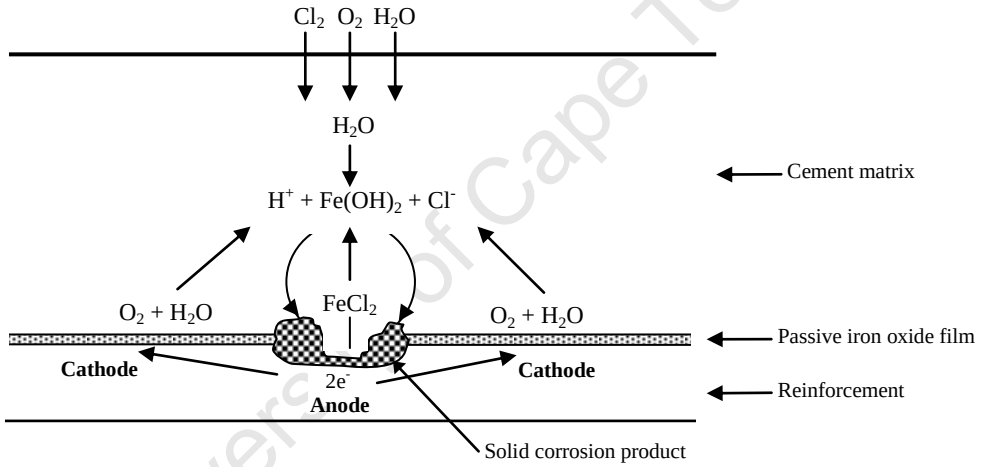

Figure 2.4: Corrosion of reinforcement in concrete exposed to chloride ions (Broomfield, 1997)

The exact manner in which chlorides break down the passive layer protecting the steel is not clearly known. There have been a number of suggestions by different researchers as to how the chloride ions actually depassivate iron under otherwise stable conditions (Foley, 1970, Shreir, 1979, Leek and Poole, 1990).

However, the exact mechanism of chloride-induced corrosion is not essential for the general understanding of the influence of chlorides on corrosion of steel in concrete. Passivity should not be viewed as a complete protection of the underlying metal but rather as an extreme or limiting value of corrosion. The passive layer is normally in a continual state of breakdown and repair under normal conditions. The presence of chloride ions will contribute towards the breakdown of the passive layer while other anions such as OH^- are responsible for its stability

and have inhibiting properties. There is a point therefore at which the concentration of aggressive ions overcomes the inhibiting ions and corrosion can initiate. This point is known as the pitting potential, below which passivity is maintained (Bockris *et al*., 1981).

2.5.3 ***Free vs. bound chlorides***

Not all of the chlorides in concrete are mobile and thus available for initiating or enhancing corrosion. Some of the chlorides are bound to the binder matrix as will be seen in the following sections. However, both free and bound chlorides usually exist simultaneously to maintain chemical equilibrium (Kropp, 1995).

(a) Free chlorides

These are the chloride ions dissolved in the concrete pore solution (Glass *et al*., 1996). Free (water soluble) chlorides are reduced with increasing concrete age due to effects such as chloride binding.

Early works suggested that only the free chlorides contribute to the corrosion process but this has been disputed as will be seen in the next section. The free chloride content may be determined by one of the following methods:

- Pore solution expression (Glass *et al*., 1996)
- Leaching techniques (Castellote *et al*., 2001)
- Use of embedded Ag/AgCl electrodes (Elsener *et al*., 2003)

(b) Bound chlorides

Chloride binding can be defined as the removal of chloride ions from the pore solution through interaction with the binder matrix. All mineral cements bind chlorides to some degree and this strongly influences the rate at which chlorides penetrate into the concrete from an external source. Chlorides in concrete can be bound chemically through a reaction with C_3A (tricalcium aluminate) or C_4AF (tetracalcium aluminoferrite) to form calcium chloro-aluminates (Boddy *et al.*, 1999).

Chloride binding effectively removes chlorides from the transport process resulting in changes to the pore solution concentration and thus the gradient driving ionic diffusion. Chloride binding may further influence chloride transport through partial blocking of pores due to the formation of the calcium chloro-aluminates (Glass *et al*., 1997).

The nature of the concrete chemistry is important in determining the penetration of chlorides through concrete and thus the level of chlorides present at the steel. For example Glass *et al*. (1997) noted a variation in the order of binding efficiency with 65% slag replacement

resulting in the greatest degree of chloride binding. The effects of cement extenders on chloride binding are graphically shown in Figure 2.5.

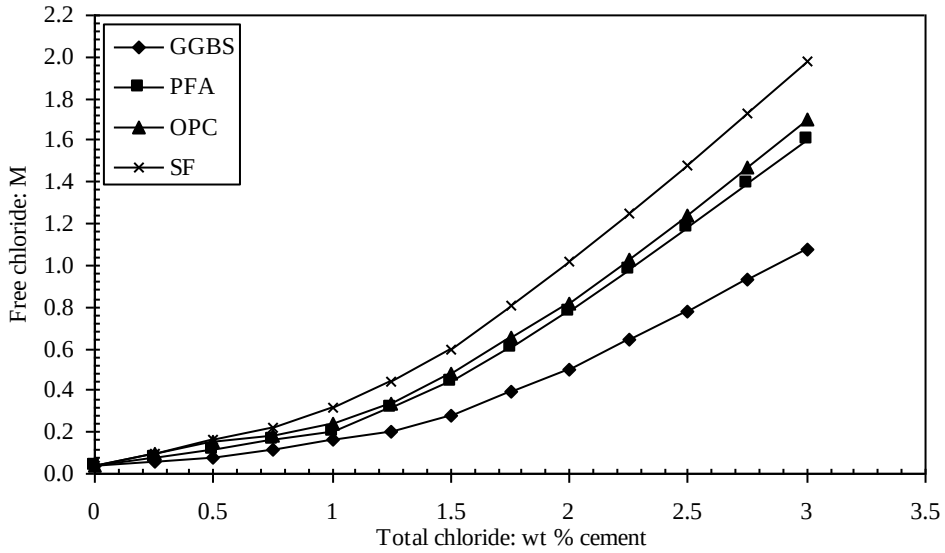

Figure 2.5: Chloride binding relationships dependant on binder type and total concentration (Glass *et al*., 1997)

(c) Participation of bound chlorides in corrosion

It has been postulated that only the remaining free chloride presents a significant corrosion risk. However, experimental evidence shows that bound chlorides may be released to participate in establishing a sustained corrosion process. Two mechanisms of releasing the bound chlorides have been proposed (Glass *et al*., 2000):

(i) The readily reversible nature of some of the chloride binding reactions.

(ii) Local acidification at the anode. In this case the local chloride ion concentration would be increased above its initial value promoting further breakdown of the passive film.

Therefore, bound chlorides may present a similar corrosion risk to free chlorides. The implications of this are that, while chloride binding retards chloride penetration, it also allows the build up of higher chloride contents that can increase the corrosion risk in some situations.

2.5.4 ***Chloride threshold level***

The chloride threshold level (or critical chloride concentration) is the concentration of chlorides necessary to break down the protective passive film on the reinforcing steel surface and initiate corrosion (Daigle *et al.*, 2004). It is the amount of chlorides that must be present at the steel surface before chloride-induced corrosion can be triggered. Knowledge of this value is important because it is a vital input parameter in service life design and service life prediction models.

The chloride threshold level is not a single value valid for all types of concretes, steels and environments, but is affected by a number of different factors such as cover thickness, temperature, relative humidity, electrical potential of the reinforcement, chemistry of the binder, proportion of total chlorides to that of free chlorides and chloride to hydroxyl ion ratio (Nilsson *et al*., 1996).

Early works suggested that only the free chlorides contribute to the corrosion process and hence the free chloride content was regarded as the best expression of the critical chloride content. These proposals have been challenged by other studies (Glass and Buenfeld, 1997) as was mentioned in section (c).

Different approaches have been used to express the chloride threshold level including the following:

(i) Free (water soluble) chloride threshold level
(ii) Total (acid soluble) chloride
(iii) $[Cl^-]/[OH^-]$ ratio

The representation of the chloride threshold level as the total chloride (acid soluble) content is the most widely used approach although there still exists controversy on the minimum total chloride content that is required at the steel level to initiate corrosion.

Generally, a large scatter is found with results from 0.02 to 3.08% total chlorides by mass of binder (over two orders of magnitude) (Table 2.1). However, a conservative value of 0.4% total chlorides by mass of cement has been given by most authors (Daigle *et al*., 2004). The increased use of mineral extenders also makes the prediction of the free chloride threshold in concrete difficult.

Table 2.1: Some published total chloride threshold values

Reference	*Binder type*	*Chloride threshold (% by mass of binder)*
Lambert *et al*., 1991	OPC, SRPC	1.0 - 3.0
Alonso *et al*., 2000	OPC	1.24 - 3.08
Trejo *et al*., 2003	OPC	0.02 - 0.24
Scott, 2004	various binders	0.08 - 0.53

The large span of results might be due to reasons such as:

(i) Sample preparation, for example whether the chlorides were added during concrete mixing (admixed), type of chloride salt (e.g. CaCl, NaCl), binder type, type of steel, etc.

(ii) Testing methodology e.g. there is no defined line between potential to corrode (half-cell potential, E_{corr}) and actual progression of steel corrosion (corrosion current density, i_{corr}).
(iii) Different exposure conditions.

All these make comparison of threshold values very tricky, and hence the controversy. It would therefore be appropriate if the total chloride threshold concentration was defined in such a way that it is binder-specific. Moreover, the variability in these values could be decreased if a standardised testing procedure is adopted.

2.5.5 ***Factors affecting time to chloride-induced corrosion initiation***

The time to corrosion initiation is dependent on the following factors:

- Chloride binding capacity of the binder
- Chloride threshold value
- Thickness of the concrete cover
- Resistance of cover zone to chloride ingress

2.5.5.1 ***Effect of chloride binding on corrosion initiation***

The effect of chloride binding on corrosion initiation is twofold: (a) the rate of chloride ionic transport in concrete is reduced since the amount of available mobile ions (free chlorides) is also reduced by the binding mechanisms and (b) the reduction of free chlorides in concrete results in lower amounts of chlorides being accumulated at the reinforcing steel surface (Hooton and Thomas, 2000).

The effects of cement extenders, and by inference chloride binding, on limiting the ingress of chlorides are provided by Tarek *et al*. (2002) in their examination of concrete after 15 years of exposure in tidal zones. For an assumed cover depth of 70 mm and a threshold value of 0.4% total chlorides by mass of cement, the time to initiation was found to be 22, 65 and 150 years for OPC, FA (10-20%) and slag (60-70%) respectively. Similar results have been obtained by Mangat *et al*. (1994) and Mackechnie and Alexander (1996). However, the increased time to corrosion initiation cannot only be attributed to chloride binding effects. Other effects such as finer pore structure in the blended cements may also contribute to the longer time to corrosion initiation.

Even after corrosion has started, the rate at which it progresses will continue to be affected by binding as there is a much slower increase in chloride level which will in turn limit the increase in corrosion rate.

The effects of ground slag (which is of interest in this study) on chloride binding will be covered in the following sections.

In South Africa, slag can be of two types depending on the iron manufacturing process used:

(i) ***Ground granulated blastfurnace slag (GGBS)***

This is a cementitious material formed when molten iron blast furnace slag is rapidly cooled by immersion in water. It is a granular product with very limited crystal formation and is cementitious in nature. South African GGBS has a typical Blaine fineness value of about 390 m^2/kg (Mackechnie *et al.*, 2003).

(ii) ***Ground granulated Corex slag (GGCS)***

This is a cementitious material produced in the Corex process at the Saldhana steel plant in the Western Cape Province, South Africa. It has been produced since 1999. GGCS is much finer than GGBS, with a Blaine fineness value of about 470 m^2/kg (Mackechnie *et al.*, 2003).

(a) Effect of slag on chloride binding capacity of concrete

Chemical compounds similar to Calcium Silicate hydrate (C-S-H) form during the hydration reactions of ground slag, causing pore refinement (Jaul and Tsay, 1998). Ground slag is efficient in blocking the pores (fine-filler effect) since it reacts not only with $Ca(OH)_2$ but also with water to form C-S-H and calcium aluminates (Bakker, 1983). Thus, the additional formation of C-S-H gel results in the absorption of more chloride ions and blocking of diffusion paths. A higher content of aluminates in ground slag can also absorb more chlorides to form Friedel's salt (Leng *et al*., 2000).

However, the chloride binding capacity of ground slag can be reduced in the presence of sulphates (Leng *et al*. 2000, Luoa *et al.*, 2003).

In general, ground slag therefore decreases the free chlorides and increases the bound chloride content in concrete, which results in a lower probability of corrosion initiation of the reinforcing steel.

(b) Effect of sulphides

Slag has a reducing character in its composition, containing manganese, iron, and other species in reduced states. The main contribution of its reducing power may be associated with the presence of soluble sulphides such as S^{2-}, HS^{-}, and S_n^{2-}, even though the total sulphide content of the slag may typically be less than 1% by mass. The reducing characteristics of granulated slag can influence the electrochemical potential of slag-OPC paste pore solutions (Pal *et al.*, 2002).

Sulphides affect the steel in two ways (West, 1980):

(i) The sulphides are oxidized to sulphate by the available oxygen thus depleting the oxygen concentration at the steel level and creating a potentially reducing environment;

(ii) The sulphides form a precipitate of FeS on the steel surface thus affecting the formation of the passive layer.

Tromans (1980) also suggested that sulphides may be incorporated into the oxide layer thus reducing its ability to protect the steel. The depletion of oxygen in the presence of sulphides limits the formation of the passive layer on the steel surface. This is because the development of this layer is dependent on the availability of sufficient oxygen to supply the cathodic reaction. The embedded steel will therefore be more susceptible to corrosion and, with the availability of the corrosive agents such as chlorides, time to corrosion initiation may be decreased.

The effect of sulphides therefore tends to downplay the improved overall concrete pore structure (mainly fine pore sizes). However, this effect may only be detrimental in the short term (depending on the sulphide content and the availability of oxygen). In the long term, the improved pore structure of the concrete due to incorporation of slag dominates and negligible corrosion rates may be noticed (Salvarezza *et al*., 1982).

2.5.5.2 ***Effect of chloride threshold level on corrosion initiation***

As was mentioned in section 2.5.4, the chloride threshold level is not a single value valid for all types of concretes, steels and environments. It is affected by a number of different factors such as cover thickness, temperature, relative humidity, electrical potential of the reinforcement and chemistry of the binder (Nilsson *et al*., 1996). These parameters vary from concrete to concrete and therefore corrosion initiation time will also have a similar variation among different binders.

The inclusion of cement extenders generally results in a lowering of the chloride threshold. The different performance of the cement extenders is attributed to the reduction in alkalinity and the presence of sulphides in the slag bearing materials (Scott, 2004). In a study using simulated pore solution, Scott (2004) found varying chloride threshold values for different binders as presented in Table 2.2.

The lower threshold values for the blended cements may be attributed to slow early hydration process leading to high short term concrete permeability. In the long term, the increased dense pore structure in these concretes may result in substantial decrease in corrosion rate or stifle the corrosion process.

Table 2.2: Variation of chloride threshold level with binder type (simulated pore solution) (Scott, 2004)

Binder Type	*Concentration (% by mass of binder)*
Ordinary Portland Cement (PC)	0.53
25/75 GGBS/PC	0.41
50/50 GGBS/PC	0.08
75/25 GGBS/PC	0.20
30/70 Fly ash/PC	0.36
50/43/7 PC/GGBS/silica fume	0.08

2.5.5.3 ***Effect of concrete cover on corrosion initiation***

The concrete cover (or *covercrete*) may be regarded as a large transition zone with properties generally being inferior to those of the bulk concrete, particularly as the exposed surface is approached (Du Preez and Alexander, 2004, Alexander and Mindess, 2005). It provides the initial resistance to the degradation agents such as chloride ions. Therefore, the thickness, quality and condition of the concrete cover all have significant effects on the processes that lead to the corrosion of steel in concrete. The protective performance of the concrete cover is often further impaired by the presence of cracks. This will be covered in section 2.6.1.6.

A significant portion of the service life of a structure may be lost if the cover thickness is reduced (Torrent *et al*., 2007). On the other hand, excessively thick covers may result in wider flexural cracks which increase the penetrability of the cover. Therefore the cover thickness can only be increased up to a limit of 80-90 mm (Neville, 1998). If this is unsatisfactory for the required durability, then the quality rather than the thickness should be increased.

2.5.6 ***Prediction of time to chloride-induced corrosion initiation***

The corrosion initiation period (t_i) for chloride-induced corrosion defines the time required for chlorides to accumulate at the steel level in sufficient concentration to break down the passive protective layer on the steel surface and thereby trigger corrosion process. No damage due to corrosion is assumed to occur during this period.

To predict chloride ingress in concrete structures the following should be considered (Daigle *et al.*, 2004):

(i) Concrete is a heterogeneous material that can include cracks.
(ii) Surface chloride concentration is known to vary with time.
(iii) Changing environmental conditions, such as temperature and humidity, affect the diffusion coefficient.

(iv) Hydration of cement paste is a chemical process that continues after the structure is put in service. This chemical reaction has an influence on the chloride diffusion coefficient.

(v) Interface between cement paste and aggregates influences chloride diffusion.

Prediction models based on consideration of diffusion alone are constructed around Fick's second law of diffusion, which concerns the rate of change of concentration with respect to time. For a semi-infinite homogeneous medium, and in spite of whether the process is in steady state or not, the law may be stated as follows (Richardson, 2002):

$$\frac{\partial C}{\partial t} = D\frac{\partial^2 C}{\partial x^2} \tag{2.11}$$

where D is the apparent diffusion coefficient. The diffusion coefficient is not only a material property but also depends on the testing conditions, with boundary conditions of:

$C_x = 0$ at $t = 0$ and $0 < x < \infty$

$C_x = C_s$ at $x = 0$ and $0 < t < \infty$

where C_x = chloride concentration at depth x at time t.

C_s = surface chloride concentration

Crank's error function solution (also called *Gauss error function*) of Fick's second law can be stated as follows (Richardson, 2002):

$$C_{x,t} = C_s\left[1 - erf\left(\frac{x}{2\sqrt{D_a t}}\right)\right] \tag{2.12}$$

where: $C_{x,t}$ = chloride concentration at the depth x at a given time t.

C_s = surface chloride concentration

D_a = apparent chloride diffusion coefficient

t = time of exposure

erf = error function

However practical observations have shown that the application of Fick's second law of diffusion entails certain conditions. Close to the surface, the concrete is exposed to a continuous cycle of wetting and subsequent evaporation (drying). Here the water carrying dissolved chlorides moves in and out; this contradicts the assumption for diffusion (Hunkeler, 2005) (Figure 2.6). Beyond this depth, diffusion is the decisive transport mechanism.

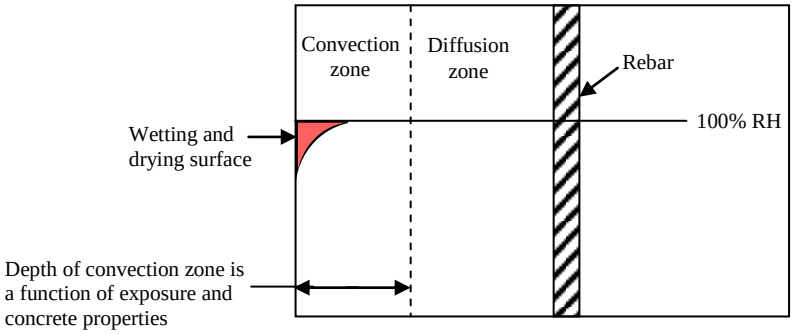

Figure 2.6: Convection zone in concrete
(ACI Committee 365: LIFE 365, 2005)

Other causes of the convection zone include the following:

(i) Leaching of chlorides in times when there is no or low chloride loading. This may occur if the concrete surface is subjected to chloride-free water.

(ii) Carbonation of surface concrete; this reduces the binding capacity of the binder and the pH drop accompanied by carbonation may result in release of bound chlorides in the zone near the surface. This enhances the chloride gradient.

Therefore, in order to describe the penetration of chlorides with the error function solution of Fick's second law of diffusion the convection zone (Δx) was introduced by Gehlen (2000, cited by Hunkeler, 2005). Beyond the convection zone, the effect of diffusion may then be described by a diffusion approach, for which the simple error function solution is again applicable. Instead of using the chloride concentration at the surface, the starting point of the calculation with the error function solution is thus the depth Δx where the concentration of chlorides is considered to remain constant over time (Figure 2.7).

$$C_{x,t} = C_i + (C_{\Delta x} - C_i).erf\left(1 - \frac{x - \Delta x}{2\sqrt{(t - t_{exp}).D_{(t)}(t)}}\right) \qquad (2.13)$$

where: $C_{x,t}$ = chloride concentration at depth x at age t (wt.-% cement)

C_i = initial chloride background level (wt.-% cement)

$C_{\Delta x}$ = chloride content in depth Δx (wt.-% cement)

$D_{(t)}$ = time-dependent apparent diffusion coefficient (m^2/s)

t_{exp} = time until first exposure to chlorides (s)

t = concrete age (s)

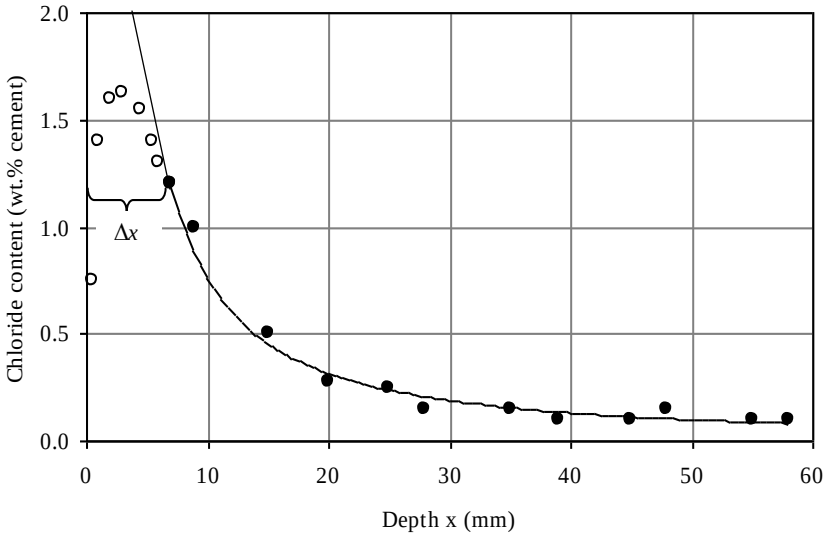

Figure 2.7: Typical chloride profile from splash zone
(profile has been fitted to error function neglecting data points in the convection zone) (Hunkeler, 2005)

The time-dependent (*time-integrated*) diffusion coefficient ($D_{(t)}$) takes into account the decrease in chloride diffusivity with time due to effects such as continued hydration and chloride binding. This is described by the relation (Mackechnie, 1996):

$$D_{(t)} = D_o\left(\frac{t_o}{t}\right)^n \tag{2.14}$$

Where D_o is the diffusion coefficient at reference time t_o (e.g. 28 days) and n is the aging coefficient (reduction factor). The value of the aging factor depends on the rate of hydration and degree of drying.

The depth of the convection zone depends on (Tuutti, 1993):

- Drying and wetting time
- Time to capillary suction during wetting
- Difference in water pressure and
- Penetrability of the concrete against water

The convection zone can be estimated by:

(i) Using chloride profiles as a maximum of the chloride concentration (Hunkeler, 2005).
(ii) Using relative humidity measurements (Tuutti, 1993).
(iii) Using conductivity measurements in concrete under cyclic wetting and drying regime (Chrisp *et al*., 2002).

Most of the existing chloride-induced corrosion initiation prediction models are based on Fick's 2nd law of diffusion. These include the following:

(i) South African chloride prediction model (Mackechnie, 2001)
(ii) DuraCrete (DuraCrete, 1998)
(iii) ClinConc (Tang, 1996, Tang, 2008)
(iv) LIFE 365 (ACI Committee 365, 2005)

2.6 ***Corrosion propagation***

When corrosion agents (O_2, CO_2, H_2O, Cl^-) continue to be available at the corrosion sites (anode and cathode) after corrosion initiation, corrosion may proceed into the propagation stage. Corrosion propagation is characterised by active corrosion and may lead to generation of cracks, delamination, and spalling of concrete cover due to expansive corrosion products (Yoon *et al*., 2000). Conventionally, it is taken that corrosion rates below 0.1µA/cm^2 characterise passive corrosion state, whereas rates above this value characterise active corrosion (Alonso *et al.,* 2002) i.e. corrosion rate of 0.1 µA/cm^2 is taken as the transition point from passive to active corrosion.

2.6.1 ***Factors affecting corrosion propagation of steel in concrete***

After corrosion initiation, the rate at which corrosion progresses agents depends on several factors including temperature, w/b ratio, binder type, presence of cracks, concentration of the corrosion agents, duration and condition of exposure, and the chemical resistance of concrete.

In this section, focus is on factors that affect corrosion rate of chloride-induced corrosion including, among others, presence of cracks on the concrete surface, w/b ratio and the effect of slag.

2.6.1.1 ***Effect of cement extenders on corrosion propagation***

Apart from having an influence on corrosion initiation, mineral cement extenders such as slag, fly ash and silica fume also have a profound effect on the rate at which it progresses (Mangat *et al*., 1994, Mackechnie and Alexander, 1996). Extensive research has been done on the use of cement extenders and as a result, a better understanding on the influence of cement extenders on the corrosion rate has been developed.

Song and Saraswathy (2006) reviewed previous studies on the corrosion resistance of reinforced steel in concrete with ground granulated blast-furnace slag and concluded that replacement of cement by 40% slag has no significant influence on corrosion rates of rebar in concrete. At 60% slag content the corrosion rate is significantly reduced. Hence, an increase

in slag proportion decreases the rate and amount of corrosion of reinforcement in slag concrete.

2.6.1.2 ***Effect of moisture content on corrosion rate***

The moisture content in concrete is an important factor for both corrosion initiation and its progress. It highly influences corrosion initiation time as it delays the intrusion of both oxygen and carbon dioxide but is an important pre-requisite for the penetration of chlorides by diffusion (section 2.5.6), (Hunkeler, 2005). In the propagation period, the rate of corrosion is also influenced by moisture condition of the concrete.

The corrosion rate is slow in dry or saturated condition, but at intermediate moisture contents, moisture acts as an electrolyte and also allows the intrusion of oxygen to the corrosion process (DuraCrete, 1998). In dry conditions, there is no moisture to support corrosion process whereas in saturated conditions, movement of oxygen through the concrete to the steel level may be significantly impaired because oxygen does not readily dissolve in water. A corrosion cell can therefore not occur if the concrete is too dry to serve as an electrolyte or too wet (saturated) to allow ingress of oxygen. Corrosion activity is most vigorous at relative humidity (RH) values above 80%. Chloride induced corrosion is at a maximum when the RH within the concrete is around 90-95% (Richardson, 2002).

There appear to be two main inter-related mechanisms for controlling the corrosion rate of steel, both dependent upon the relative humidity of the concrete. The movement of O_2 from the atmosphere to the surface of steel is a function of the diffusion coefficient (the ease with which O_2 can move through concrete) and the depth of the steel. The diffusion coefficient is in turn affected by both the w/b ratio (through the permeability of the concrete) and the RH of the concrete. The movement of O_2 through concrete is significantly reduced by an increase in the proportion of water-filled voids. The O_2 diffusion coefficients for two w/b ratios of cement paste at various RH are provided in Figure 2.8.

The moisture condition (or relative humidity) of concrete is therefore an important factor in controlling corrosion rate. It mainly affects the availability of oxygen depending on whether the concrete is dry or saturated. In between, there is an optimum RH range for chloride induced corrosion.

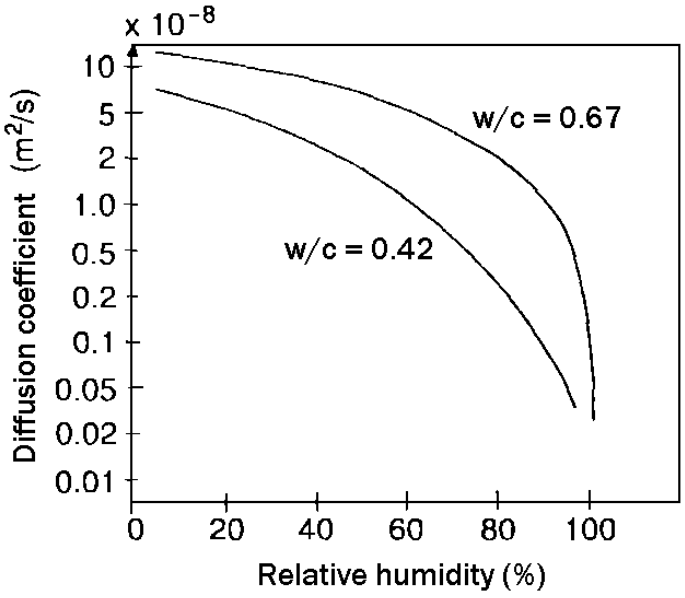

Figure 2.8: Influence of w/c ratio and RH on the diffusion coefficient for O_2 (Bentur *et al*., 1997)

2.6.1.3 ***Influence of temperature on corrosion rate***

The significance and influence of temperature as a factor in steel reinforcement corrosion rate is evaluated by means of the universal dependence of chemical reactions on the surrounding temperature. According to this, the rate of chemical reaction is accelerated as the surrounding temperature is increased. But experimentally it has been found that dependence of the rate of steel reinforcement corrosion on the surrounding temperature is more complex. This complexity has been shown by an accelerating effect up to a temperature of 40 °C followed by an inhibiting effect occurring above this temperature. The main cause of this phenomenon is attributed to the decreasing oxygen solubility in the pore solution when the surrounding temperature is increased (Zivica, 2003).

2.6.1.4 ***Influence of water/binder ratio and binder content on corrosion rate***

The water/binder (w/b) ratio affects the corrosion characteristics of the concrete primarily by governing the pore structure. High w/b ratio has a negative effect on the steel reinforcement corrosion mainly due to increased permeability of concrete. The effect is due to faster diffusion of chloride ions to the steel level, easier oxygen penetration and lower concrete electrical resistivity of the concrete (Petterson, 1995).

For concrete in a moist environment, the cathodic reaction rate depends on the availability of oxygen and the corrosion rate may therefore be limited by the cathodic reaction. With a decrease in w/b ratio, the quantity of oxygen decreases due to decreased concrete permeability. Therefore, decreasing the w/b ratio suppresses the cathodic reaction and

subsequently a decrease in the corrosion rate. In addition, the concrete resistivity increases with a decrease in the w/b ratio. If sufficient oxygen is available to support higher corrosion rate, concrete resistivity may be the controlling factor that determines the maximum possible corrosion rate. Scott and Alexander (2007) proposed a relationship between corrosion rate, oxygen availability and resistivity (Figure 2.9).

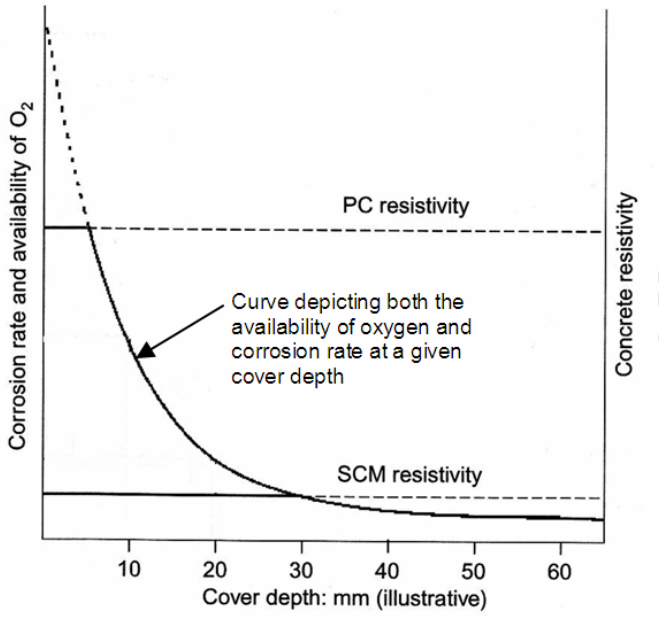

Figure 2.9 : Schematic of the relationship between corrosion rate, O_2 availability and resistivity (PC: ordinary Portland cement, SCM: supplementary cementitious materials) (Scott and Alexander, 2007)

The resistivity controls are shown as horizontal lines PC resistivity and SCM resistivity, where PC would be representative of OPC concretes and SCM of concretes produced with supplementary cementitious materials.

Corrosion rates for 12 mm deformed steel cast in concrete, with a cover of 10 mm, and three different w/b ratios and cement contents, were examined by Mangat and Molloy (1994). The specimens were exposed to cyclic periods of wetting and drying after 14 days air curing. The results are provided in Table 2.3.

It is evident that w/b ratio had a significant impact upon the corrosion rate of steel in concrete as opposed to cement content. The highest corrosion rate was observed in the 0.76 w/b ratio with the accompanying highest chloride concentration while the lowest corrosion rate of 0.13 $\mu A/cm^2$ was found to occur in the w/b 0.45 sample despite having higher chloride content than the 0.58 w/b with 530 kg cement. The effects of the material are thus more significant

than simply limiting the chloride ingress. The cement content was shown not to significantly affect the corrosion rate.

Table 2.3: Influence of w/b and cement content on corrosion rates (Mangat and Molloy, 1994)

w/b	*Cement content* (kg/m^3)	i_{corr} (uA/cm^2)
0.45	430	0.13
0.58	430	0.65
0.58	330	0.62
0.58	530	0.52
0.76	430	2.16

The effects of w/b ratio and hence permeability on corrosion characteristics are even more severe considering that 530 kg of cement resulted in a Cl^-/OH^- ratio of 6 compared to 11 for the 0.45 w/b ratio with 430 kg cement. Thus the physical effects of the concrete appear to dominate the chemical contributions of the hydroxyl ions in the pore water.

The influence of w/b ratio on corrosion rate is therefore significant and should be taken into account at the concrete mix design stage if the RC structure will be exposed to aggressive environments during its service life. For less aggressive environments, careful selection of w/b ratio may as well be successfully used to limit corrosion.

2.6.1.5 ***Influence of concrete cover thickness on corrosion rate***

Concrete cover thickness influences mainly the ingress of chlorides and oxygen into the concrete. The quality of the concrete cover especially with respect to its penetrability determines the ease of ingress of the chloride ions. Reduction of concrete cover reduces the travel path for the chloride ions and oxygen to reach the embedded steel in concrete (Hawkins and McKenzie, 1996).

The effects of cover on the diffusion of O_2 are shown in Figure 2.10. It can be depicted from the graph that an increase in cover depth from 20 to 50 mm results in a reduction in the availability of O_2 at 60% RH, (Bentur *et al*., 1997). Thus the coupled effect of an increasing cover depth and a shift in RH from 60 to 80% results in approximately twice the decrease in the availability of O_2. The increased cover depth is also likely to minimize the influence of the external drying at the depth of the steel thus sustaining a fairly high RH. The phenomenon of oxygen availability with varying cover depth can also be explained using Scott and Alexander's (2007) schematic previously presented in Figure 2.9.

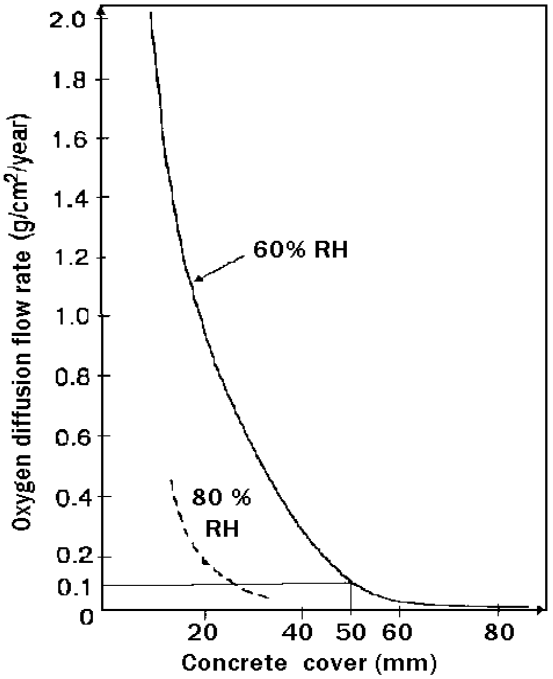

Figure 2.10: Effect of concrete cover on the diffusion of O_2
(Bentur *et al*., 1997)

Concrete cover therefore affects the corrosion rate mainly by either decreasing or increasing the travel path of the corrosion agents (oxygen, moisture, chlorides). Just like w/b ratio, concrete cover may also be used to inhibit corrosion. In fact, when w/b ratio, cover, binder type and binder content are carefully chosen, corrosion may be significantly inhibited during the service life of a RC structure. In general, a small concrete cover may be used for a high quality (less penetrable) concrete while the same cover thickness may not apply for a lower quality concrete cover.

2.6.1.6 ***Influence of cracks on corrosion***

The ACI 201 defines a crack as a *complete or incomplete separation of concrete or masonry, into two or more parts, produced by breaking or fracturing*. Concrete is essentially waterproof in an uncracked state when properly placed, compacted, and adequately cured. However, it may gradually lose its water-tightness in the course of its service life due to the formation of cracks, and then become vulnerable to deterioration by corrosion of reinforcement.

While cracks may develop in concrete from a variety of causes, the underlying principle cause is the relatively low tensile strength of concrete. Concrete is a quasi-brittle material with a low capacity for deformation under tensile stress. Cracking occurs when the applied tensile stresses exceed the tensile strength of the concrete.

Two forms of cracks are of interest when evaluating the condition of a reinforced concrete structure; those present before the onset of corrosion which might assist the corrosion processes, and those produced as a direct consequence of corrosion. This study is interested in the former.

In most instances, cracks do not affect the load-carrying capacity of the concrete structure. However, in extreme cases, they may affect the structural integrity of the concrete member and may also adversely affect its durability by providing easy access to aggressive agents, especially chloride ions in marine environments (Transportation Research Circular E-C107, 2006). The effects of cracks in concrete cover vary not only with their effective depth, but also with their width, frequency and orientation (relative to the steel reinforcement). These factors will be explored in this section.

(a) Autogenous healing of cracks in concrete

The term autogenous healing (also referred to as *self-healing*) refers to the ability of the cementitious material to heal cracks in concrete. The process involves both physico-chemical and mechanical processes. The following physical, chemical, and mechanical processes have been suggested to be the main reasons for the autogenous healing of concrete (Edvardsen, 1999):

(i) Swelling and hydration of cement paste
(ii) Precipitation of calcium carbonate crystals
(iii) Ettringite formation
(iv) Blocking of flow path by impurities in water and
(v) Blocking of flow path by the concrete particles (debris) broken from the crack surface due to cracking.

The most significant factor, which influences autogenous healing, is the precipitation of calcium carbonate ($CaCO_3$) (Schiessl and Edvardsen, 1993). However, regardless of the origin, the occurrence and benefits of self-healing are especially significant in the reduction in concrete penetrability and hence improving the protection of the embedded steel from corrosion (Neville, 2002).

To a considerable degree, the autogenous healing process is influenced by the crack width and the prevailing water pressure, whereas the type of binder, aggregate, and filler and the hardness of the water are of a lesser influence (Edvardsen, 1999). Smaller cracks are therefore more likely to heal (faster) than larger ones.

An important practical question is: what is the maximum crack width that can be closed by autogenous healing? Various researchers have reported different maximum crack widths for which autogenous healing is possible but this is not surprising because the testing conditions also vary a lot. The following may vary from one experiment to another:

- How the cracks were produced e.g. by shrinkage, application of flexural tension, or by direct tension
- The age at which the cracks were opened and for how long they were monitored
- Type of water used e.g. fresh, sea water, lime-saturated water
- The material undergoing the autogenous healing (concrete or mortar)

The combinations of these conditions are numerous, so that generalizations about the maximum width of cracks that will heal are not possible. Table 2.4 presents some of the findings of various researchers.

Table 2.4 : Some studies on autogenous crack healing
(Summarised from Neville, 2002)

Reference	*Results*
Wagner (1974)	A 0.33 mm crack (in a mortar lining of metal pipes) was still open after 30 days' immersion in city water, but healing had taken place below the surface.
Vennesland and Gjorv (1981)	Corrosion was observed in all RC blocks with crack widths of 0.4 mm or more
Gautefall and Vennesland (1983)	Specimens with cracks more than 0.6 mm wide were susceptible to corrosion attack but this did not happen when the cracks were less than 0.4 mm wide Immersed in seawater (ample oxygen was available at a separate cathode, which was remote from the anode)
Edvardsen (1999)	25-50% of the 0.20 mm cracks wide healed completely after 7 weeks of water exposure. The proportion of cracks closed depended on the water pressure

However, regardless of the maximum crack width at which autogenous healing is possible, cracks up to a certain width in RC are inevitable and acceptable, hence the concept of acceptable or allowable crack widths. The next section will cover this briefly.

(b) Allowable crack widths

The maximum crack width considered acceptable depends on the type of structure, the location within the structure, the environment (exposure conditions), and the consequences of excessive cracking (Park and Paulay, 1975, Ismail *et al*., 2004).

Some concrete design codes limit the surface transverse crack widths to control corrosion of steel in concrete (e.g. British Standards Institution (BS 8110: Part 1) 1997). On the contrary, European design code (Comite´ Euro-International du Be´ton (CEB), 1989) recommends that the limitation of crack widths is no means to avoid the attack to the reinforcement in the case of severe chloride attack to horizontal concrete surfaces. This may be due to the ponding effect of the chlorides on the concrete surface hence faster ingress of the chlorides into the concrete.

To ensure durability, maximum crack width in a corrosive and aggressive environment may need to be considerably smaller. Results of exposure tests and site inspections confirm that within a common range of crack widths (up to 0.4 mm), the influence of the transverse crack on the corrosion rate of steel bars is relatively small (CEB/FIP model code, 1992). Hence most codes adopt a crack width of 0.4 mm as a threshold value.

At this point, it must be mentioned that crack widths and crack profiles are inherently subject to wide scatter (Nejadi, 2005) even in carefully monitored laboratory tests and are influenced by shrinkage and other time-dependent effects.

In designing a concrete structure against corrosion, several codes and specifications provide equations to predict the maximum crack widths that are expected to result from the loads and stresses carried by the structure e.g. ACI 318, 1995 (Table 2.5). Some give the designer both the option of predicting the maximum crack width e.g. British Standards Institution (BS 8110: Part 1, 1997 and BS 5400 Part 4, 1990) (Table 2.5).

Table 2.5: Examples of crack width prediction formulae

Code/Specification	*Crack width prediction equation (W_{max})*
ACI 318 (1995)	$0.132z$
BS 8110: Part 1 (1997) and BS 5400: Part 4 (1990)	$\frac{3a_{cr} \in_m}{1+2\left(\frac{a_{cr}-c}{h-d_c}\right)}$

where: a_{cr} = distance from crack to nearest bar surface which controls width

$\in_m$ = calculated strain at the level where cracking is considered

h = overall depth of section

d_c = depth of concrete in compression

c = cover to outermost reinforcement

z = $f_s(cA_e)^{1/3}$

A_e = effective area of concrete

It appears that there is no single answer to the question on permissible crack widths. Complex inter-relations among properties of the concrete cover, exposure conditions, and designed service life of the structure should be used to determine the crack widths that can be tolerated without significant corrosion.

(c) Effect of cracking on chloride ion penetration

Cracks in concrete may cause localised chloride ingress and hence localised steel corrosion. Mass transfer of corrosion species in cracked concrete, e.g. chloride ion diffusion, has been shown to increase after cracking of concrete (Sagues and Kranc, 1998).

Transverse crack width (with respect to the reinforcing bar orientation) in the tension zone of about 0.1 mm has been interpreted to allow proportionately greater penetration of chlorides in the vicinity of the cracks due to microcracking internal to the concrete near the bar. This may be caused by bond-related transfer of tensile strain within the concrete adjacent to the reinforcement or by temperature or other strains (Bentur *et al.*, 1997). The damage decreases with distance from the (transverse) macrocrack implying non-homogeneity in concrete permeability (Schiessl 1998).

In a study by Scott (2004) on cracked steel reinforced concrete specimens made with a constant w/b ratio of 0.58 but using different binder types, chloride concentrations were determined at two locations: 30 mm along the steel on either side of the crack (near crack), and from 30 mm to 90 mm from the crack at one side along the steel (remote from crack) (Table 2.6).

Table 2.6: Chloride concentrations for near crack and remote from crack section (Specimen age: 86 weeks, cover depth: 20 mm) (Scott, 2004)

Binder type	*Chloride concentration (% mass of cement)*			
	Near crack		*Remote from crack*	
	0.2 mm	*0.7 mm*	*0.2 mm*	*0.7 mm*
100 % CEM I (OPC)	4.36	4.15	1.78	1.73
50/50 CEM I/GGBS	1.86	2.25	0.22	0.28
70/30 CEM I/Fly ash	1.91	2.05	0.25	0.21
50/43/7 CEM I /GGBS/Silica fume	2.47	2.92	0.39	0.92

It can be noted that generally, an increase in crack width resulted in an overall increase in the chloride concentration and hence chloride penetration. There is also a significant difference in chloride concentration in the vicinity of the crack between those concretes made with 100% CEM I and those made using blended cements regardless of the crack width of cover depth.

(d) Effect of crack width on corrosion rate

There is no general agreement on the relationship between crack width and corrosion. Bentur *et al*. (1997) indicated that for two reinforced concrete specimens that differ only in crack width, the time required to initiate corrosion is shorter for one with wider cracks, but the corrosion rates are not significantly influenced by crack width. However, Beeby (1983) and Arya and Wood (1995) suggest that there is no direct relationship between crack width and corrosion rate. They consider more important factors to be the following:

(i) Crack properties, for instance whether the crack is active or dormant
(ii) Concrete and steel properties, whereby low permeability of the concrete will limit ionic transport, high moisture contents will limit oxygen ingress and increased strength leads to better bond and less slip at the steel-concrete interface, and
(iii) Service environment.

Pettersson and Jorgensen (1996) investigated the influence of crack width on corrosion process using different mix proportions and found that when the crack widths remained <0.4 mm, cover was shown to affect corrosion rates; however, for cracks >0.4 mm, it was shown that cover had negligible effect on corrosion.

Francois and Maso (1988) initiated a long-term study on reinforced concrete beams loaded in three-point flexure. The generated crack widths were between 0.05 and 0.5 mm. They concluded that chlorides penetrate rapidly through cracks.

Suzuki *et al*., (1990) support the argument of limited effect of crack width on corrosion rate, though they note some early-age differences in corrosion rate based on crack width, but these decrease with time due to crack healing. The w/b ratio was found to have a more significant impact on corrosion rate than crack width.

In a study by Scott (2004) using South African materials, different binder types (OPC, Slag and Silica fume) were used. Surface crack widths of 0.2 mm and 0.7 mm were introduced in the concrete specimens by the slipping of plain round bars. 5% NaCl solution was used while the w/b ratio was constant at 0.58. Two different concrete covers (20 mm and 40 mm) were used. From the study, it was concluded that binder type, crack width and concrete cover thickness all affect the corrosion rate of the steel. It was also found that for an OPC concrete, at a constant crack width, the decrease in the concrete cover results in a significant increase in corrosion rate compared to concrete made with blended cements. Generally, the corrosion rate increases as the concrete cover thickness decreases (Table 2.7). The same trend was observed for the 0.7 mm crack width using the same cover thicknesses of 20 mm and 40 mm.

The effect of concrete cover depth can therefore be deduced to have a profound effect on corrosion rate of OPC concretes, other factors being constant.

It can be depicted that for a constant concrete cover, increasing the surface crack width for a given concrete cover results in higher corrosion rates. This is expected because, at a constant cover, increasing the surface crack width results in a greater steel surface being exposed, assuming the crack is wedge-shaped. This raises serious concerns relating to corrosion rate inter-study comparisons that are done taking into consideration only the similarity in surface crack width and disregarding the influence of cover depth amongst other factors.

Table 2.7 : Influence of crack width and cover on corrosion rate

(Scott, 2004)

Binder type	*Corrosion rate (μA/cm^2)*			
	0.2 mm crack width		*0.7 mm crack width*	
	20 mm cover	*40 mm cover*	*20 mm cover*	*40 mm cover*
100 % CEM I (OPC)	2.65	1.20	3.23	1.48
50/50 GGBS/CEM I	0.39	0.35	0.51	0.53
30/70 Fly ash/CEM I	0.64	0.39	0.71	0.50
50/43/7 CEM I /GGBS/Silica fume	0.67	0.59	1.12	1.03

(e) Effect of crack frequency on corrosion rate

Crack frequency refers to the number of cracks present on the concrete surface per given length. Current theory of crack formation agrees that where many surface cracks exist in concrete, crack frequency (or *crack density*) is more important than crack width.

A study by Arya and Ofori-Darko (1996) confirmed this after conducting tests by varying the crack frequency from approximately 0-20 cracks per metre length. The equally spaced parallel-sided cracks had a constant width and depth of 0.3 mm and 40 mm respectively. A concrete cover of 42 mm was used for all the specimens. Two series of tests were conducted using two different NaCl concentrations of 3% and 5%. The concrete had a w/b ratio of 0.65. Figure 2.11 shows a plot of the cumulative mass loss of the reinforcement steel against time. It is clear that the corrosion rate increases with the increase in the crack frequency. They also concluded that while cracks may accelerate corrosion initiation, the subsequent influence of transverse cracks on corrosion rate may not be significant.

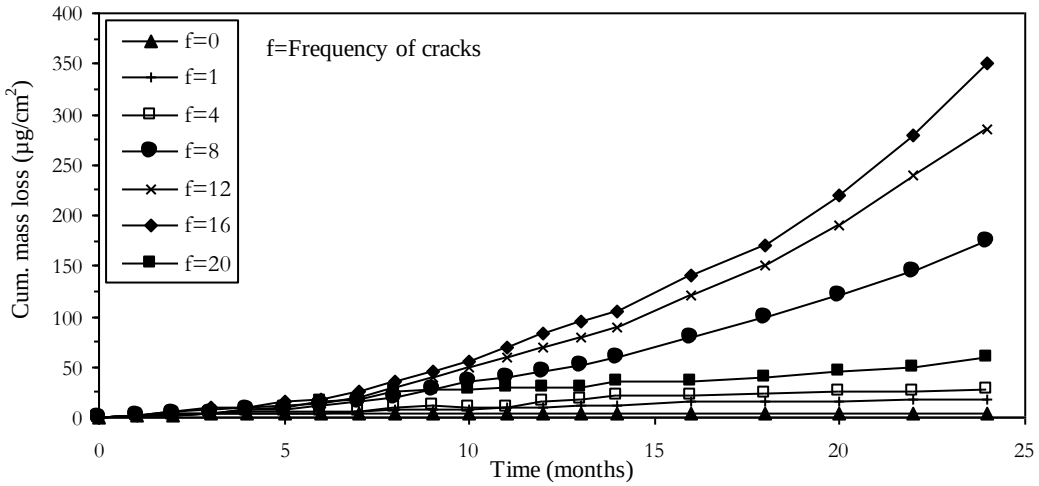

Figure 2.11: Effect of crack frequency on cumulative mass loss due to corrosion (Arya and Ofori-Darko, 1996)

The cumulative mass loss (Figure 2.11) gives an indication of the corrosion rate of the steel. It can therefore be concluded that the corrosion rate increases with increasing crack frequency. This can be attributed to the increase in the (a) permeability of the concrete hence ease of chloride ions ingress into the concrete and (b) total area of steel undergoing corrosion. It must be noticed that the specimens with the highest crack frequency of 20 did not correspond to the highest corrosion rate. The crack frequency of 16 may be the optimum under the given set of experimental conditions above which corrosion rate decreases.

(f) Effect of crack orientation on corrosion rate

Orientation of cracks with respect to reinforcement is an important factor influencing crack-induced corrosion. According to their orientation, cracks can be grouped as either longitudinal (along the line of the reinforcement) or transverse (across the reinforcement).

Longitudinal (or coincident) cracks can be induced by various mechanisms including plastic settlement, plastic shrinkage and bond failure. With regards to chloride-induced corrosion, this type of cracking is extremely dangerous, since chlorides, moisture, and oxygen can easily penetrate to the embedded steel and attack large areas of steel in the corrosion process.

In the case of transverse (or intersecting) cracks, the cathodic areas of reinforcement mostly occur in the crack-free regions. Therefore, moisture and oxygen that enter through the cracks do not significantly affect the rate of corrosion (Arya and Xu, 1995).

Longitudinal cracking has been found to be more likely to result in higher corrosion rates than intersecting cracks (Arya and Wood, 1995, Arya and Ofori-Darko, 1996, Bentur *et al.*, 1997). However, for concrete in service, transverse cracks are more frequent in tensile- stressed areas

of a RC structure than longitudinal cracks. The latter are more associated with corrosion cracks along the longitudinal reinforcement due to the large volume (or expansive nature) of corrosion products.

2.6.1.7 ***Effect of cyclic wetting and drying on corrosion rate***

Cyclic wetting and drying of concrete causes continuous moisture movement through concrete pores. This cyclic action accelerates durability problems by subjecting concrete to the accumulation of harmful materials such as sulphates, alkalis, acids, and chlorides.

Chloride ingress is also strongly influenced by the sequence and duration of cyclic wetting and drying. Specifically, the degree of dryness and therefore the surrounding drying conditions are very important (Hong and Hooton, 1999). The degree of drying influences the extent to which the chlorides travel into the concrete by capillary action. To investigate the effect of cycle period on chloride ingress into concrete, Hong and Hooton (1999) carried out experiments by subjecting concrete samples (made with w/b ratio of 0.4 and cured in a saturated $Ca(OH)_2$ solution for 28 days) to two wetting and drying regimes viz 1-day and 3-day cycle periods with 1.0 M NaCl solution at 23 ^{o}C for 120 days or 1 year . The results showed that both the duration of wetting/drying and the number of cycles affect the depth of chloride ingress into concrete (Figure 2.12 and Figure 2.13).

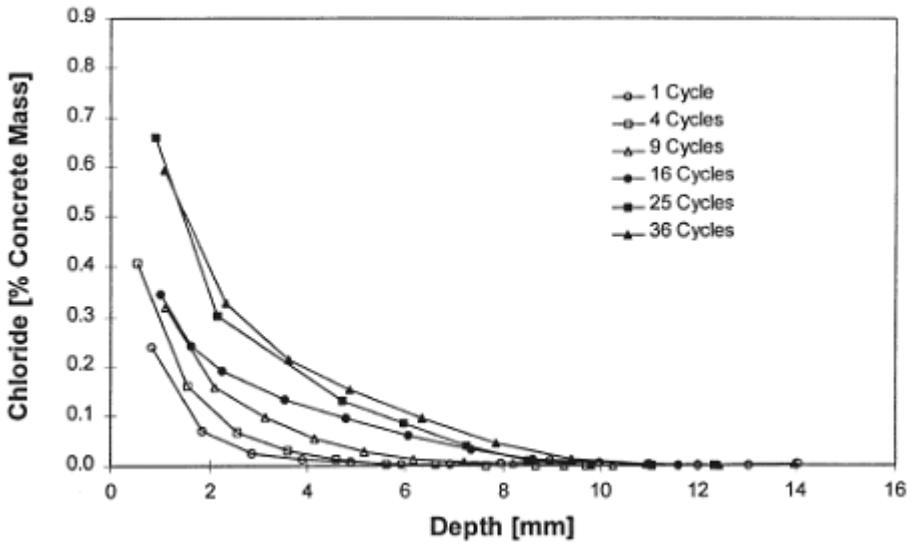

Figure 2.12: Chloride profiles for concrete with 25% slag, 1-day cycle for 120 days (Hong and Hooton, 1999)

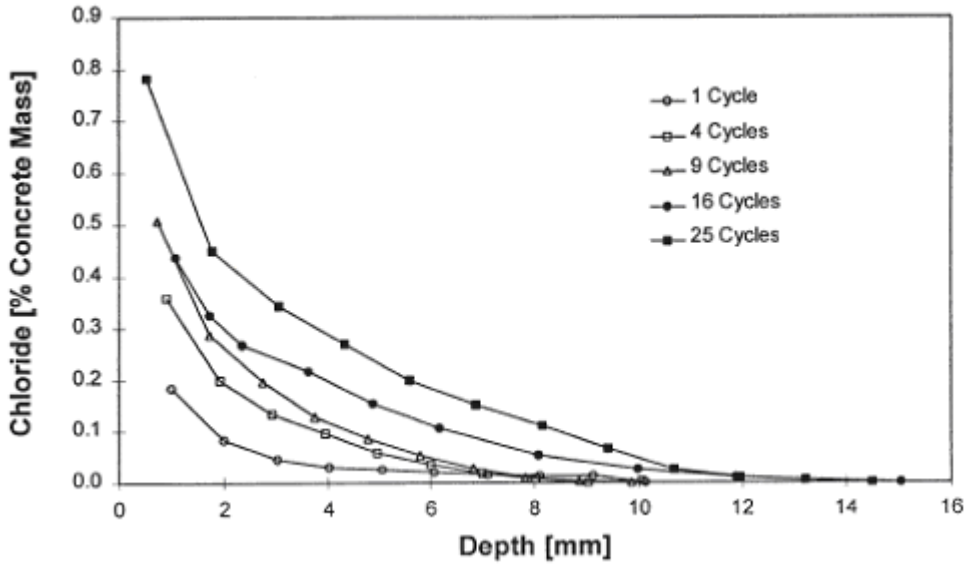

Figure 2.13: Chloride profiles for concrete with 25% slag, 3-day cycle for 120 days (Hong and Hooton, 1999)

From these figures, it is can be seen that a 3-day cycle results in a higher chloride concentration than a 1-day cycle. However, it is also clear that for a given cycle regime (1-day or 3-day), the chloride ion concentration at a given depth of the concrete cover increases with an increase in the number of cycles. It can therefore be concluded that both the cycling duration and the number of cycles affect chloride ingress into concrete keeping other factors constant.

Cyclic wetting and drying can increase the rate of corrosion in reinforced concrete structures as a result of two actions. First, cyclic wetting and drying concentrates ions, such as chlorides, and can increase the rate of corrosion by the evaporation of water during the drying phase, allowing oxygen ingress. Secondly, once chloride thresholds have been reached at the depth of the steel, drying of the concrete increases the availability of oxygen required for steel corrosion, because oxygen has a substantially lower diffusion coefficient in saturated concrete (Hong and Hooton, 1999). Concrete structures subjected to cyclic wetting and drying by seawater (tidal zone) are therefore more prone to deterioration by reinforcement corrosion than those permanently submerged (submerged zone).

2.6.1.8 ***Effect of sustained loading and loading history on corrosion rate***

Cracks increase in number, width and depth under the effect of sustained and/or cyclic loading. Cracks that are generated by sustained loads or overloads, or both, may influence the corrosion response of the reinforcing steel. The growth rate of cracks is considerably faster, and hence concrete may deteriorate more rapidly, under cyclic loading than under sustained

loading (Ahn and Reddy 2001). It has been observed that, under sustained loading, cracks grow in width but at a decreasing rate (ACI-224, 2001).

Yoon *et al*. (2000) studied the influence of pre-loading (or pre-cracking) and sustained loading on corrosion propagation using 100 x 150 x 1170 mm beam specimens made with w/b ratio of 0.5 and a concrete cover of 30 mm. The pre-loaded specimens were loaded to 45% and 75% of the ultimate flexural load and unloaded, while the specimens under sustained loading were loaded to 20, 45, 60 and 75% of the ultimate flexural load and the load sustained on the specimens during the corrosion tests. The respective load levels were maintained by checking beam deflections using linear variable displacement transducers (LVDTs). The specimens were subjected to a cycle of 4 days wetting and 3 days drying with 3% NaCl solution. The following conclusions were made:

- For both the sustained load and pre-loaded specimens, corrosion rate was higher in the specimens loaded to higher load levels e.g. specimens loaded to 75% of the ultimate flexural load had higher corrosion rates (measured in terms of steel mass loss) than those loaded to 45% of the ultimate flexural load (Figure 2.14)
- For the same loading level, specimens under sustained loading had higher corrosion rates than the pre-cracked ones (Figure 2.14).

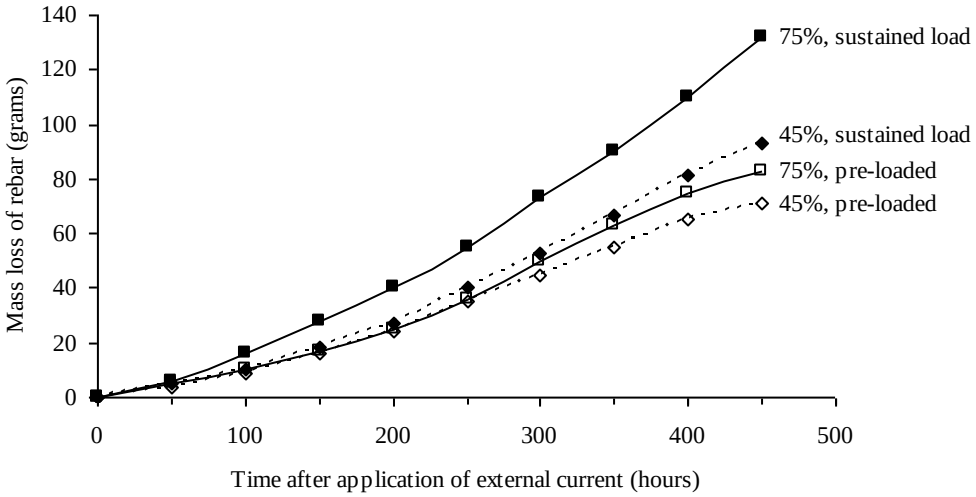

Figure 2.14: Effect of pre-loading and sustained loading on corrosion propagation (Yoon *et al*., 2000)

The high corrosion rates in the specimens under sustained loading and those at higher loading levels was attributed to increased number, size and interconnectivity of cracks which increase the penetrability of the concrete. The low corrosion rates in the pre-loaded specimens was attributed to cracks being closed or becoming smaller and less connected after unloading thus slowing down penetration of corrosion agents (chlorides and oxygen) and thus reducing

corrosion rate. Crack self sealing may also be an explanation to the low corrosion rates in the pre-loaded specimens but this was not explored in this study.

It can therefore be concluded that both the loading history and loading level play important roles in corrosion propagation.

2.6.1.9 ***Influence of concrete resistivity***

Electrical resistivity is an important physico-chemical property of concrete that affects a variety of its applications. It is a geometry independent material property which describes the electrical resistance of a material (Rilem TC 154-EMC, 2000). It is fundamentally related to the penetrability of fluids and diffusivity of ions through porous materials such as concrete (Marta and Jezierski, 2005).

In spite of the studies done on concrete resistivity, it is not yet possible to accurately predict the resistivity of a given concrete from knowledge of the respective constituents and mixture proportions alone. This is because the resistivity of concrete is affected by both intrinsic and extrinsic factors as will be seen.

Nevertheless, electrical resistivity can be used as an indirect measure of the probability of corrosion initiation and corrosion rate. A resistivity of less than 5 kΩ-cm can support very rapid corrosion of steel (Brown, 1980). If the electrolyte has high resistance to the passage of current, or if the concrete is dry and unable to support ionic flow, then corrosion will occur only at a very low rate. Corrosion can therefore be limited by increasing concrete resistivity.

The electrical resistivity of concrete may vary over a wide range, from 1 to 10^4 kΩ-cm. It is influenced by many factors including the binder type and content, w/b ratio, degree of pore saturation, type of aggregate, presence of salts such as chlorides, temperature and age of the concrete (Gjorv *et al*., 1977).

There are no generally accepted rules relating resistivity to corrosion rate. The relationship between concrete resistivity and corrosion rate is still a subject under study. However, a commonly used guide has been suggested for the interpretation of measurements of the likelihood of significant corrosion for non-saturated concrete as presented in Table 2.8 (Andrade and Alonso, 1996).

Table 2.8: Relationship between resistivity and corrosion risk (Andrade and Alonso, 1996)

Resistivity (kΩ-cm)	*Risk level*
> 100 - 200	Very low Corrosion rate even if chloride contaminated
50 - 100	Low corrosion rate
10 - 50	Moderate to high corrosion rate
< 10	Resistivity is not the controlling parameter

Further, the corrosion rate has been shown to be inversely proportional to the resistivity of concrete or directly proportional to its conductivity (Hunkeler, 2005):

$$i_{corr} \, \alpha \, \frac{1}{R_c} = \sigma_c \qquad (2.15)$$

where: i_{corr} = corrosion rate (A/cm^2)
R_c = concrete resistance (Ω)
σ_c = concrete conductivity

However, this is subject to a number of factors such as cover to reinforcement, degree of concrete water saturation, presence of cracks, presence of salt ions, w/b ratio etc. Therefore, resistivity must be analysed in conjunction with other factors influencing corrosion.

2.6.2 ***Prediction of corrosion propagation period***

The propagation period (t_p) defines the time necessary for sufficient corrosion to occur and cause unacceptable level of damage to the RC structure or element. The length of this period depends on the definition of *unacceptable damage* or an *acceptable limit state*. This level of damage will vary depending on the requirements of the owner and the nature or use of the structure. For example, the ACI committee 365 (2005) defines the propagation period as the *time to first repair*.

Consequently, the length of the propagation period depends principally on the corrosion rate, which in most cases is related to loss of steel cross sectional area, time to cracking, and gradual loss of steel/concrete bond (Andrade and Alonso, 1996). However, most service life prediction models do not explicitly account for these effects. The following sections will cover briefly some of the criteria used to predict the duration of the corrosion propagation period.

(a) Prediction based on loss of steel cross-sectional area

The design of a structure is dependant upon the various national codes which govern design and construction from one country to another but there is generally quite a large safety factor built into the calculations to accommodate variations in material properties, construction and loading. These safety factors can effectively accommodate a certain loss in cross sectional area which may be used to define the *acceptable damage*. Andrade and Alonso (1996) suggest a loss of cross sectional area between 5% and 25% to define the end of service life of the structure. This range seems to be a reasonable estimate for the end of a structure's service life, taking into account the inbuilt safety factors already mentioned.

The relationship between corrosion rate and loss of cross section is based on Faraday's Law (Stansbury and Buchanan, 2000):

$$m = \frac{MIt}{zF} \tag{2.16}$$

where: m = mass of metal entering solution (g)
M = atomic mass (g/mol)
I = corrosion current (A)
t = time (seconds)
z = valency of metal
F = Faraday's constant (96,500 A.s)

(b) Prediction based on time to corrosion-induced cracking

Corrosion cracks, unlike service cracks, run longitudinal with the steel and may allow for a significant acceleration of the corrosion rate as the steel is more directly exposed to the atmosphere and the ability of the cement extenders to provide protection is reduced. Thus the onset of corrosion-induced cracking may also provide a reasonable, though conservative, estimate to the end of a structure's life and can therefore be used to estimate the propagation period (Liu and Weyers, 1998).

Several models have been developed to predict the time to cracking, for example Bazant's physical-mathematical model (1979), Cady and Weyers' model (1983), Liu and Weyers' mathematical model (1998), and El Maaddawy and Soudki's mathematical model (2006)). Liu and Weyers' (1998) model is presented here as an example. It is related to the critical mass of corrosion products and corrosion rate and is given by the equation:

$$T_{cr} = \frac{W_{crit}^2}{2k_p} \tag{2.17}$$

where: T_{cr} = time to cracking (years)

W_{crit} = critical volume of rust products required to induce cracking

k_p = $0.098(1/\alpha)\pi D i_{corr}$

D = diameter of reinforcing

α = 0.57

i_{corr} = annual mean corrosion current density (mA/ft^2)

A detailed description of the model and its development can be found in Liu and Weyers (1998). The other time-to-cracking models mentioned can be found in the respective references.

The following sections will cover the various methods that can be used to assess corrosion, with a focus on chloride-induced corrosion.

2.7 ***Corrosion assessment***

The evaluation of the condition of corroding RC structures is normally a two-stage process involving both preliminary and detailed assessment. The preliminary assessment characterises the nature of the corrosion and gives guidance in planning a detailed measurement. It involves a visual inspection such as probing of cracks and spalls to see their extent. The detailed assessment will then confirm the cause and quantify the extent of corrosion. This stage will show the extent of damage that has occurred and the cause(s) of the damage. Table 2.9 lists some of the techniques that can be used for corrosion assessment and what they detect.

Table 2.9: Corrosion assessment techniques
(Heckroodt, 2002)

Classification	*Assessment*	*Detects*
Preliminary	– Visual inspection	– Surface defects such as cracks, rust stains, spalling
	– Half-cell potential	– Probability of corrosion (Electrochemical state of the steel)
	– Resistivity measurements	– Probability of corrosion
Detailed	– Carbonation depth	– Carbonation ingress
	– Chloride content	– Chloride ingress
	– Linear polarization	– Corrosion rate

2.7.1 ***Visual inspection***

Visual inspection is usually the first step in an investigation. The aim is to give a first indication of what is wrong and how extensive the corrosion damage is. For example, if the concrete is spalling, this can be used as a measure of extent of damage. However, visual inspection can only provide useful information when done in a rational and systematic manner. Classification of visual evidence of deterioration must be done objectively, following clear guidelines that define damage in terms of appearance, location and cause. Defects may be defined in terms of (Heckroodt, 2002):

- Cracks: caused by corrosion, temperature gradient, shrinkage or fatigue
- Joint deficiencies: joint spalls, upward movement, lateral movement, seal damage
- Surface damage: abrasion, rust stains, delaminations, popouts, spalls
- Changes in member shape: curling, deflection, settlement, deformation
- Textural features: blow holes, honeycombing, sand pockets, segregation

Visual survey should be followed up by testing to confirm the cause of corrosion (Rodriguez *et al*., 1994). It must also be noted that corrosion-induced structural deterioration is a gradual process with a commencement time not always obvious from external examination (Li *et al.*, 2008).

Visual inspection therefore only serves as an indication of an already ongoing corrosion process in the concrete. Moreover, it may come too late for cost-effective repairs because reinforcement corrosion damage only manifests itself at the surface after significant deterioration has occurred.

2.7.2 ***Half-cell potential measurement***

This is an electrochemical method (also referred to as *open circuit* or *corrosion potential*) and is currently one of the most widely used methods for the detection of the potential for steel reinforcement corrosion in concrete. The principle of this method is based on the measurement of the potential difference between the reinforcement and a reference electrode in the form of a half-cell (Rodriguez *et al.*, 1994, Broomfield *et al*., 2002). The technique is particularly useful because it can be utilized to evaluate the probability of corrosion before damage is evident at the surface of a RC structure.

The half-cell is a simple device consisting of an electrode and an electrolyte. The electrolyte is normally made from a soluble salt of the electrode metal i.e. the reference electrode is a piece of metal in a solution of its own ions, such as copper/copper sulphate ($Cu/CuSO_4$), Calomel (Hg/Hg_2C1_2) and silver/silver chloride (Ag/AgCl).

Half-cell potential (E_{corr}) measurement is based on the electrical and electrolytic continuity between the embedded steel, reference electrode on the concrete surface and the voltmeter. Electrical conduction between the reference electrode and the concrete is established by the transport of ions. This can be ensured by placing a wet sponge between the reference electrode and the concrete surface.

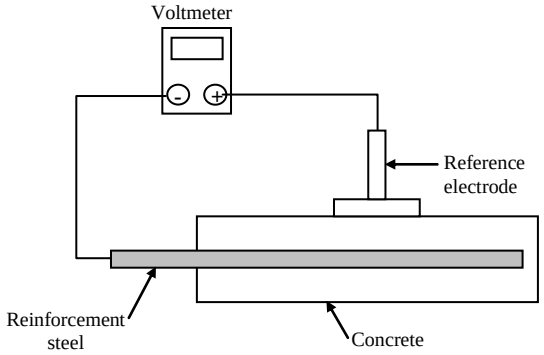

Figure 2.15: Schematic of half-cell potential measurement
(Broomfield *et al*., 2002)

The numerical value of the measured potential between the embedded steel and the reference electrode depends on the type of reference electrode used and the corrosion condition of the steel in the concrete. It is therefore important to quote the reference electrode being used for half-cell potential measurements. For site work, saturated $Cu/CuSO_4$ electrode is most robust and is sufficiently accurate, although errors may arise due to contamination of the concrete surface with copper sulphate. Calomel and silver chloride electrodes are used more in laboratory work due to their stability and robustness.

Half-cell potential measurements can be used to detect the likely corrosion state of corroding steel bars. The criteria for corrosion are illustrated in Table 2.10. It is important to note that HCP measurements only give an indication of the corrosion risk of steel and are linked empirically to the probability of corrosion.

Table 2.10: Criteria for corrosion of steel in concrete
(ASTM C876-91, 1999)

$Cu/CuSO_4$ electrode	*Ag/AgCl electrode*	*Likely corrosion condition*
> -200 mV	> -106 mV	Low (10% risk of corrosion)
-200 to -350 mV	-106 to -256 mV	Intermediate corrosion risk
< -350 mV	< -256 mV	High (>90% risk of corrosion)
< - 500 mV	< - 406 mV	Severe corrosion

2.7.3 Concrete resistivity measurement as a corrosion assessment criteria

The relationship between concrete resistivity and corrosion rate was covered in section 2.6.1.9 and will therefore not be reviewed here again. Concrete resistivity measurement techniques include the following:

(i) Single electrode technique
(ii) Two-probe technique
(iii) Four-probe (Wenner) technique

The Wenner technique is of interest in this study and will be briefly covered.

2.7.3.1 Four-probe (Wenner) resistivity measurement technique

The four-probe (Wenner) method is currently the most widely used technique for measurement of concrete resistivity. The apparatus consists of four electrodes equally spaced (Figure 2.16). A small current of low frequency is applied between the outer probes and potential drop measured between the inner probes (Millard *et al*., 1990). This approach eliminates any effects due to surface contact resistances.

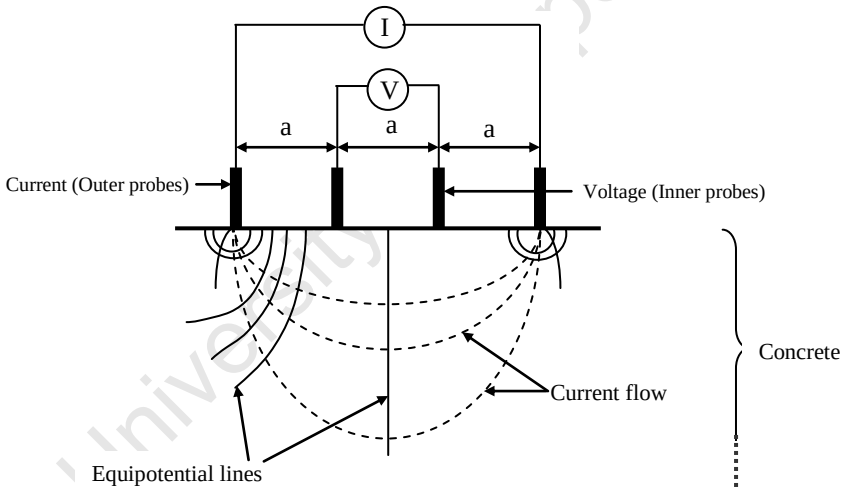

Figure 2.16: Schematic drawing of four-probe (Wenner) method resistivity measurement (Vienna, 2002)

The apparent resistivity (ρ) in Ω-cm may be expressed as:

$$\rho = \frac{2\pi aV}{I} \qquad (2.18)$$

where: V = voltage drop (Volts)
I = applied current (Amperes)
a = electrode spacing (cm)

One advantage of this technique over the two-probe arrangement is that it measures the resistivity of the concrete area between the inner probes which is a larger area than that of the probe tip. The influence of aggregate can therefore be avoided when the spacing between the inner electrodes exceeds the maximum size of the aggregate particles. This will yield a more reliable resistivity reading. A spacing of 50 mm is sufficient to give relatively accurate resistivity readings for most concrete structures (Millard, 1990).

Other factors which influence the resistivity measurement using the four-probe technique include (Whiting and Nagi, 2003):

(i) geometrical constraints
(ii) surface contact
(iii) concrete non-homogeneity
(iv) presence of steel reinforcing bars
(v) surface layer(s) having different resistivity than the bulk of the concrete and
(vi) ambient environmental conditions

A more detailed literature on these factors can be found in a study by Gowers and Millard (1999).

*2.7.4 **Linear polarization resistance (LPR) measurement***

The theory of linear polarization, also known as polarisation resistance, relies on the relationship between the half-cell potential of a piece of corroding steel and an external current or potential applied to it i.e. the reinforcing steel is perturbed by a small amount of potential from its equilibrium potential.

Three electrodes are used, viz counter/auxilliary, working, and reference electrodes. The counter electrode applies current or potential to the embedded steel reinforcement, which is the working electrode. The reference electrode (e.g. Ag/AgCl) measures the change in potential due to applied current or potential.

A schematic of the linear polarization set-up is shown in Figure 2.17. It has a control box (pulse generator) that applies the current or potential, a multimeter and a data logger that records the measurement, a half cell to measure the potential and its change and a counter electrode to pass the applied current/potential to the working electrode (corroding reinforcement) (Broomfield, 1997).

Measurements are performed by applying a potential either as a constant pulse (potentiostatic), or a potential sweep (potentiodynamic), and measuring the current response

using the data logger. Alternatively, a current pulse (galvanostatic) or a current sweep (galvanodynamic) can be applied, and the potential response measured.

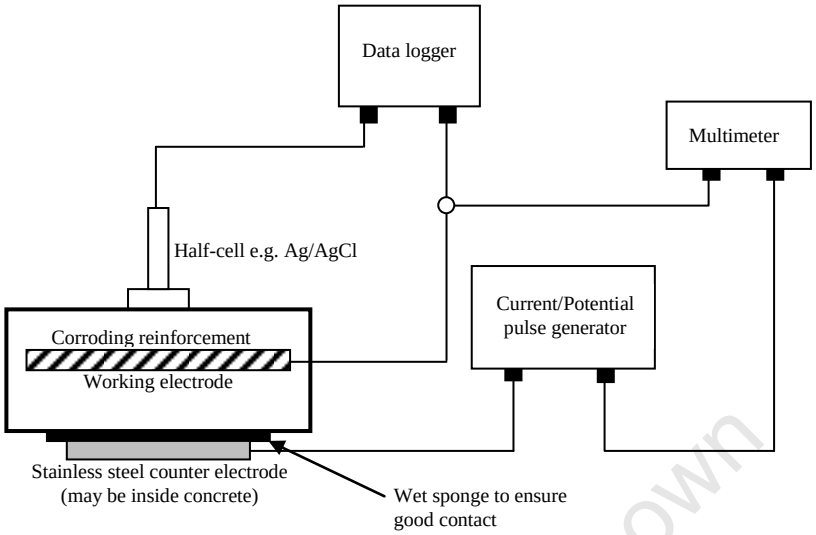

Figure 2.17: Schematic of polarisation resistance measurement device (Richardson, 2002)

In each case, the conditions are selected such that the shift in potential, ΔE falls within the linear Stern-Geary range of ±10 to 20 mV (Figure 2.18). As shown in Figure 2.18 there is an approximately linear region in the region of the open circuit/half-cell potential.

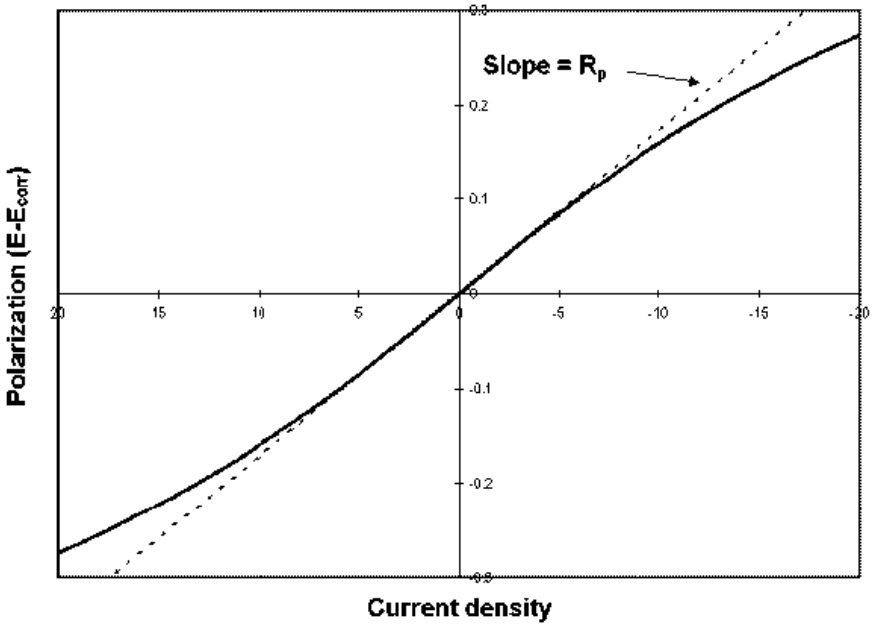

Figure 2.18: Linear polarisation curve (Stern and Geary, 1957)

The ratio of the applied potential to resulting current (ΔE/ΔI) is called the polarization resistance (Rp) and is inversely proportional to the corrosion current, I_{corr}, (Stern and Geary, 1957):

$$I_{corr} = \frac{B}{R_p} \tag{2.19}$$

where:

R_p = change in potential (ΔE)/change in current (ΔI)

B = a constant parameter (Stern-Geary constant) varying from 26 to 52mV depending on the passive (52 mV) or active (26 mV) condition of the steel.

The corrosion rate (in terms of current density per given steel surface area) can be deduced as follows:

$$\text{Corrosion rate} = \frac{I_{corr}}{A}\ (\mu A/cm^2) \tag{2.20}$$

Where A is the polarized steel surface area (A=ЛDl cm^2 where D is the diameter of the steel and l is the length of the polarized steel area).

The major limitation of this technique is difficulty in knowing the actual surface area of steel that is polarized by the applied potential, or the area which is actively corroding. Therefore, the corrosion is generally considered to be uniform over the polarized area and the measured corrosion current is divided by the estimated polarized area to give an average corrosion rate.

An additional limitation is that this is an instantaneous corrosion rate and (*a*) gives no indication of how long corrosion has been going on or (*b*) how the corrosion rate varies with time and ambient conditions. A fundamental drawback of these measurements is that artificial corrosion damage and rebar surface changes can be induced at relatively high polarization levels.

Despite this, the LPR technique is popular for measuring corrosion rate because: (*i*) it is a non-destructive technique; (*ii*) it is simple to apply and (*iii*) it usually needs only a few minutes for corrosion rate determination.

Classification of measured corrosion rates as proposed by Rodriugiez *et al.,* (1994) is given in Table 2.11.

Table 2.11: Interpretation of measurements
(Rodriugiez *et al.*, 1994)

Current density ($\mu A/cm^2$)	*Corrosion state*
< 0.1 - 0.2	Passive condition
0.2 - 0.5	Low to moderate
0.5 - 1.0	Moderate to high
> 1.0	High

To overcome the problem of accurate determination of the actual area of steel polarised (especially for on-site application), commercial LPR devices such as GECOR-6 and GECOR-8 make use of a guard ring around the counter/auxilliary electrode to constrain the applied electric field from the counter electrode. This ensures that a measurement is taken from a defined area of steel and prevents gross errors in the estimation of area of steel (Figure 2.19).

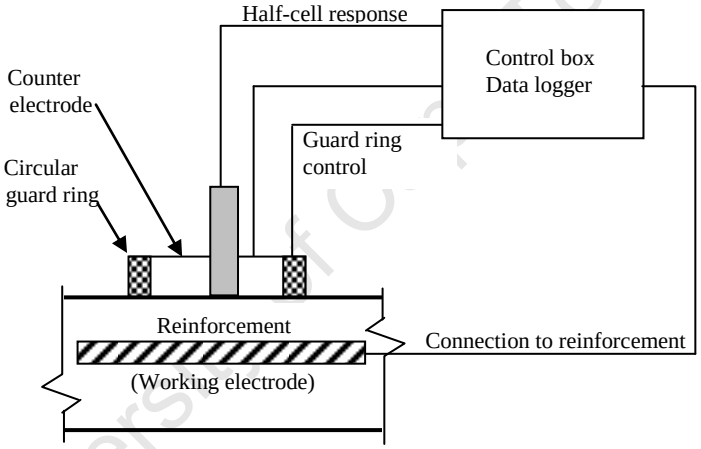

Figure 2.19: Schematic of polarisation resistance measurement with a guard-ring incorporated
(Modified from Richardson, 2002)

2.7.5 ***Coulostatic technique***

The coulostatic technique is essentially a galvanostatic LPR technique which measures the relaxation of the potential after a small fixed current (ΔI) is applied to the reinforcing steel for a known duration in the order of milliseconds. Corrosion rates are related to a time constant describing the potential decay (ΔE) induced by a small potential (10-20 mV) disturbance.

A high corrosion current will lead to a rapid decay of the potential transient whereas with a lower corrosion current the decay of the potential after the perturbation will take a longer time. The potential transient is described by the equation (Glass, 1995, Hassanein *et al.*, 1998):

$$n_t = n_o \exp\left(\frac{-t}{\tau_c}\right) \tag{2.21}$$

where: n_t = potential shift at time t
n_o = initial potential shift
τ_c = time constant

The polarization resistance R_p is then obtained from the time constant and capacitance (C) information, with q_s being the applied charge density.

$$\tau_c = CR_p \tag{2.22}$$

$$C = \frac{q_s}{n_o} \tag{2.23}$$

Potential measurements are taken 0.1 seconds after the termination of the charge which allows many of the very early transients to dissipate. The remaining early additional transients are unlikely to significantly effect the corrosion rate measurements as potential readings are taken for at least 30 seconds thus the overall shape of the curve and the resulting equation are still valid.

The duration of the charge has been shown by Glass (1995) to have an effect on the shape of the relaxation transient with longer perturbations resulting in progressively flatter relaxation curves (Figure 2.20), resulting in under-estimation of polarisation resistance (R_p) which then translates to over-estimation of the corrosion rate. The flatter relaxation curves may be caused by an effective shift in time zero leading to the loss of the fast components of the transient related to the charging process as well as significant mass transfer occurring during the perturbation period which then affects the subsequent decay.

The advantages of the coulostatic method include:

(i) A very small perturbation is applied during which its effects on diffusion process can be minimised by keeping the perturbation period short
(ii) No need to compensate the result for the effects of the electrolyte
(iii) The determination of the interfacial capacitance as part of the measurement
(iv) Its suitability for low frequency work when compared with impedance measurements
(v) The insensitivity of the time constant to the steel surface area

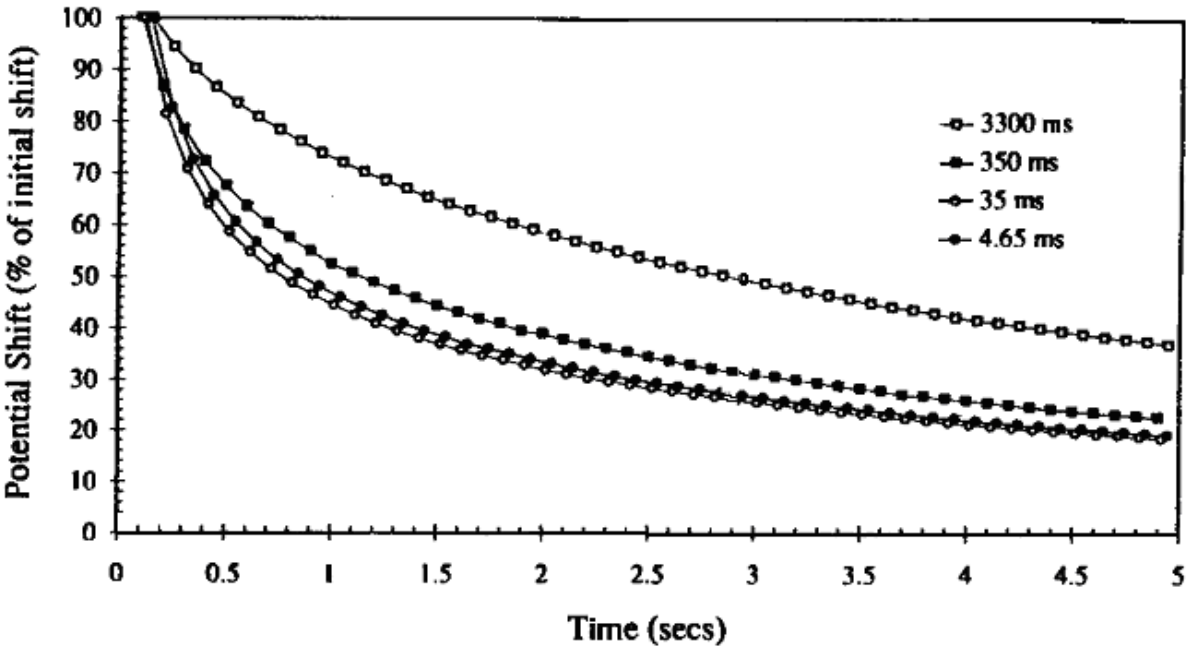

Figure 2.20: Effect of perturbation duration on shape of potential transients (Glass 1995)

The disadvantages include:

(i) The long time required to determine the transient compared to direct polarisation resistance measurements particularly for passive steel
(ii) Determination of the actual area of the embedded steel that is corroding
(iii) It neither gives an indication of how long corrosion has been going on nor how the corrosion rate varies with time and ambient conditions.

*2.7.6 **Cyclic potentiodynamic polarization***

This is a non-destructive technique that provides information on the corrosion rate, corrosion potential and susceptibility to pitting corrosion of the metal in the test environment (in this case concrete), as well as information about the expected behaviour of the steel should its potential be changed, for example, due to exposure to stray currents, coupling with other metals, or the surrounding concrete becoming anaerobic (Hansson *et al*., 2007).

In this method, the potential of the specimen is changed continuously or in steps, while the resulting current is monitored. Like most electrochemical techniques, cyclic polarization is carried out with three electrodes viz, a working electrode (the reinforcing steel), a counter electrode and a reference electrode.

Cyclic polarization is most useful in the laboratory but has the same limitation of LPR of knowing the actual polarized area of the steel, as well as taking a longer time to perform. It is the test method adopted in the ASTM standard G61-86 (2003).

2.8 ***Closure***

The two major corrosion-inducing mechanisms are carbonation and chloride-induced corrosion. However, chloride-induced corrosion still remains one of the main durability-threatening mechanisms for reinforced concrete (RC) structures exposed to aggressive environments such as marine. This chapter has covered chloride-induced corrosion at length because it is the focus of this study.

The corrosion process in RC is divided into two main stages i.e. initiation and propagation stages. For chloride-induced corrosion, the initiation period depends on the chloride threshold level which varies with binder type but it is conventionally taken to be 0.4% total chlorides by mass of binder. The presentation of chloride threshold level as total chlorides is the most common approach to stating the chloride threshold level but other approaches such as free chlorides and the Cl^-/OH^- ratio are also used.

The mechanism of chloride-induced corrosion in reinforced concrete is still not well understood especially with respect to the destruction of the passive layer (γ-Fe_2O_3) protecting the steel in an alkaline concrete medium. There have been a number of suggestions by different authors but a general conclusion has not been reached. It is however realised that chloride-induced corrosion initiation not only depends on the breakdown of the passive film, but also on the propagation of this initially localised action to produce a more sustained process.

Several factors have been mentioned to affect the corrosion process in steel RC. The use of mineral extenders, concrete cover, moisture content of the concrete, temperature, applied stress and strain, w/b ratio and the presence of cracks are some of these factors. The influence of ground slag, cracks, w/b ratio and cover depth have been covered at length in this chapter mainly because they are of interest in this study. With typical replacement levels of between 35-65%, ground slag has been found to be of benefit with regard to mitigating chloride-induced corrosion. One of the main benefits is its ability to substantially reduce the pore sizes and cumulative pore volume of hardened concrete resulting in a more impermeable and durable concrete. The use of slag also results in significant chloride binding, depending on the replacement level. Chloride binding effects of ground slag results in a delay in the corrosion initiation due to the reduction in the free chlorides in the concrete pore solution.

The influence of concrete cover (thickness, quality and condition) and the presence of surface cracks in the concrete are also important. Corrosion rate has been found to be inversely related to the depth of concrete cover, with high concrete cover resulting in longer time to corrosion initiation. This has been attributed to the longer travel paths for the corrosive

species to reach the embedded steel level in the concrete. However, concrete resistivity and oxygen availability may influence corrosion rate by affecting the cathodic reaction.

Cracking significantly increases concrete penetrability and has been mentioned by different authors to have varied effects on the corrosion initiation and progress, with some suggesting that they shorten the time to corrosion initiation while others say otherwise. Some studies have also concluded that concrete quality is more influential than the crack width. The controversy surrounding the influence of cracks on corrosion may be as a result of varied experimental testing methods and specimen preparation e.g. concrete quality (binder type, w/b ratio), how the cracks were induced, etc. A crack width of 0.4 mm is generally taken as a conservative value in many design codes and specifications to limit chloride-induced corrosion.

Factors such as w/b ratio, moisture content and temperature affect the corrosion rate in RC structures although in different magnitudes and up to certain limits. For example an increase in the w/b ratio results in higher concrete penetrability. This in turn encourages faster chloride ion penetration into the concrete to the steel level resulting in an increased corrosion rate.
Cyclic wetting and drying of the concrete affects corrosion rate, with high corrosion rates being recorded as the drying period is increased relative to the wetting period. The corrosion rate has also been reported to be proportional to the number of cycles the concrete is subjected to the wetting/drying regime.

Several techniques may be used to assess the corrosion process in RC structures or elements. These techniques include visual inspection, chloride content measurement, half-cell potential measurement, concrete resistivity measurement and electrochemical techniques such as the linear polarisation methods (LPR). This chapter focused mainly on methods used for chloride-induced corrosion. Electrochemical methods are today the most popular used to assess chloride-induced corrosion despite the limitations they have. This has been partly because they are quick to carry out both in the laboratory and in the field. The most common of these methods are the linear polarisation resistance (LPR) techniques such as the coulostatic technique, which was adopted in this study. A drawback to the LPR techniques in the accurate determination of the actual area of steel polarised. An improvement to the LPR methods to tackle this problem has been to include a guard ring to limit the extent of the current pulse to a specific area. Instruments with the guard ring incorporated such as the GECOR are commercially available.

The next chapter will cover the experimental details and methods used in this study.

2.9 ***References***

ACI Committee 224R-01, (2001), Control of cracking in concrete structures, *American Concrete Institute*.

Aldea, C. M., Shah, S. P. and Karr, A., (1999), Permeability of cracked concrete, *Materials and Structures*, (32), June, pp. 370-376.

Alexander, M. G. and Mindess, S., (2005), *Aggregates in Concrete*, published by Taylor and Francis.

Alonso, C., Castellote, M., Andrade, C., (2002), Chloride threshold dependence of pitting potential of reinforcements, *Electrochimica Acta* ,47, pp. 3469-3481.

Alonso, C., Andrade, C., Castellote, M. and Castro, P., (2000), Chloride threshold values to depassivate reinforcing bars embedded in a standardized OPC mortar, *Cement and Concrete Research*, 30(7), pp. 1047-1055.

Andrade, C., (1993), Calculation of Chloride Diffusion Coefficients in Concrete from Ionic Migration Measurements, *Cement and Concrete Research*, 23(3), pp. 724-742.

Andrade, C. and Alonso, C., (1996), Corrosion Rate Monitoring in the Laboratory and on-Site, *Construction and Building Materials*, 10(5), pp. 315-328.

Andrade, C., Polder, R. and Besheer, M., (2007), Non-destructive methods to measure ion migration, Chapter five, *RILEM TC 189-NEC: State-of-the-art report*, Non-destructive evaluation of the penetrability and thickness of the cover, pp. 91-112.

Arya, C. and Ofori-Darko, F. K., (1996), Influence of crack frequency on reinforcement corrosion in concrete, *Cement and Concrete Research*, 26(3), pp. 333-353.

Arya, C. and Wood, L., (1995), The relevance of cracking in concrete to corrosion of reinforcement, *Concrete Society*, Technical report No. 44.

Arya, C. and Xu, Y., (1995), Effects of cement type on chloride binding and corrosion of steel in concrete, *Cement and Concrete Research*, 25(4), pp. 893-902.

ASTM C876-91, (1999) Standard test method for half-cell potentials of uncoated reinforcing steel in concrete, ASTM.

ASTM G61-86, (2003) Standard test method for conducting cyclic potentiodynamic polarisation measurements for localised corrosion susceptibility of Iron, Nickel- or Cobalt-based alloys.

Bakker, R.F.M., (1983), Permeability of blended cement concretes, *Proceedings of the CANMET/ACI First International conference on the use of Fly ash, Silica fume, Slag and other mineral by-products in concrete*, pp. 589-605.

Bazant, Z. P., (1979), Physical model for steel corrosion in concrete sea structures – application, *ASCE Structural Division Journal*, 105(6), pp. 1155-1166.

Beeby, A., (1983), Cracking, cover and corrosion of reinforcement, *Concrete International*, February, pp. 35-40.

Bentur, A., Diamond, S. and Berke, N., (1997), *Steel corrosion in concrete, Fundamentals and Civil Engineering Practice*, London: E & FN Spon, pp. 41-43.

Bockris, J., Conway, B., Yeager, E. and White, R. ed., (1981), Comprehensive treatise of electrochemistry, *Electrochemical Materials Science*, Vol. 4, Plenum Press: New York.

Boddy, A., Bentz, E., Thomas, M. D .A. and Hooton, R. D., (1999), An overview and sensitivity study of a multi-mechanistic chloride transport model, *Cement and Concrete Research*, (29), pp.827-837.

Breysse, D. and Gerard, B., (1997), Transport of fluids in cracked Media, *RILEM report 16* – Barriers to organic and contaminating liquids, ed. Reinhardt H. W., published by E & FN SPON, London, pp. 123-153.

Broomfield, J. P., (1997), *Corrosion of Steel in Concrete: Understanding, Investigation and Repair*, London, UK: E & FN Spon.

Broomfield, J. P., Davies, K., Hladky, K., (2002), The use of permanent corrosion monitoring in new and existing reinforced concrete structures, *Cement & Concrete Composites*, (24), pp. 27-34.

British Standards Institute BS 5400-4, (1990), Code of practice for design of Concrete Bridges.

British Standards Institute BS 8110-1, (1997), *Structural use of concrete* - Part 1: Code of practice for design and construction.

Buenfeld, N. R., Shurafa-Daoudi, M. T. S., and McLoughlin, I. M., (1997), Chloride transport due to wick action in concrete. In Nilsson L. O., and Olliver J. P., *Proceedings of RILEM international workshop on chloride penetration into concrete*, Paris: RILEM.

Cady, P. D. and Weyers, R. E., (1983), Chloride penetration and the deterioration of concrete bridge decks, *Cement, Concrete & Aggregate*, 5(2), pp. 81-87.

Castellote, M., Alonso, C., Andrade, C., Castro, P., and Echeverrõ, M., (2001), Alkaline leaching method for the determination of the chloride content in the aqueous phase of hardened cementitious materials, *Cement and Concrete Research*, 31, pp. 233-238.

Chrisp, T. M., McCarter, W. J., Starrs, G. , Basheer, P. A. M. and Blewett, J., (2002), Depth-related variation in conductivity to study cover-zone concrete during wetting and drying, *Cement and Concrete Composites*, 24, pp. 415-426.

Daigle, L., Lounis, Z., Cusson, D., (2004), Numerical prediction of early-age cracking and corrosion in high performance concrete bridges – Case study; *Proceedings of Annual conference of the Transportation Association of Canada Innovations in Bridge Engineering*, Québec city, Québec.

DuraCrete, (1998), Probabilistic performance based durability design: modelling of degradation, *DuraCrete project document*, BE95-1347/R4-5, The Netherlands.

Du Preez, A. A. and Alexander, M. G., (2004), A site study of durability indexes for concrete in marine conditions, Materials and Structures, 37, pp. 146-154.

Edvardsen, C., (1999), Water permeability and autogenous healing of crack in concrete, *ACI Materials Journal*, 96(4), pp. 448-454.

El Maaddawy, T. and Soudki, K., (2006), A model for prediction of time from corrosion initiation to corrosion cracking, *Cement & Concrete Composites*, 29(3), pp. 168-175.

Elsener, B., Zimmermann, L. and Böhni, H., (2003), Non destructive determination of the free chloride content in cement based materials, *Materials and Corrosion*, 54, pp. 440-446.

Flis, J., Sehgal, A., Li D., Young, Tai K., Sabotl, S., Pickering, H., Osseo- Asare, K., Cady, P., (1993), Condition evaluation of concrete bridges relative to reinforcement corrosion: Method for measuring corrosion rate of reinforcing steel, Vol. 2. SHRP-S-324, *National Research Council*. Washington, D.C.

Foley, R., (1970), Role of the Chloride Ions in Iron Corrosion, *Corrosion*, 26(2), pp. 58-70.

Francois, R., and Maso, J. C., (1988), Effect of damage in reinforced concrete on carbonation or chloride penetration, *Cement and Concrete Research*, 18, pp. 961-970.

Frederiksen, J. M., Nilsson, L. O., Sandberg, P., Poulsen, E., Tang, L., and Andersen, A., (1997), A system for estimation of chloride ingress into concrete, Theoretical background, *HETEK report* No. 83, The Danish Road Directorate.

GECOR, GEOCISA, Madrid, Spain, http://www.geocisa.com.ingteyes/eindex.htm.

Gerard, B. and Marchand, J., (2000), Influence of cracking on the diffusion properties of cement-based materials, Part 1: Influence of continuous cracks on the steady-state regime, *Cement and Concrete Research*, 30(1), pp. 37-43.

Gjorv, O. E., Vennesland, O. and E1-Busaidy, A. H. S., (1977), Electrical resistivity of concrete in the oceans, *9th annual offshore technology conference*, Houston, paper 2803, pp. 581-588.

Glass, G. K., (1995), An assessment of the coulostatic method applied to the corrosion of steel in concrete, *Corrosion Science*, 37(4), pp. 597-605.

Glass, G. K. and Wang Y. and Buenfeld, N.R., (1996), An investigation of experimental methods used to determine free and total chloride contents, *Cement and Concrete Research*, 26, pp. 1443-1449.

Glass, G. K. and Buenfeld, N. R., (1997), Presentation of the chloride threshold for corrosion of steel in concrete, *Corrosion Science*, 39(5), pp. 1001-1013.

Glass, G. K., Hassanein, N. M. and Buenfeld, N. R., (1997), Neural network modelling of chloride binding, *Magazine of Concrete Research*, 49, pp. 323-335.

Glass, G. K., Reddy, B. and Buenfeld, N. R., (2000), The participation of bound chloride in passive film breakdown on steel in concrete, *Corrosion Science*, 42(11), pp. 2013-2021.

Gowers, K. R. and Millard, S. G., (1999), Measurement of concrete resistivity for assessment of corrosion severity of steel using Wenner technique, *ACI Materials Journal*, 96(5), pp. 536-542.

Hansson, C. M., Poursaee, A., and Jaffer, S. J., (2007), Corrosion of reinforcing bars in concrete, *Portland Cement Association*.

Hassanein, A., Glass, G. and Buenfled, N., (1998), The use of small electrochemcial perturbations to assess the corrosion of steel in concrete, *NDT and E International*, 31(4), pp. 265-272.

Hawkins, C. and Mckenzie, M., (1996), Environmental effects on reinforcement corrosion rates, *Proceedings of the fourth international symposium on corrosion of reinforcement in concrete construction*, pp. 166-175.

Heckroodt, R. O., 2002, *Guide to deterioration and failure of building materials*, published by Thomas Telford Ltd, 1 Heron Quay, London E14 4JD.

Hong, K. and Hooton, R. D., (1999), Effects of cyclic chloride exposure on penetration of concrete cover, *Cement and Concrete Research*, 29, pp. 1379-1386.

Hunkeler, F., (2005), *Corrosion in reinforced concrete structures*, Ed. Hans B., published by Woodhead publishing limited, Abington Hall, Abington Cambridge CBI 6AH, England, pp. 1-45.

Ismail, M., Toumi, A., François, R. and Gagné, R., (2004), Effect of crack opening on the local diffusion of chloride in inert materials, *Cement and Concrete Research*, 34(4), April, pp. 711-716.

Jaul, W. C. and Tsay, D. S., (1998), A study of the basic engineering properties of slag cement concrete and its resistance to seawater corrosion, *Cement and Concrete Research*, 28 (10), pp. 1363-1371.

Kim, A. T. and Stewart, M. G., (2000), Structural reliability of concrete bridges including improved chloride-induced corrosion models, *Structural Safety*, 22(4), pp. 313-333.

Kropp, J., (1995), Performance criteria for concrete durability: state of the art report, *RILEM Technical Committee 116-PCD*, published by Taylor & Francis.

Kropp, J. and Alexander, M. G., (2007), Transport mechanisms and reference tests, *chapter two, RILEM TC 189-NEC: state-of-the-art report*, Non-destructive evaluation of the penetrability and thickness of the cover, pp. 13-34.

Lambert, P., Page G. L. and Vassie P. R., (1991), Investigations of reinforcement corrosion, Electrochemical monitoring of steel in chloride-contaminated concrete, *Materials and Structures*, 24, pp. 351-358.

Leek, D. S. and Poole, A. S., (1990), The Breakdown of the passive film on high yield mild steel by chloride ions, *Corrosion of Reinforcement in Concrete*, Society of Chemical Industry, Elsevier, London, pp. 65-73.

Leng, F., Feng, N. and Lu, X., (2000), An experimental study on the properties of resistance to diffusion of chloride ions of fly ash and blast furnace slag concrete, *Cement and Concrete Research*, 30, pp. 989-992.

Li, C. Q., Yang Y. and Melchers, R., (2008), Prediction of reinforcement corrosion in concrete and its effects on concrete cracking and strength reduction, *ACI Materials Journal*, 105(1), pp. 3-10.

LIFE-365, Service life prediction model (2005), Computer program for predicting the service life and life-cycle costs of reinforced concrete exposed to chlorides, *ACI Committee 365*.

Liu, Y. and Weyers, R. E., (1998), Modelling the time-to-corrosion cracking in chloride contaminated reinforced concrete structures, *ACI Materials Journal*, 95(6), pp. 675-681.

Luoa, R., Caib, Y. and Wang, C., Huanga, X., (2003), Study of chloride binding and diffusion in GGBS concrete, *Cement and Concrete Research*, 33 (1), pp.1-7.

Mackechnie, J. R., (1996), Predictions of reinforced concrete durability in the marine environment, *PhD Thesis*, University of Cape Town.

Mackechnie, J. and Alexander, M. G., (1996), Marine exposure of concrete under selected South African conditions, *Proceedings of 3rd ACI/CANMET Int. conference on the performance of concrete in marine environment*, St. Andrews, Canada, pp. 205-216.

Mackechnie, J. R., (2001), Predictions of reinforced concrete durability in the marine environment, *Research monograph No. 1*, Department of Civil Engineering, University of Cape Town.

Mackechnie, J. R. and Alexander, M. G., (2001), Repair principles for corrosion-damaged reinforced concrete structures, *Research monograph No. 5*, Department of Civil Engineering, University of Cape Town.

Mackechnie, J. R., Alexander, M. G. and Jaufeerally, H., (2003), Structural and durability properties of concrete made with Corex slag, *Research monograph No. 6*, Department of Civil Engineering, University of Cape Town.

Mangat, P., Khatib, J. and Molloy, B., (1994), Microstructure, chloride diffusion and reinforcement corrosion in blended cement paste and concrete, *Cement and Concrete Composites*, 16, pp. 73-81.

Marsavina, L., De Schutter, G., Audenaert, K., Marsavina, D. And Faur, N., (2007), The influence of cracks on chloride penetration in concrete structures. Part II - Numerical simulation, The International *RILEM Workshop on Transport Mechanisms in Cracked Concrete*, Ghent, Belgium, 3-7 September 2007.

Marta, K-K. and Jezierski, W., (2005), Evaluation of concrete resistance to chloride ion penetration by means of electrical resistivity monitoring, *Journal of Engineering Management*, 11(2), pp. 109-114.

McCarter, W. J. and Watson, D., (1997), *Proceedings of the Institute of Civil Engineers*: Structures and Buildings, 22 (2).

Melchers, R. E. and Li, C. Q., (2006), Phenomenological modelling of reinforcement corrosion in marine environments, *ACI Materials Journal*, 103(1).

Millard, S. G., Ghassemi, M. H, Bugey, J. Jafar M. I., (1990), Assessing the electrical resistivity of concrete structures for corrosion durability studies, corrosion of reinforcement in concrete (Eds.: Page, Treadaway, Bamforth), Elsevier, London, pp. 303-313.

Mohamed, B., Sakai, K., Banthia, N., and Yoshida, H., (2003), Prediction of chloride ions ingress in uncracked and cracked concrete, *ACI Materials Journal*, 100(1), pp. 38-48.

Nanukuttan, S. V., Basheer, L., McCarter, W. J., Robinson, J., and Basheer, P. A. M., (2008), Full-scale marine exposure tests on treated and untreated concretes - Initial 7-year results, *ACI Materials Journal*, 105,(1), pp. 81-87.

Nejadi, S., (2005), Time dependent cracking and crack control in reinforced concrete structures, *PhD Thesis*, University of New South Wales, Sydney Australia.

Neville, A. M., (1996), *Properties of concrete*, 4th Ed., Longman, New York.

Neville, A. M., (1998), Concrete cover to reinforcement – or cover up?, *Concrete International*, 20(11), pp. 25-29.

Neville, A. M., (2002), Autogenous healing – A concrete miracle?, *Concrete International*, November issue, pp. 76-82.

Nilssson, L. O., Poulsen, E., Sandberg, P., Sorensen, H. E. and Klinghoffer, O., (1996), Chloride penetration into concrete, state-of-the-art, transport processes, corrosion initiation, test methods and prediction models, *HETEK Report No. 53*.

Pal, S. C., Mukherjee, A. and Pathak, S. R., (2002), Corrosion behaviour of reinforcement in slag concrete, *ACI Materials Journal*, 99(6), pp. 1-7.

Park, R. and Pauley, T., (1975), *Reinforced concrete structures*, John Wiley and Sons, New York.

Parrott, L. J., (1987), A review of carbonation in reinforced concrete, *Cement and Concrete Association*, United Kingdom, Waxham Springs, Slough.

Paulsson, J. T. and Johan, S., (2002), Estimation of chloride ingress in uncracked and cracked concrete using measured surface concentrations, *ACI Materials Journal*, 99(1).

Perez, B. M, Zibara, H. and Hooton, R. D., (2000), A study of the effect of chloride binding on service life predictions, *Cement Concrete Research*, 30(8), pp. 1215–1223.

Pettersson, K., (1995), Chloride threshold value and the corrosion rate in reinforced concrete, *Proceedings of Nordic Seminar*, Lund.

Pettersson, K. and Jorgensen, O., (1996), The effect of cracks on reinforcement corrosion in high-performance concrete in a marine environment, *Proceedings third ACI/CANMET Int. conference on the Performance of Concrete in Marine Environment*, St. Andrews by-the Sea, Canada, pp. 185-200.

Rilem TC 154-EMC, (2000), Electrochemical techniques for measuring metallic corrosion, *Materials and Structures*, (33), pp 603-611.

Richardson, M. G., (2002), *Fundamentals of durable concrete, modern concrete technology*, published by Spon Press, London.

Rodriguez, P., Ramirez and Bonzalez, E J. A., (1994), Methods for studying corrosion in reinforced concrete, *Magazine of Concrete Research*, 46(167), pp. 81-90.

Rodriguez, O. G., (2001), Influence of cracks on chloride ingress into concrete, *MSc. Thesis*, University of Toronto, Graduate Department of Civil Engineering.

Sageus, A. A, Kranc, S. C., (1998), Computation of corrosion distribution of reinforcing steel in cracked concrete, *Proceedings of the international conference on corrosion and rehabilitation of reinforced concrete structures*, Orlando, Florida, US: University of South Florida, pp. 1-12.

Salvarezza, R., Videla, H. and Arvia, A., (1982), The electrodissolution and passivation of mild steel in alkaline sulphide solutions, *Corrosion Science*, 22(9), pp. 815-829.

Samaha, H. R. and Hover, K. C., (1992), Influence of microcracking on the mass transport properties of concrete, *ACI Materials Journal*, 89(4), pp. 1416-1424.

Schiessl, P., and Edvardsen, C., (1993), Autogenous healing of cracks in concrete structures subjected to water pressure, *No. F361*, Institute of Building Materials Research, University of Technology, Aachen.

Schiessl, P. and Raupach, M., (1997), Laboratory studies and calculations on the influence of crack width on chloride-induced corrosion of steel in concrete, *ACI Materials Journal*, 94(1).

Schiessl, P. ed., (1998), *Corrosion of Steel in Concrete*, Chapman and Hall Ltd, London.

Scott, A. N., (2004), The influence of binder type and cracking on reinforcing steel corrosion in concrete, *PhD Thesis*, University of Cape town.

Scott, A. N. and Alexander, M. G., (2007), The influence of binder type, cracking and cover on corrosion rates of steel in chloride-contaminated concrete, *Magazine of Concrete Research*, 59(7), pp. 495-505.

Sharif, A., Loughlin, K. F., Azad, A. K. and Nawaz, C. M., (1999), Determination of the effective diffusion coefficient in concrete via a gas diffusion technique, *Proceedings of the international conference on concrete durability and repair technology*, Edited by Dhir R. K. and McCarthy M. J., published by Thomas Telford.

Shreir, L. ed., (1979), *Corrosion Volume 1*, Metal/Environment Reactions, Newnes-Butterworths: London cited by Scott A.N. (2004), The Influence of Binder Type and Cracking on Reinforcing Steel Corrosion in Concrete, *PhD Thesis*, University of Cape town.

Sisomphon, K. and Franke, L., (2007), Carbonation rates of concrete containing high volume of pozzolanic materials, *Cement and Concrete Research*, 37, pp. 1647-1653.

Song, H. W. and Saraswathy, V., (2006), Studies on the corrosion resistance of reinforced steel in concrete with ground granulated blast-furnace slag - an overview, *Journal of Hazardous Materials*, 16, pp. 226-233.

Stanish, K., Hooton, R. D. and Thomas, M. D. A., (2004), A novel method for describing chloride ion transport due to an electrical gradient in concrete: Part 1. Theoretical description, *Cement and Concrete Research*, 34, pp. 43-49.

Stansbury, G. and Buchanan, R., (2000), Fundamentals of Electrochemical Corrosion, ASM International, Ohio.

Stern, M. and Geary, A. L., (1957), Electrochemical polarization I: theoretical analysis of shape of polarization curves, *Journal of Electrochemistry Society*, (104), pp. 56-63, cited by Poupard *et al*., (2006), Characterizing Reinforced Concrete Beams Exposed During 40 years in a Natural Marine Envirinment - Presentation of the French Project Benchmark des Poutres de la Rance, *proceedings of the 7th CANMET/ACI international conference on durability of concrete*, Montreal Canada, American Concrete Institute SP 134, pp. 17-30.

Suzuki, K., Ohno, Y., Praparntanatorn, S. and Tamura, H., (1990), Mechanism of steel corrosion in cracked concrete, *Corrosion of reinforcement in concrete*, Ed. Page, C., Treadaway, K. and Bramforth, P., London: Society of Chemical Industry, pp. 19-28.

Tang, L., (1996), Chloride transport in concrete: measurement and prediction, *PhD thesis*, Publication P-96:6, Department of Building Materials, Chalmers University of Technology, Gothenburg, Sweden.

Tang, L., (2008), Engineering expression of the ClinConc model for prediction of free and total chloride ingress in submerged marine concrete, *Cement and Concrete Research*, (3).

Tarek, U. M., Yamaji, T. and Hamada, H., (2002), Chloride diffusion, microstructure and mineralogy of concrete after 15 years of exposure in tidal environment, *ACI Materials Journal*, 99(3), pp. 256-263.

Terheiden, K., (2008), diffusive and convective salt transport in building materials depending on pore solution concentration and moisture content, *Journal of Building Physics*, 31(3), pp. 199-211.

Torrent, R., Alexander, M. G. and Kropp, J., (2007), Introduction and problem statement, Chapter one, *RILEM TC 189-NEC: State-of-the-art report, non-destructive evaluation of the penetrability and thickness of the cover*, pp. 1-11.

Transportation Research Circular E-C107, (2006), Control of cracking in concrete - state of the art, *Transportation Research Board*, October, Washington, DC 20001.

Trejo, D. and Pillai, R.G., (2003), Accelerated chloride threshold testing: Part I - ASTM A-615 and A-706 reinforcement, *ACI Materials Journal*, 100(6), pp. 519-527.

Tritthart, J., (1989), Chloride binding: II, The influence of the hydroxide concentration in the pore solution of hardened cement paste on chloride binding, *Cement and Concrete Research*, (19), pp. 683–691.

Tromans, D., (1980), Anodic polarization behaviour of mild steel in hot alkaline sulfide solutions, *Journal of Electrochemical Society*, June, pp. 1253-1256 cited by Scott A.N. (2004), The influence of binder type and cracking on reinforcing steel corrosion in concrete, *PhD Thesis*, University of Cape town.

Tuutti, K., (1982), Corrosion of steel in concrete, *Swedish Cement and Concrete Research Institute*, Stockholm, Report No.CBI Research 4:82, pp. 468.

Tuutti, K., (1993), Effect of cement type and different additions on service life. In: R.K. Dhir and M.R. Jones, Editors, *Proceedings of the international conference concrete 2000 - economic and durable construction through excellence*, E&FN Spon, London, pp. 1285-1295.

Vienna, (2002), Guidebook on non-destructive testing of concrete structures, *International Atomic Energy Agency*.

Weiss, J., Radalinska, A., Paradis, F., Niemuth, M. and Sant, G., (2007), Cracks in concrete: An overview of an approach to assess their development, their physical features, and their impact on durability, The international *RILEM workshop on transport mechanisms in cracked concrete*, Ghent, Belgium, 3-7 September 2007.

West, J., (1980), *Basic Corrosion and Oxidation*, Ellis Horwood Limited, London.

Whiting, D. A. and Nagi, M. A., (2003), Electrical resistivity of concrete-A literature review, *Portland Cement Association*, Illinois, pp 56.

Yoon, S., Wang, K., Weis, W. J., and Shah, S. P., (2000), Interaction between loading, corrosion, and serviceability of reinforced concrete, *ACI Materials Journal*, 97(6), pp. 637-644.

Zivica, (2003), Influence of w/c ratio on rate of chloride induced corrosion of steel reinforcement and its dependence on ambient temperature, *Bull. Materials Science*, 26(5), pp. 471-475.

Chapter 3

3 EXPERIMENTAL DETAILS

3.1 Introduction

This chapter presents the salient details of experiments performed during the study (Figure 3.1). Details of specimen design, sample preparation, mix proportions and test methods are given.

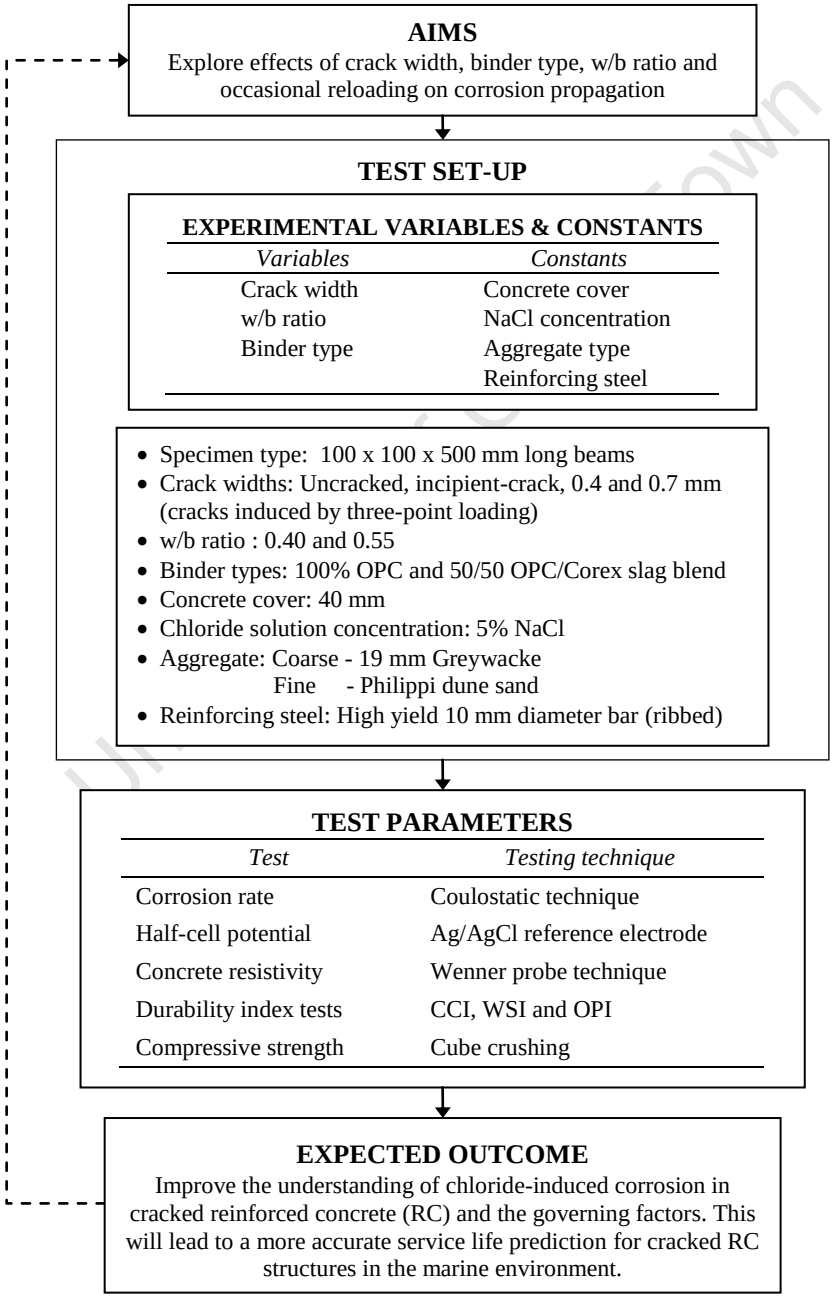

Figure 3.1: Flow chart of experimental set-up

*3.2 **Experimental variables***

*3.2.1 **Crack widths***

The crack widths investigated in this study were limited to 0.7 mm, 0.4 mm and incipient crack*. Uncracked specimens were also included to act as reference specimens.

* Incipient crack as used in this study refers to a crack just induced by three-point loading of beam specimens and thereafter unloading. The incipient cracks were visually detected using a hand lens.

The incipient-cracked specimens were selected to investigate the effect of crack width on self-healing in RC structures and how it affects the corrosion initiation and propagation. 0.4 mm crack width is generally taken as the threshold crack width, below which corrosion may proceed similar to uncracked concrete as discussed in Chapter 2. The selection of 0.7 mm crack width was to simulate adverse crack widths, which are rarely encountered, but may pose corrosion threat to the RC structure.

*3.2.2 **Binder types***

Two types of binders were used in this study viz:

- CEM I 42.5N from Riebeek West PPC factory in the Western Cape Province, South Africa. This is an ordinary Portland cement (OPC). All the cement was obtained from the same factory. A typical oxide composition of the OPC used is given Table 3.1.

  Table 3.1: Typical oxide analysis of OPC used
  (Riebeek PPC Cement factory product data sheet)

Constituent	CaO	SiO_2	Al_2O_3	MgO	TiO_2	Fe_2O_3	MnO	K_2O	Na_2O	SO_3
% Composition	66.17	21.1	4.58	1.24	0.30	3.45	0.10	0.66	0.09	1.96

- Corex slag is a latent hydraulic binder i.e. it hardens slowly in the presence of water but is much more reactive in an alkaline environment. It is a widely used cementitious material produced in the Corex process at the Saldhana steel plant in the Western Cape Province, South Africa and marketed by PPC Cement factory. In South Africa, similar to GGBS, its use has been predominantly at 50% of cement due to convenience for proportioning. At this replacement level, optimum chloride resistance is achieved while replacement levels below 25% provide only little increase in chloride resistance (Mackechnie *et al*., 2003). A 50/50 OPC/Corex slag blend was therefore adopted for the study. Corex slag contains the same oxides as OPC but in different proportions. A typical oxide composition of GGCS is given in Table 3.2.

Table 3.2: Typical oxide analysis of GGCS used

(Mackechnie *et al.,* 2003)

Constituent	CaO	SiO_2	Al_2O_3	MgO	TiO_2	Fe_2O_3	MnO	K_2O	Na_2O	SO_3
% Composition	37.2	30.8	16.0	13.7	0.51	0.87	0.09	0.35	0.12	3.19

*3.2.3 **Water/binder ratio***

Water/binder (w/b) ratios of 0.55 and 0.40 were used. 0.55 is the maximum w/b ratio specified by the South African concrete design code (SANS 10100-2, 1992) for the design of RC structures in aggressive environments, in this case marine environment. A lower w/b ratio of 0.40 was used to investigate the effects of a less permeable concrete on corrosion rate in the presence of cracks. Water/binder ratio relates to concrete strength inversely. The w/b ratio also affects the penetrability of concrete which is very influential for the ingress of aggressive corrosion agents (chloride ions, moisture and oxygen) in concrete.

*3.2.4 **Concrete cover to reinforcement***

To reduce the likelihood of corrosion of embedded steel owing to the ingress of chlorides from an external source, it is essential to ensure adequate cover to reinforcement. The South African concrete design code (SANS 10100:2, 1994) recommends a minimum concrete cover of 40 mm for normal density concrete exposed to severe environmental conditions such as marine environments. A cover of 40 mm was used for all the beam specimens.

*3.2.5 **Reinforcing steel***

High yield 10 mm diameter steel reinforcement bars (ribbed) were used for all the beam specimens. It is the most common type of reinforcing steel used in practice and is therefore preferable for investigating corrosion.

*3.2.6 **Chloride solution***

A 5% NaCl solution was used to simulate the marine environment. Tap (potable) water was used in the preparation of the solution.

*3.2.7 **Aggregate***

(a) Coarse aggregate

Greywacke (also known as *Malmesbury shale*) is a fine-grained glassy rock consisting of quartz, feldspar, mica and iron oxides. It is developed by thermal metamorphism of argillaceous rocks of the Malmesbury group (Brink, 2003). Greywacke does not crush to a good cubical particle shape and hence tends to be elongated and flaky. Consequently, the

workability of concrete made with this aggregate may be negatively affected. The grading curve for 19 mm greywacke used is given in Figure 3.2 (see appendix A for details).

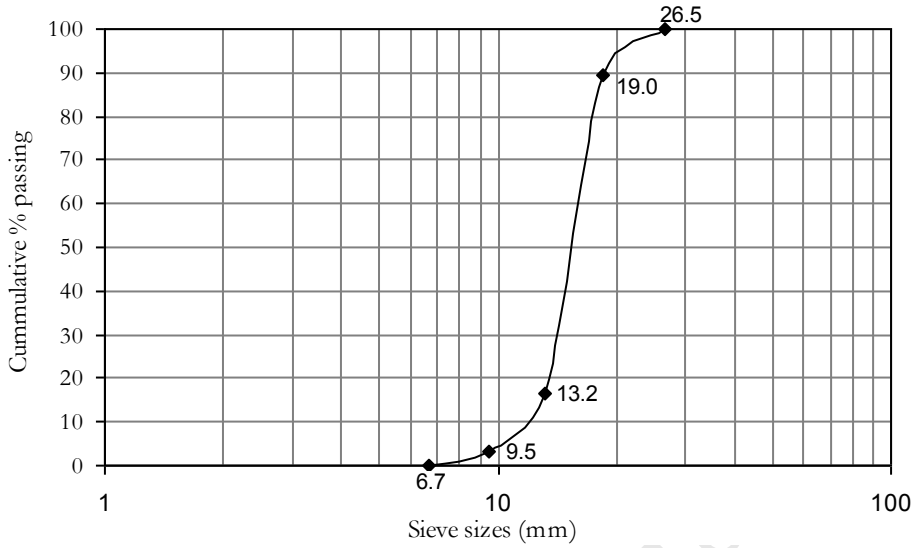

Figure 3.2: Grading curve of coarse aggregate (Greywacke)

It is notable from the grading curve that the coarse aggregate sample contained sizes other than 19 mm and is therefore not single-sized. Based on the ASTM C125 definition, a 19 mm *nominal maximum stone size* (i.e. the smallest sieve opening through which the entire amount of aggregate is permitted to pass) must have the entire aggregate pass through the 25-mm sieve, which is the case for the stone grading in Figure 3.2.

Table 3.3 gives some of the typical characteristics of greywacke. Greywacke is a highly reactive material with respect to alkali-silica reaction (Alexander and Davis, 1991).

Table 3.3: Typical characteristics of greywacke
(Alexander and Davis, 1991)

Aggregate property	*Value*
Relative density	2.72
10% Fines Aggregate Crushing Value (kN)	140 – 300
Unconfined compressive strength (MPa)	297 – 308
Elastic Modulus (GPa)	68 – 77
Coefficient of thermal expansion ($x10^{-6}/^{o}C$)	10.9
Water absorption (%)	0.41

(b) Fine aggregate

Philippi dune sand from the Cape Flats was used in this study. This is one of the main sources of concrete sand is used in the Cape Peninsula area. It is a shell-bearing dune sand with a shell content of approximately 25 to 30% (measured as carbonate) (Grieve, 2001). The grading curve for the Philippi dune sand used is given in Figure 3.3 (see appendix A for details). Because of their well-rounded grains, they produce concrete with low to medium standard water requirement (water demand) of about 200 l/m^3 (Grieve, 2001).

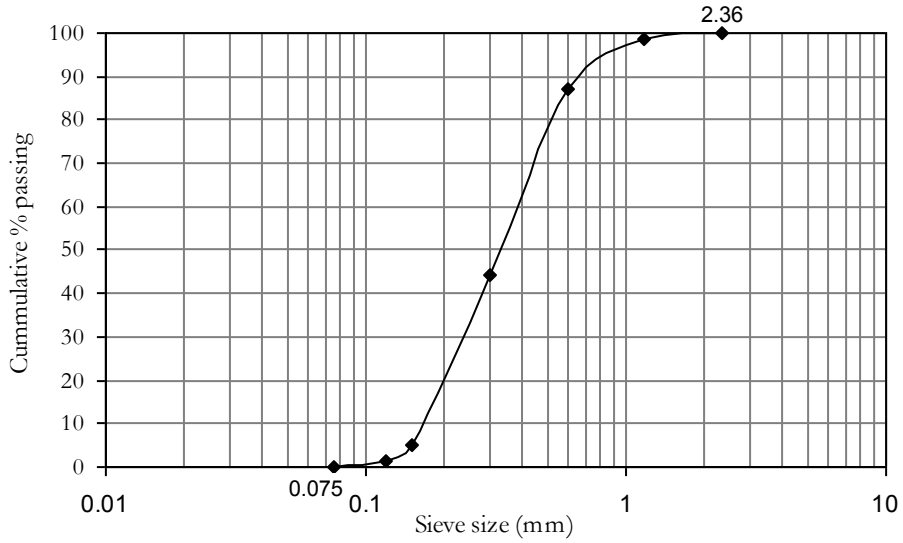

Figure 3.3: Grading curve of fine aggregate (Philippi dune sand)

3.3 ***Concrete mix design and mix proportions***

Concrete mix design is a process of selecting the mixture of ingredients required to meet anticipated properties of both fresh and hardened concrete. It is a well established practice around the world and as such, most countries have standardised their concrete mix design methods. These methods are mostly based on empirical relations, charts, graphs, and tables developed as outcomes of extensive experiments and investigations of locally available materials.

In South Africa, the Cement and Concrete Institute (C&CI) volumetric mix design method is used (Addis, 2002), and was adopted for this study. It is derived from the ACI 211.1-91 method and modified to suit South African practice. In this approach, the mix constituents are calculated by mass, with the requirement that the absolute volumes should sum to the total volume of the concrete.

The flow chart in Figure 3.4 shows the basic mix design procedure used (modified to suit this study).

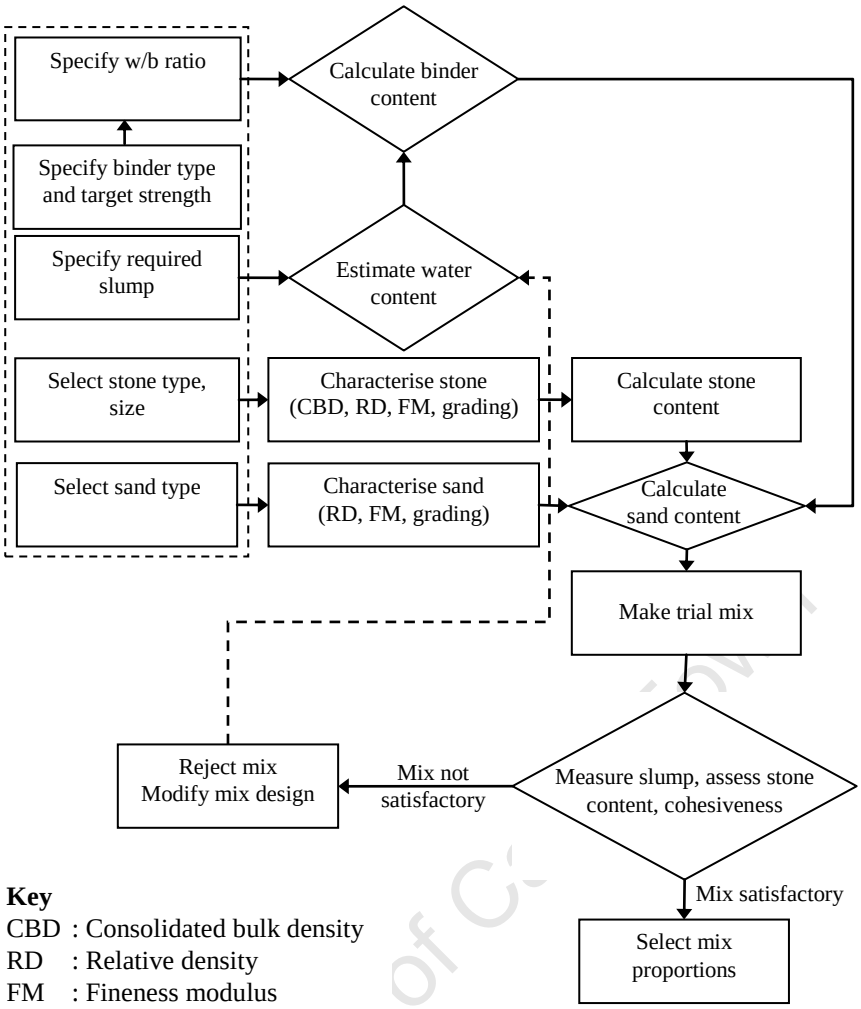

Figure 3.4: Concrete mix design flow chart (Volumetric method)

A summary of the mix proportions used to make the beam and cube specimens is given in Table 3.4.

Table 3.4: Summary of mix proportions used

	100 % OPC		*50/50 OPC Corex Slag*	
Material (*kg/m*^{3})	*PC-40*	*PC-55*	*SL-40*	*SL-55*
OPC	463	336	231	168
Corex Slag	-	-	231	168
Fine aggregate (sand)	749	855	749	855
Coarse aggregate: 19 mm max.	1040	1040	1040	1040
Water content	185	185	185	185
Water/binder ratio	0.40	0.55	0.40	0.55
28 day Compressive strength (MPa)	50	33	52	33

*3.4 **Number of specimens***

100 x 100 x 500 mm long beam specimens (Figure 3.5) were used. For each binder type, crack width and w/b ratio (see Figure 3.6), three beam specimens were cast, resulting in a total number of 48 specimens. For each concrete mix, 3 cube samples were tested for compressive strength at the desired ages i.e. 7, 28 and 90 day strengths. Three cube samples per mix were also cast for durability index testing of discs cored from the cubes.

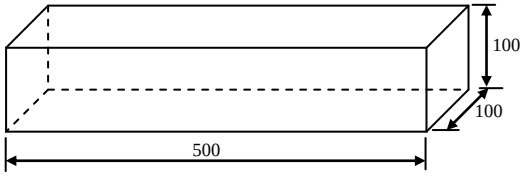

Figure 3.5 : Typical beam specimen (Dimensions in millimetres)

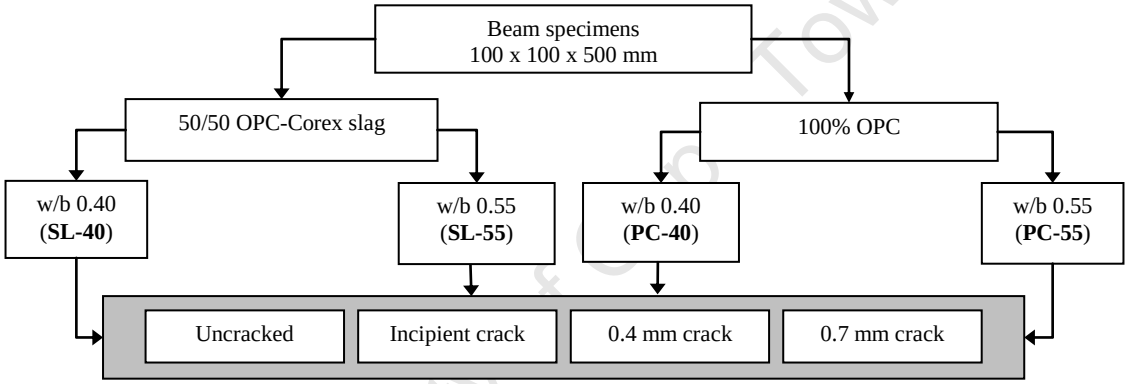

Figure 3.6: Summary of binder types, w/b ratio and crack widths used

*3.5 **Casting of specimens***

The beam specimens were cast face-down with the concrete cover to steel (40 mm) provided from the base of the mould as shown in Figure 3.7. The steel bar was held in place using 100 x 40 x 50 mm mortar spacer blocks.

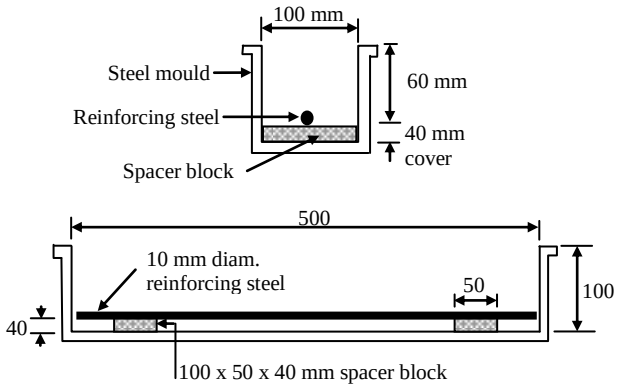

Figure 3.7: Positioning of reinforcing steel in the steel mould prior to casting

Prior to casting, the reinforcing bars were wire-brushed to remove mill scale and thoroughly cleaned. A wire was attached to one end and both ends were epoxy-coated to provide an effective exposed surface area of approximately 94 cm^2 (Figure 3.8). Just before casting, the bars were again cleaned and de-greased with acetone.

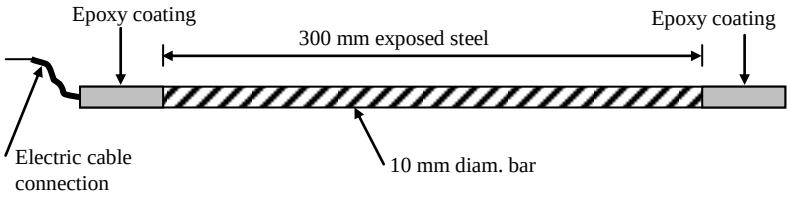

Figure 3.8: Typical reinforcing steel bar after preparation

10 mm diameter x 100 mm long stainless steel 303 bars were placed in the concrete during casting to act as counter electrodes for the purpose of corrosion rate measurements.

Both the beam and cube samples were compacted using a vibrating table (for 10 seconds) immediately after placing concrete.

3.6 ***Curing of specimens***

Immediately after casting, the cube and beam specimens were covered with polythene sheets for 24 hours (in the laboratory) at room temperature after which they were stripped and placed in a tap water bath at 23 ± 2 ^oC for curing. The beam specimens were cured for 28 days while the cubes were cured for (a) 7, 28 and 90 days to obtain the respective compressive strengths, and (b) 28 days to obtain the durability indexes.

3.7 ***Crack inducement, measurement and loading criteria***

To facilitate the formation of cracks at approximately the centre of the beam specimens during machine loading, 1.0 mm thick PVC sheets were placed at the center of each beam during casting as shown in Figure 3.9. The PVC sheets were 10 mm deep.

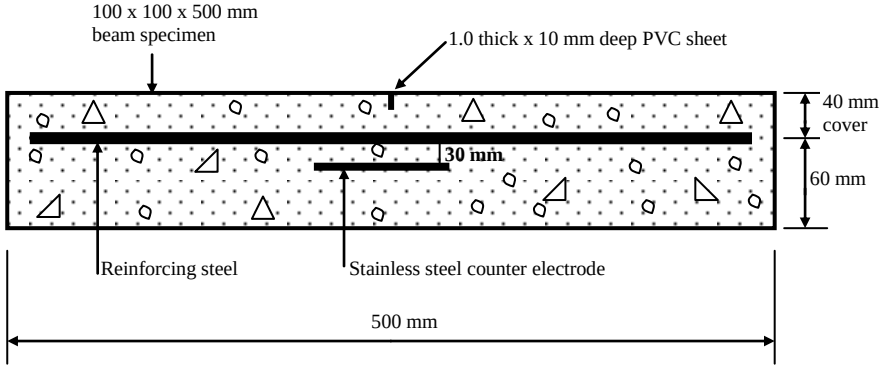

Figure 3.9: Schematic of a beam specimen with 1.0 mm thick PVC sheet

The PVC sheet acted as a notch and hence a line of stress concentration. This increases the probability of obtaining a more or less centrally placed flexural crack under three point loading.

The beams were pre-cracked under three-point flexural machine loading. Crack widths were measured using a crack width detection microscope with a magnification of X40 and accuracy of 0.02 mm. Thereafter, the respective crack widths (except the incipient crack) were maintained using the loading rig shown in Figure 3.10. The loading set-up is also a three-point loading system. The cracks were introduced after 28 days water curing of the specimens followed by 10 days drying.

The cracking loads (see Appendix A for details) for the various crack widths were used to calculate the stress level in the steel to check whether the steel yielded. None of the steel yielded. The load used to obtain the incipient crack was released and hence the stress in the steel was assumed to be zero.

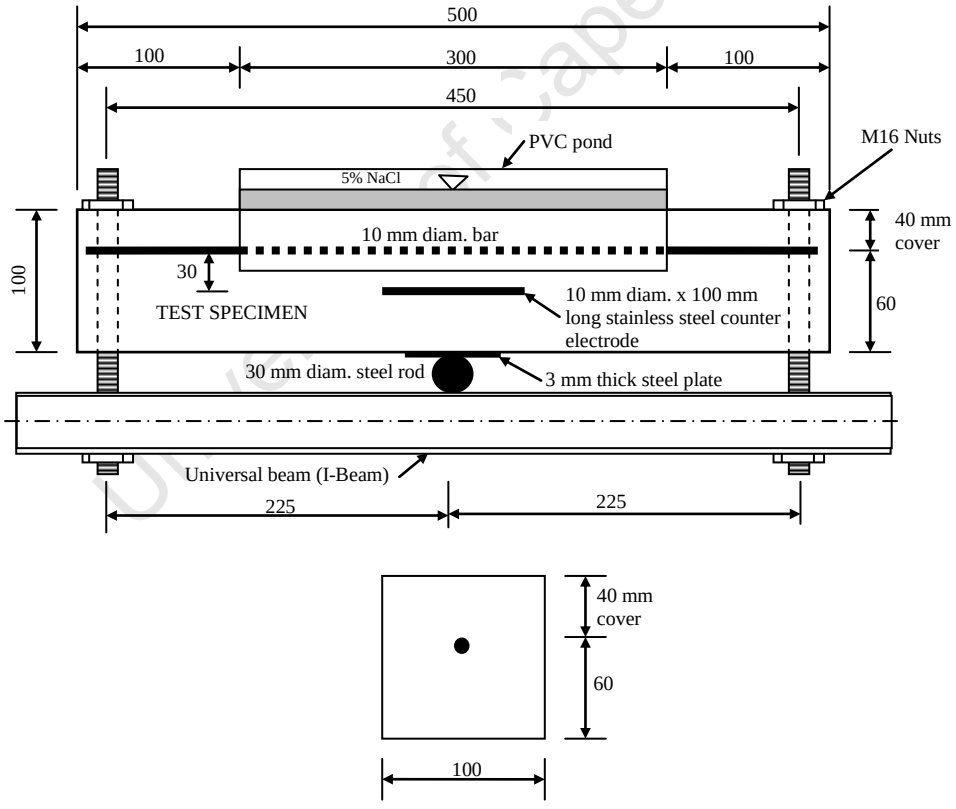

Figure 3.10: Experiment beam loading set-up and cross section
(All dimensions in millimetres, drawing not to scale)

3.8 ***Exposure conditions***

Both the cracked and uncracked beam specimens were monitored for corrosion rate, resistivity and half-cell potential at ambient conditions (Table 3.5).

Table 3.5: Temperature and relative humidity ranges during test period (February-August, 2008)

Parameter	*Range (approximate)*
Temperature (^{o}C)	16 - 24
Relative humidity (%)	60 - 80

3.9 ***Drying and wetting cycles***

Cyclic wetting and drying causes a continuous movement of moisture through the concrete pores. All the beam specimens were subjected to a weekly cycle of 3 days ponding with 5% NaCl solution and 4 days drying.

3.10 ***Reference specimens***

The uncracked specimens (both 100% OPC and 50/50 OPC/Corex slag) were used as reference specimens. These served as benchmarks for comparison purposes in this study.

3.11 ***Reloading of beam specimens***

The beam specimens were reloaded on the basis of corrosion rate trend i.e. when corrosion rates were reasonably stable. It was expected that the reloading would reactivate the sealed cracks and hence increase corrosion rate. Reloading was done as follows: The 0.4 mm cracks were opened (by tightening the nuts in the loading rig, Figure 3.10) up to 0.6 mm, the 0.7 mm cracks were opened to 1.0 mm wide, while the incipient cracked specimens were opened to 0.2 mm wide. The reloading crack widths were selected based on the maximum crack width that the 0.7 mm crack could be opened without the yielding of steel i.e. 1.0 mm. The crack widths at reloading (0.2, 0.6 and 1.0 mm) were maintained for about 24 hours before being relaxed to their original respective widths i.e. incipient crack, 0.4 and 0.7 mm. The first reloading was done between weeks 9 and 10, and the second between weeks 18 and 19.

3.12 ***Sample monitoring***

3.12.1 ***Corrosion rate measurement***

Corrosion rate measurement was carried out using the coulostatic technique. A schematic diagram is shown in Figure 3.11. In this method, a small charge is applied to the reinforcing steel and the relaxation of the potential monitored over a fairly short period of time (see chapter two, section 2.7.5 for details).

Corrosion rate data was collected using a HP 34970A data acquisition unit and analysed using MATLAB (a programming language/software). A typical potential transient monitored over 25 seconds is shown in Figure 3.12. The samples were monitored weekly for corrosion rate.

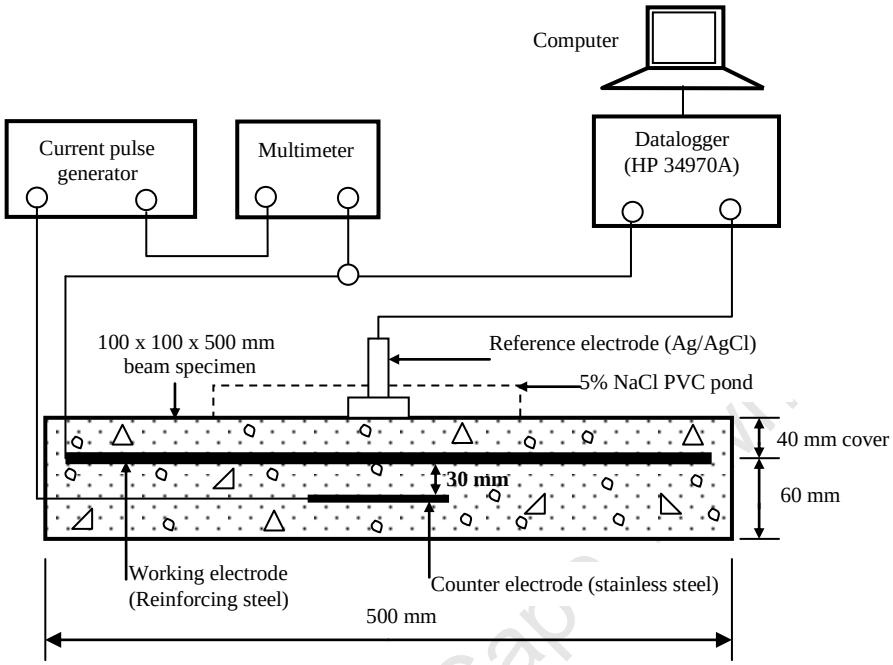

Figure 3.11: Schematic diagram of the coulostatic corrosion rate measurement set-up

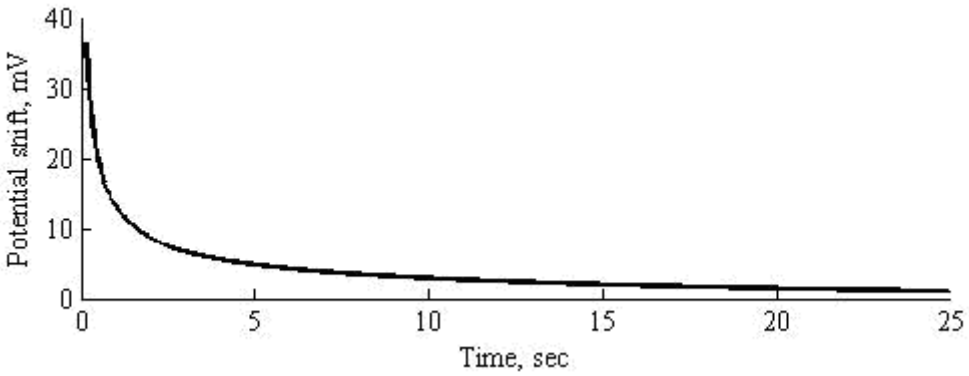

Figure 3.12: Potential transient of steel electrode after application of small charge

Figure 3.13 is a photograph taken during a corrosion rate (and half-cell potential) monitoring session. All the beam specimens were connected to the 'specimen connection board' to ease the monitoring process.

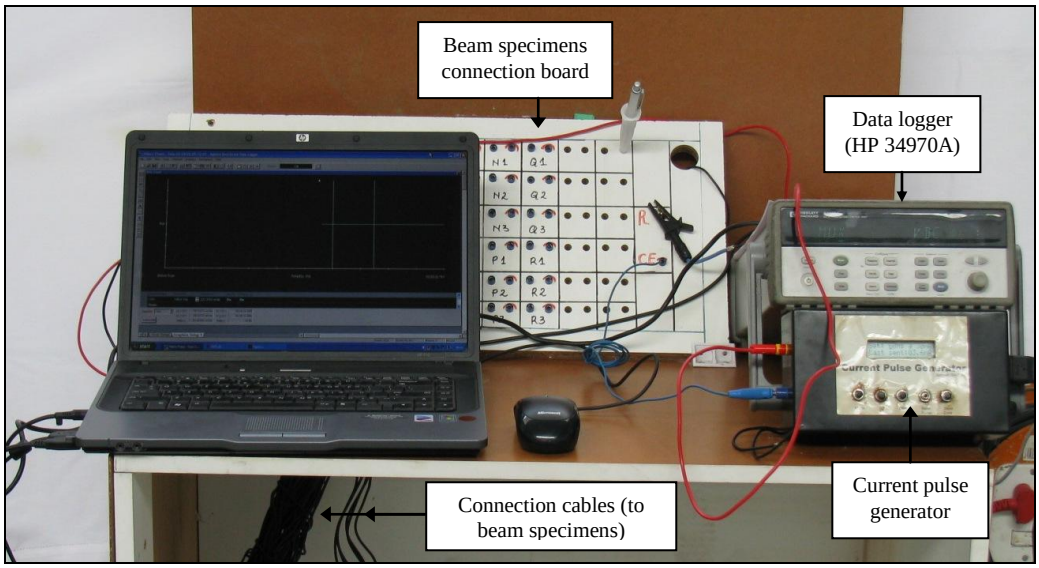

Figure 3.13: Photograph of corrosion rate measurement set-up

*3.12.2 **Half-cell potential (HCP) measurement***

HCP readings were taken simultaneously during corrosion rate measurements using a Ag/AgCl reference electrode (according to ASTM C876-91, 1999) and registered in the HP 34970A data acquisition unit together with the potential changes due to the applied pulse. A schematic illustration is given in Figure 3.11. The samples were monitored weekly for half-cell potentials.

*3.12.3 **Concrete resistivity measurement***

The four point Wenner probe (using a direct current) apparatus at a probe spacing of 50 mm was used to measure the concrete resistivity.

The probe spacing (a = 50 mm) was chosen based on results of laboratory studies by Gowers and Millard (1999) where:

a > 40 mm is given as the lower limit (minimum probe spacing) or

a ≥ 1.5 x max. aggregate size (max. aggregate size = 19 mm in this study)

whichever is greater.

In this study, maximum aggregate size = 19 mm, hence a ≥ 28 mm. Hence the lower limit of a > 40 mm applies. The chosen probe distance (a = 50 mm) is therefore sufficient.

The samples were monitored weekly (at the end of the 4 days wetting period) for concrete resistivity. The Wenner probes were placed across the crack as shown below:

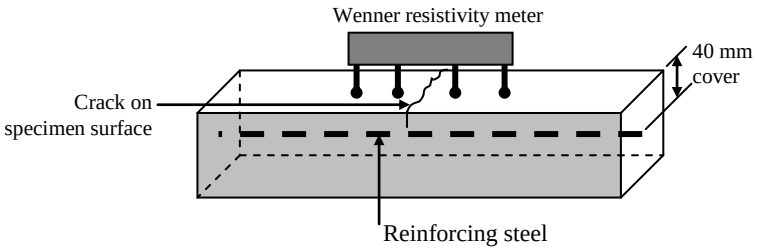

Figure 3.14 : Resistivity measurement across the crack

*3.12.4 **Crack width monitoring***

To ensure that the 0.4 and 0.7 mm crack widths remained constant, reference studs (Demec studs) were carefully placed on the concrete surface across the crack (Figure 3.15). The distance between these reference studs was monitored weekly using a demountable mechanical (Demec) gauge at a gauge length of 100 mm. The loading rig (via the bolts and nuts) was then used to adjust the crack widths as required.

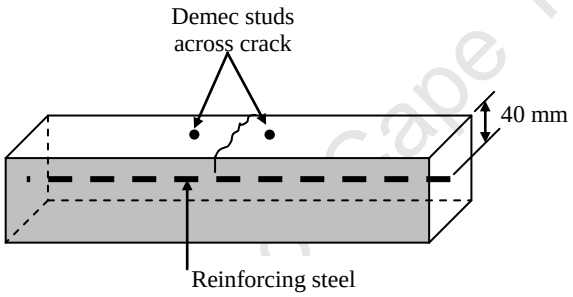

Figure 3.15: Position of reference studs for monitoring 0.4 and 0.7 mm crack widths

During the study period, it was noticed that the crack widths were gradually opening (increasing in width). To ensure that the respective crack widths remained as desired (0.4 and 0.7 mm), the nuts in the loading rig (Figure 3.10) were loosened from time to time as required. This can be attributed to either creep or corrosion of the reinforcing steel. As corrosion proceeds, steel cross sectional area is lost resulting in a reduction in the load carrying capacity of the beam i.e. a reduction in the ultimate moment of the beam; hence the load applied initially has to be reduced (by loosening the nuts).

*3.13 **Tests***

*3.13.1 **Durability indexes***

Potential durability may be inferred by measuring the resistance of the cover layer to transport mechanisms such as permeation, absorption and diffusion. Three durability index tests have been developed that measure the resistance of cover concrete to the transport of fluids and ions that affect deterioration (Alexander *et al*., 2001). The purpose of the tests is not to

determine absolute or intrinsic material properties but to produce reliable index values to be used for characterisation.

Although the values obtained from these tests may not be entirely representative of the fundamental material characteristics, the results will be used to provide indexes which can be used to predict likely material performance. An attempt will also be made to find correlation between the durability indexes and corrosion rate.

The durability index tests comprise of:

(i) Chloride Conductivity Index Test (CCI)
(ii) Oxygen Permeability Index Test (OPI)
(iii) Water Sorptivity Index Test (WSI)

A detailed literature on the above mentioned tests is outlined in Appendix B as well as in the Durability Index Testing Manual (Alexander *et al.,* 1999) published by the University of Cape Town.

3.13.2 ***Compressive strength***

The compressive strengths of the concrete used to prepare the specimens were obtained by performing standard cube (100 x 100 x 100 mm) crushing tests. The specimens were tested for 7, 28 and 90 day compressive strengths according to SANS 5863 (1994).

Concrete exhibits loading-rate sensitivity relative to compressive strength (or precisely, concrete exhibits strain-rate sensitivity behaviour in tension) (Gedney, 2008). All the tests were performed using a manually-operated hydraulic AMSLER compression machine at a loading rate of 0.25 MPa/sec up to failure load. The South African standard code of practice SANS 5863 (1994), recommends a loading rate of 0.3 ± 0.l MPa/sec.

The next chapter will present the analysis and discussion/interpretation of the experimental results obtained during the study period.

3.14 ***References***

ACI Committee 211, (2001), Guide for use of normal weight and heavy weight aggregates in Concrete, ACI 211R-96 (Re-approved 2001), *American Concrete Institute manual for concrete practice*, Farmington Hills, MI: American Concrete Institute.

Alexander, M. G., Ballim, Y. and Mackechnie, J. R., (2001), Use of durability indexes to achieve durable cover concrete in reinforced concrete structures, *Materials Science of Concrete*, VI, pp. 483-511.

Alexander, M. G. and Davis, D. E., (1991), Aggregates in concrete - a new assessment of their role, *Concrete Beton*, 59, pp. 10-20.

Alexander, M. G. and Mindess, S., (2005), *Aggregates in Concrete*, published by Taylor and Francis

ASTM C876-91, (1999), Standard test method for half-cell potentials of uncoated reinforcing steel in concrete.

ASTM C125, Standard terminology relating to concrete and concrete aggregates.

Brink, A. C., (2003), Modelling aggregate interlock load transfer at concrete pavement joints, *PhD Thesis*, University of Pretoria, South Africa.

Gedney, R., (2008), Productivity tools for the concrete testing laboratory, *Concrete International*, 30(6), pp. 52-54.

Grieve, G., (2001), Aggregates for concrete, *Fulton's Concrete technology*, 8th edition, pp. 25-59.

Gowers, K. R. and Millard, S. G., (1999), Measurement of concrete resistivity for assessment of corrosion severity of steel using Wenner technique, *ACI Materials Journal*, 96(5), pp. 536-541.

Mackechnie, J. R., Alexander, M. G. and Jaufeerally, H., (2003), Structural and durability properties of concrete made with Corex slag, *Research monograph No. 6*, Department of Civil Engineering, University of Cape Town.

Quinn, G. P. and Keough, M. J., (2006), *Experimental Design and Data Analysis for Biologists*, Published by The Press Syndicate of the University of Cambridge.

SANS 10100-2, (1994), *South African Standard Code of practice*, The structural use of concrete, Part 2: Materials and execution of work (as amended, 1994).

SANS 5861-1, (1994), *South African Standard Code of practice*, First revision, Concrete tests - Mixing fresh concrete in the laboratory.

SANS 5861-2, (1994), *South African Standard Code of practice*, First revision, Concrete tests - Sampling of freshly mixed concrete.

SANS 5861-3, (1994), *South African Standard Code of practice*, First revision, Concrete tests - Making and curing of test specimens.

SANS 5863, (1994), *South African Standard Code of practice*, First revision, Concrete tests - compressive strength of hardened concrete.

4 RESULTS AND DISCUSSION

4.1 ***Introduction***

This chapter presents the results, analysis and discussion of the various corrosion assessments outlined in Chapter 3. These include corrosion rate, half-cell potential, concrete resistivity and visual assessment. The various durability index test results are also discussed.

4.2 ***General observations***

Figure 4.1 to Figure 4.8 show 3-point moving average (see Appendix A, section A5 for definition) corrosion rates for the uncracked, incipient-cracked, 0.4 mm and 0.7 mm cracked beam specimens for the different binder types.

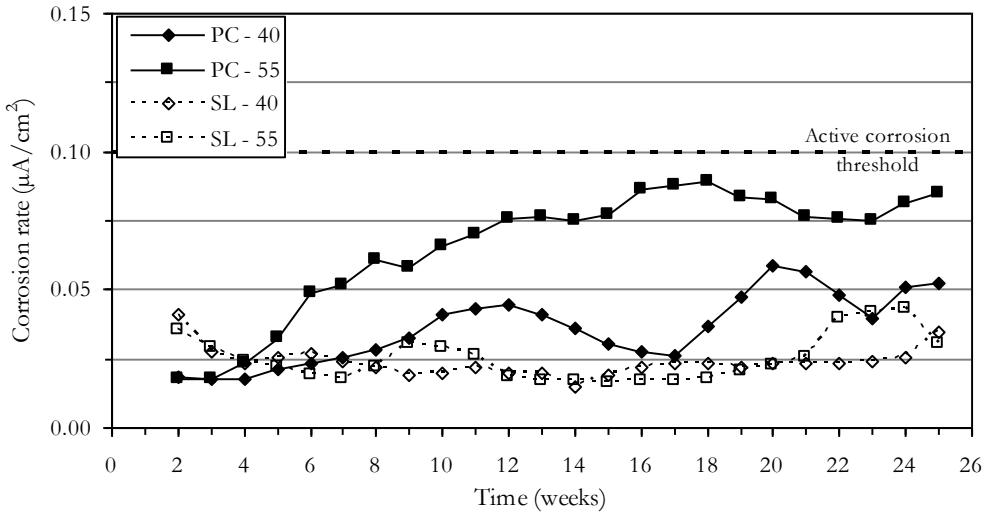

Figure 4.1: 3-point moving average corrosion rates for uncracked specimens

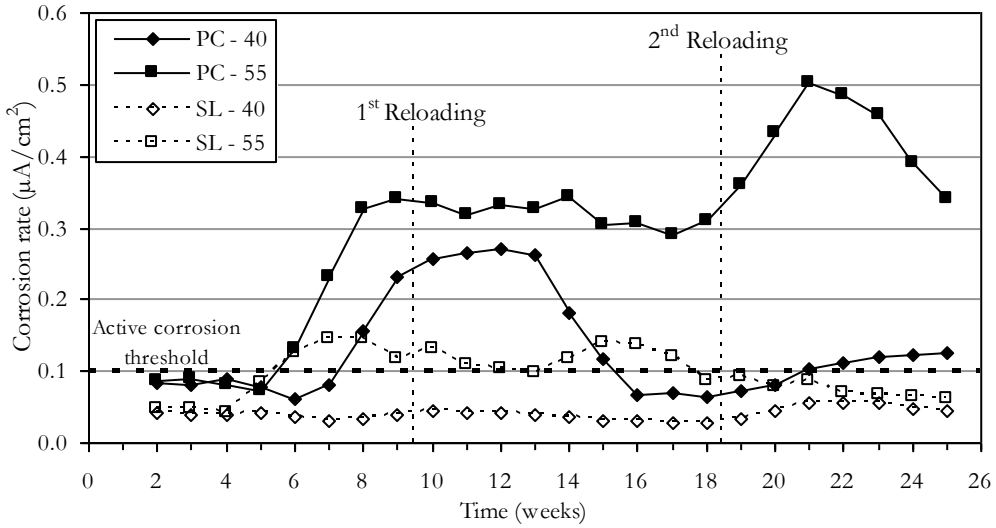

Figure 4.2: 3-point moving average corrosion rates for incipient-cracked specimens

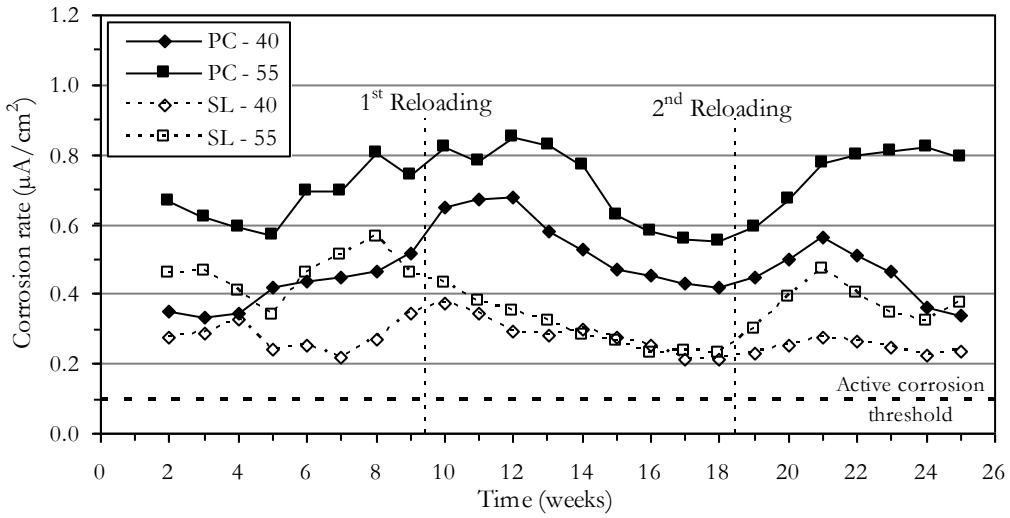

Figure 4.3: 3-point moving average corrosion rates for 0.4 mm cracked specimens

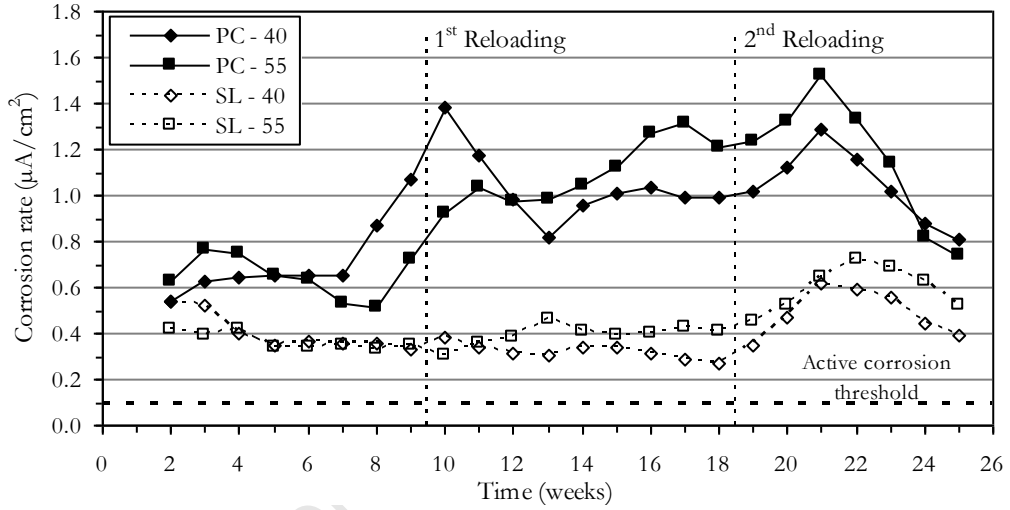

Figure 4.4: 3-point moving average corrosion rates for 0.7 mm cracked specimens

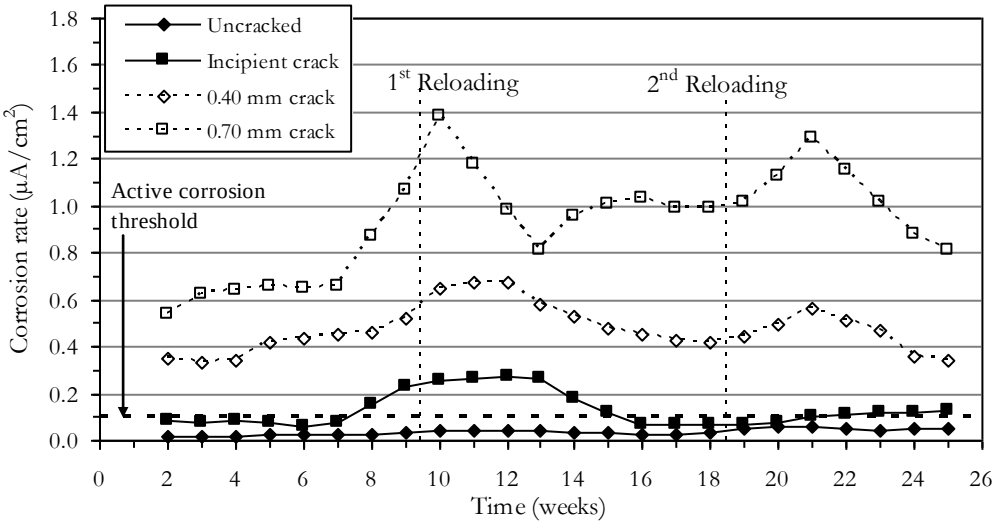

Figure 4.5: 3-point moving average corrosion rates - PC-40 mix

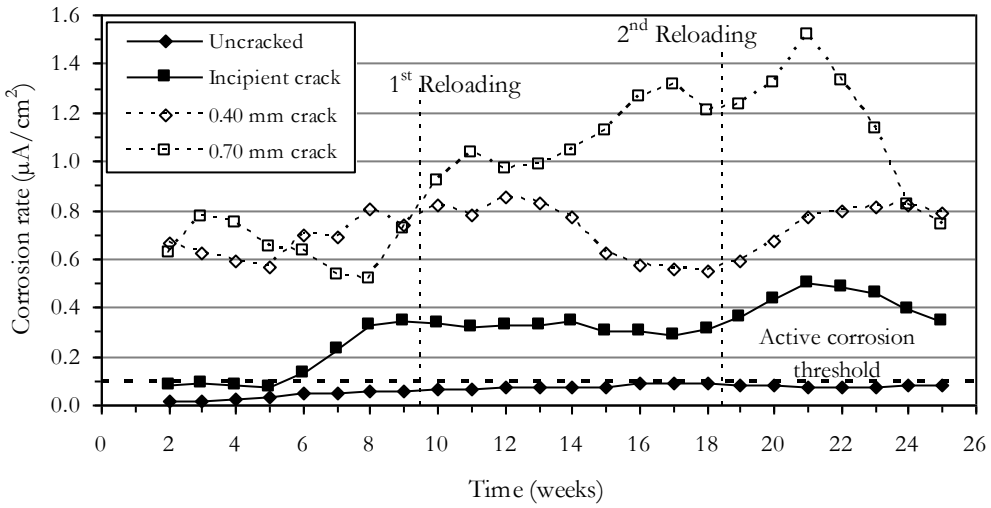

Figure 4.6: 3-point moving average corrosion rates - PC-55 mix

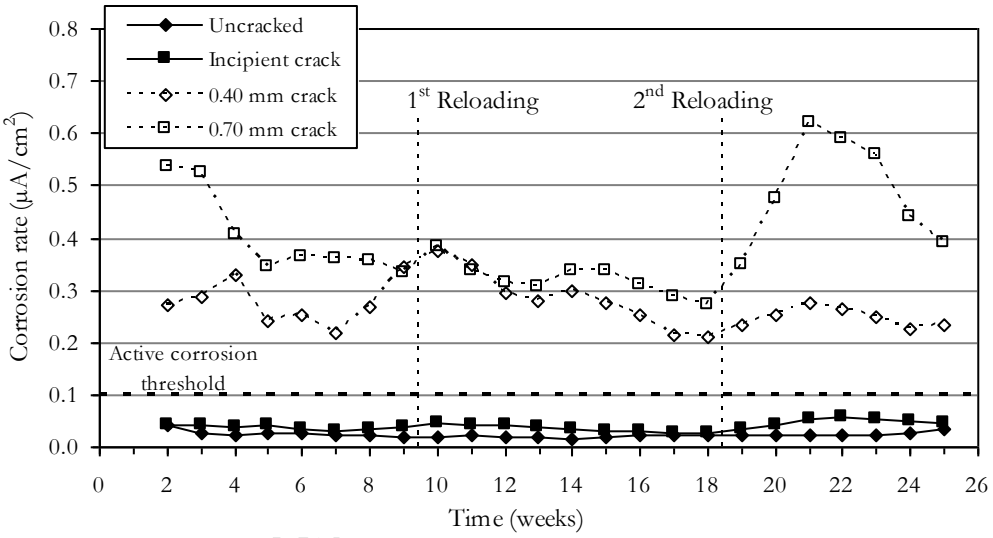

Figure 4.7: 3-point moving average corrosion rates - SL-40 mix

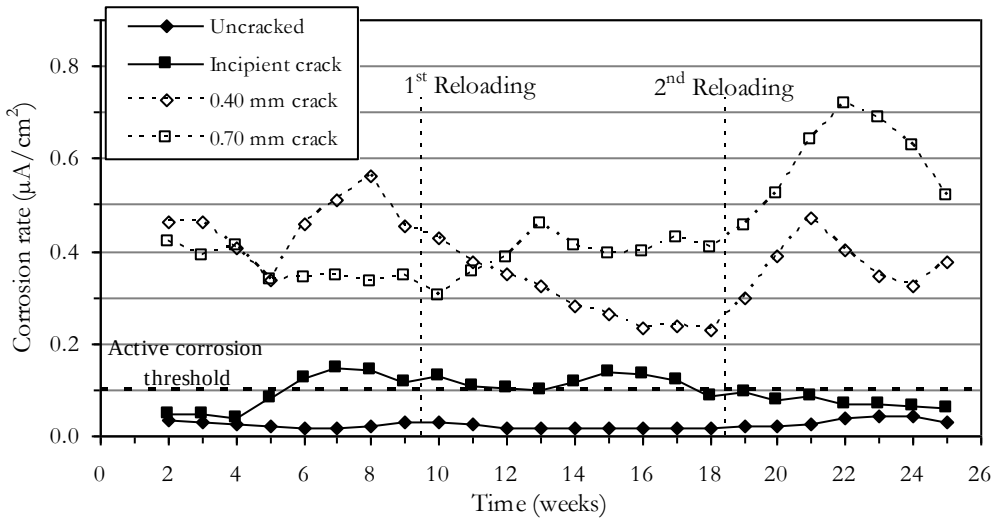

Figure 4.8: 3-point moving average corrosion rates - SL-55 mix

It is notable that for the uncracked specimens (Figure 4.1), the corrosion rates (up to about the 4th week) for Corex slag specimens (SL-40 and SL-55) are higher than those of OPC specimens (PC-40 and PC-55). This can be attributed to the presence of sulphides and thiosulphates (with oxygen reducing characteristics) in Corex slag concretes (Scott, 2004). The formation of the passive protective layer on the steel surface requires adequate dissolved oxygen which, in the case of Corex slag concrete, is consumed in the oxidation of sulphides to thiosulphates and ultimately sulphates. The effect is to decrease the dissolved oxygen concentration thereby delaying the formation of the passive protective layer on the steel surface. However, after the 6th week, Corex slag specimens recorded lower corrosion rates than the corresponding OPC specimens. At this time, it is expected that most of the sulphides and thiosulphates had been oxidised and hence there was sufficient oxygen to allow the formation of the passive protective layer on the steel surface. The low corrosion rates may be attributed to higher chloride binding effects (Glass *et al*., 1997) and high concrete resistivity of slag compared to OPC.

The high early corrosion rates of the uncracked Corex slag specimens also correspond to the high early half-cell potentials (approx. -300 mV Ag/AgCl) (Figure A.4, page 127). According to ASTM C876-91, if the half-cell potential (HCP) measured is lower (more negative) than -256 mV (Ag/AgCl), there is a 90% probability that the reinforcement is actively corroding. In other words, the more negative the value of the HCP, the greater is the tendency of the steel to corrode i.e. lose its electrons. However, in this case, the negative potentials may be attributed to the reducing environment caused by the presence of sulphide ions i.e. oxygen deficiency at the steel level. Studies have shown that the HCP of passive steel in concrete depends on the oxygen availability (moisture content) and can vary over a wide range of potentials (Andrade *et al*., 2003). This trend was not observed in the cracked Corex slag specimens and may be attributed to the availability of sufficient oxygen to simultaneously oxidise the sulphides and thiosulphates and also to support the cathodic corrosion process.

Cracked beam specimens had higher corrosion rates compared to uncracked specimens. For a given binder type and w/b ratio, the corrosion rates increased in the following order: incipient-cracked < 0.4 mm < 0.7 mm. For a given crack width, corrosion generally rates decreased in the following order: PC-55 > PC-40 > SL-55 > SL-40. Therefore, both the binder type (concrete quality) and crack width had an influence on the early corrosion rates. Generally, Corex slag specimens showed lower corrosion rates compared to the corresponding OPC specimens. Replacement of OPC with ground slag results in a finer and denser hardened cement paste (Bakker, 1983) thereby reducing the overall concrete penetrability.

From Figure 4.1 to Figure 4.4, it can be seen that there is a noticeable difference in the corrosion rates for the cracked OPC specimens, as opposed to Corex slag specimens. Furthermore, there is less difference in the corrosion rate between the uncracked and incipient-cracked Corex slag specimens (Figure 4.7 and Figure 4.8) as opposed to that between 0.4 and 0.7 mm cracked specimens of the same binder. The little difference in the corrosion rate between uncracked and incipient-cracked specimens can be attributed to crack self-healing (in the incipient-cracked specimens), chloride binding effects, and most importantly high concrete resistivity.

The decrease in corrosion rates for specimens with incipient and 0.4 mm cracks (Figure 4.2 and Figure 4.3) before the second reloading can be attributed to crack self healing. Gautefall and Vennesland (1983) reported that dormant cracks with a width less than 0.4 mm are prone to self healing when exposed to marine water. Studies by Clear (1985), Hearn and Morley (1997) and Hearn (1998) also suggest that crack self-healing should be expected in crack widths up to 0.3 mm and that the smaller the crack width, the more profound the effect. By inference, it can therefore be expected that the 0.4 mm and incipient-cracked specimens in this study were more likely to experience crack self-healing than the 0.7 mm cracked specimens. Immediately after the second reloading, the corrosion rates in the cracked specimens were noticed to increase. The effects of reloading will be discussed in section 4.5.

Table 4.1 shows the average corrosion rates and half-cell potentials values for the different binder types between week 12 and 18 (before the 2nd reloading), when the corrosion rates were reasonably stable (Figure 4.5 to Figure 4.8). The average concrete resistivities are presented in Table 4.2. The objective of determining the stable corrosion rates was to enable the comparison (and correlation) between corrosion rate with other test results; resistivity, half-cell potential and the chloride conductivity index.

From Figure 4.9, it can be noted that only the uncracked and incipient-cracked specimens for Corex slag had not attained the active corrosion threshold rate (i.e. 0.1 µA/cm^2) at 18 weeks. This is in direct contrast to the OPC specimens where only the uncracked specimens were passively corroding.

Table 4.1: Average corrosion rates and half-cell potentials (week 12-18)

Specimen condition	*Mix label*	*Corrosion rate ($\mu A/cm^2$)*	*Half-cell potential (-mV, Ag/AgCl)*
Uncracked	PC - 40	0.03	280
	PC - 55	0.08	338
	SL - 40	0.02	166
	SL - 55	0.02	205
Incipient-cracked	PC - 40	0.16	390
	PC - 55	0.32	356
	SL - 40	0.04	258
	SL - 55	0.06	284
0.4 mm cracked	PC - 40	0.51	404
	PC - 55	0.70	455
	SL - 40	0.29	401
	SL - 55	0.31	420
0.7 mm cracked	PC - 40	0.92	579
	PC - 55	1.12	571
	SL - 40	0.33	444
	SL - 55	0.39	478

Table 4.2: Average resistivities (week 12-18)

Mix label	*Resistivity ($k\Omega$-cm)*
PC - 40	15
PC - 55	9
SL - 40	43
SL - 55	41

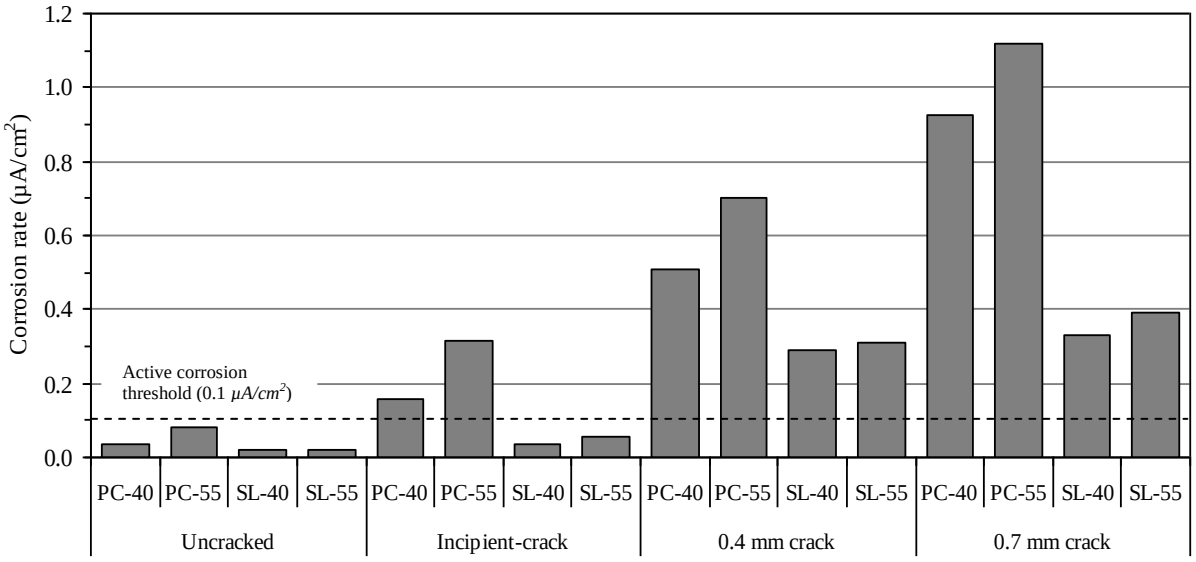

Figure 4.9: Average corrosion rates (week 12-18)

*4.3 **Effect of cracks and crack width on corrosion rate***

From the results, it is evident that the corrosion rates for the cracked specimens for a given binder type are higher than those of uncracked specimens (Figure 4.10 to Figure 4.12).

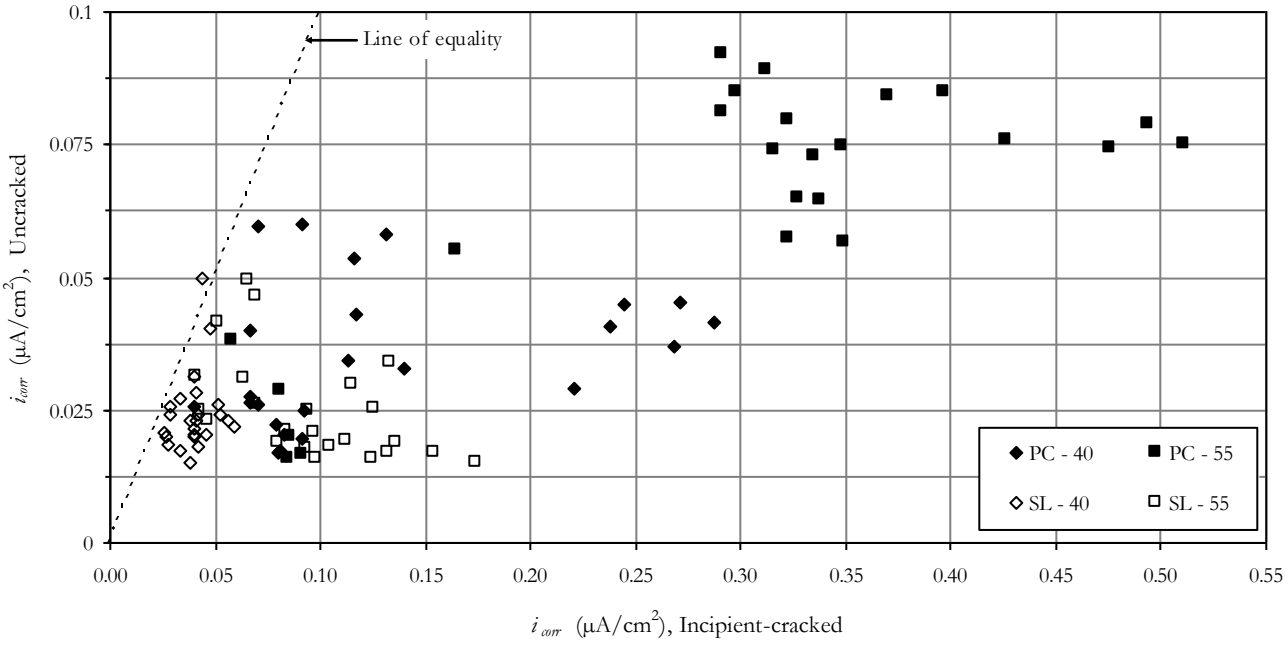

Figure 4.10: Comparison of corrosion rates for uncracked and incipient-cracked specimens

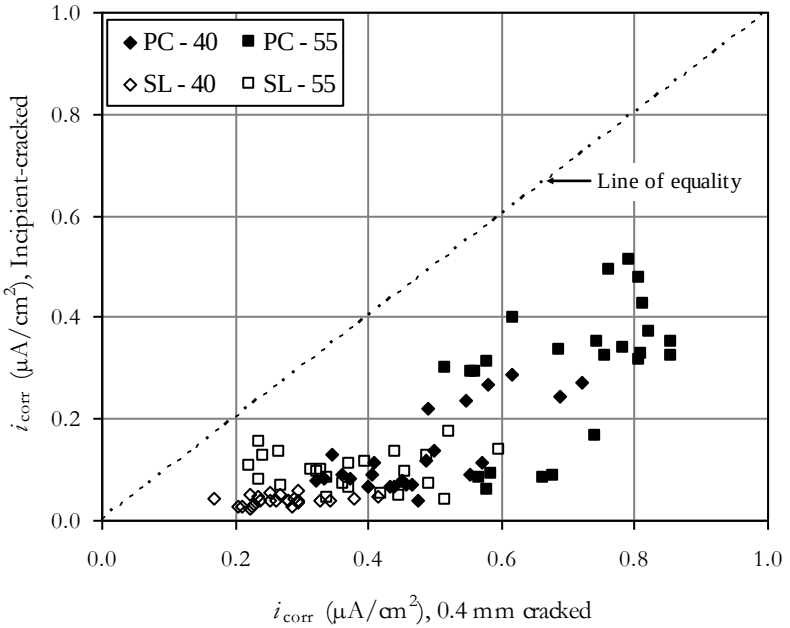

Figure 4.11: Comparison of corrosion rates for incipient-cracked and 0.4 mm cracked specimens

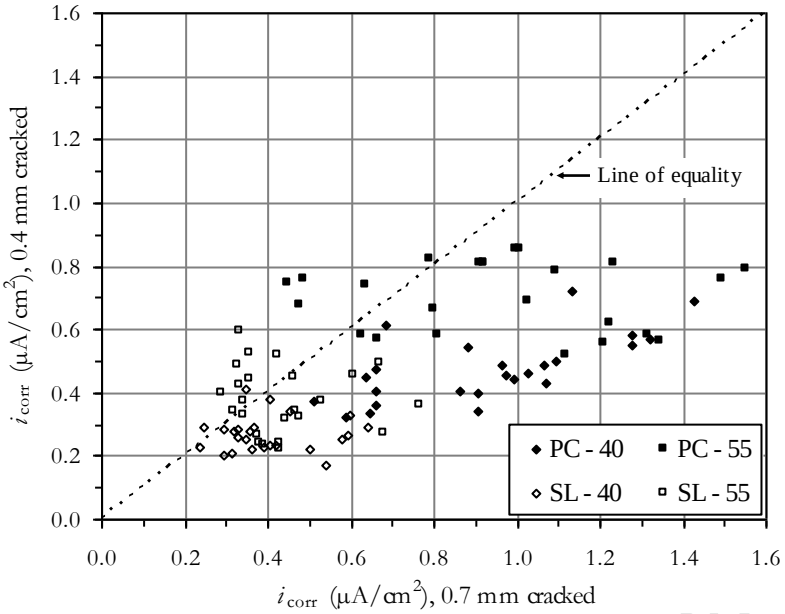

Figure 4.12: Comparison of corrosion rates for 0.4 and 0.7 mm cracked specimens

From Figure 4.10 to Figure 4.12, the following are evident:

- Even incipient cracks have a large impact on corrosion rate compared to the uncracked specimens.
- The influence of binder type can be seen by the clustering of corrosion rate values for a given binder. However, this is less notable between the 0.4 and 0.7 mm cracked specimens as it is between the uncracked and incipient-cracked specimens.
- The major changes in corrosion rate are exhibited for uncracked to incipient-cracked, then to a '*real*' crack (quantifiable cracks i.e. 0.4 and 0.7 mm); these differences are more pronounced for the OPC concrete than for Corex slag concrete specimens.

Previous studies have shown that the presence of cracks increases concrete penetrability and hence ingress of corrosion agents (oxygen, moisture and chlorides) into concrete to the reinforcing steel (Wang *et al.*, 1997, Mohamed *et al.*, 2003). The result is increased corrosion rates.

With respect to loading level, Yoon *et al*., (2000) established that high corrosion rates should be expected when the flexural loading level (or stress in the steel) is increased. According to the flexural cracking loads for the respective crack widths in this study (see Appendix A), the stress in the steel was estimated to be approximately 25, 55 and 60% of the steel yield stress for incipient-cracked, 0.4 mm and 0.7 mm cracked specimens respectively.

The following reasons can also be cited to explain the increase in corrosion rate with increasing surface crack width:

(i) Large cracks expose a greater surface area of the steel, considering wedge-shaped cracks that propagate beyond the steel level.
(ii) Larger cracks provide larger reservoirs for the chloride solution and a faster movement of oxygen during the drying period.
(iii) Smaller cracks (incipient crack and 0.4 mm crack) are prone to crack self-healing thus limiting the ingress of corrosion agents to the steel as was discussed in section 4.2.

The effect of concrete cover thickness on corrosion rate may not be cited as a contributing factor in the observed results because it was kept constant. However, at a constant concrete cover and considering wedge-shaped cracks that propagate beyond the steel level, as was visually observed in the cracked specimens, the surface area of exposed steel in the specimens with 0.7 mm crack widths is higher than that in the 0.4 mm crack widths. This may result in an increase in corrosion rate, in the presence of oxygen at the cathode (Figure 4.13). The exposed steel at the bottom of the crack is a possible locus of the anode, where the actual corrosion occurs.

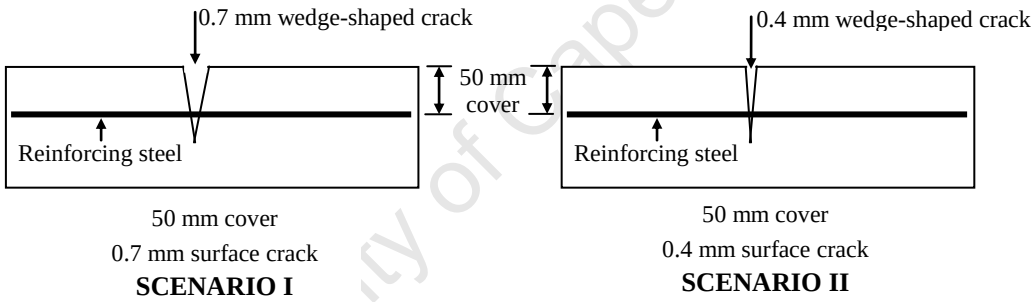

Figure 4.13: Effect of concrete cover thickness on exposed steel area

However, corrosion rate may still be limited by the area of the cathode, even in the presence of adequate oxygen. In tests on RC concrete immersed in sea water, Vennesland and Gjorv (1981) confirmed that the corrosion of the exposed steel in the crack was a function of the ratio of the area of the cathode to that of that anode. The main problem is that the area of the cathode cannot be estimated. Furthermore, at a constant cover, concrete resistivity may also be a governing factor especially for blended cements (SL-40 and SL-55) depending on whether the cathodic reaction is the governing mechanism as in the case of OPC concretes (Scott, 2004).

In the presence of cracks, it would therefore be reasonable if the surface crack widths were specified for specific cover depths. In this way, comparison between different surface crack widths will be valid. For example a crack width of 0.7 mm and a 50 mm cover may not have the same effects (in terms of corrosion) as a 0.7 mm crack and a 20 mm cover and hence

comparison based on crack width alone is limited. A second option would be to either specify the crack width at the level of the reinforcing steel or report the effective cover from the root of the crack to the steel surface (if it does not reach the steel level) but these may not be practical in certain cases. Moreover, the effect of concrete cover quality (as depicted by the chloride conductivity and oxygen permeability indexes, section 4.4) cannot be ruled out especially for purposes of comparison of the uncracked specimens. From the results obtained, the uncracked Corex slag specimens (SL-40 and SL-55) showed lower corrosion rates compared to the uncracked OPC specimens (PC-40 and PC-55) (Figure 4.1).

4.4 ***Relationship between corrosion rate and cover quality***

The three durability index tests (OPI, WSI and CCI) measure the resistance of cover concrete to the transport of fluids (moisture, oxygen) and ions (chlorides) that affect deterioration (see Appendix B for details). The cover quality of the specimens made using the different binder types will therefore be discussed together with the durability index test results. Table 4.3 gives a summary of the durability index tests for the various binders. Notice that only the 90 day CCI value was determined due to a limited number of test samples. The 90 day CCI value will be used in Scott's (2004) corrosion rate prediction model in sub-section (c) of this section.

Table 4.3: Durability Index (DI) test results

DI Test	*Age*	*100 % OPC*		*50/50 OPC-Corex slag*	
	(days)	*PC-40*	*PC-55*	*SL-40*	*SL-55*
OPI (log scale)	28	10.16	10.19	10.42	10.25
WSI (mm/√h)	28	6.7	7.6	6.5	7.4
CCI (mS/cm)	28	1.05	1.50	0.25	0.34
	90	0.86	0.83	0.16	0.23

(a) Oxygen permeability index

Oxygen permeability index (OPI) represents the negative log of the coefficient of oxygen permeability, k, (m/s) through a concrete sample (i.e. $-\log_{10} k$). A poor concrete with connectivity of the pores will therefore have a high coefficient of permeability (low OPI value) and would allow easy access of oxygen (and carbon dioxide) through the concrete. Concretes with very low coefficients of permeability (high OPI value) would impede the access of oxygen to the steel and limit the corrosion progress, given sufficient (thickness and /or quality) concrete cover. The corresponding values of oxygen permeability coefficients at 28 days for the concrete mixes are given in Table 4.4.

Table 4.4: Oxygen permeability coefficients at 28 days

Concrete mix label	*Oxygen permeability* (k x 10^{-11} *m/s*)
PC-40	6.92
PC-55	6.46
SL-40	3.80
SL-55	5.62

From the results obtained, the different concretes used can be graded in terms of ease of oxygen access as SL-40 < SL-55 ≈ PC-40 ≈ PC-55. The grading is done at a 95% confidence level (see Appendix A for details). The reduction in the OPI value with increasing w/b ratio in the Corex slag specimens is as a result of a less dense microstructure. At the same degree of hydration, a low w/b ratio produces fewer and finer pores, whereas a high w/b ratio leads to more pores of larger diameter. However, the OPI (and the corresponding oxygen permeability coefficients) results for the OPC specimens do not clearly depict this trend. The OPC specimens at w/b ratio of 0.40 were expected to have a higher OPI value than those made at w/b ratio of 0.55. The cause of this deviation is not known. These results will therefore not be used in further discussions.

(b) Water sorptivity index

Sorptivity is the movement of a wetting front through a porous medium due to capillary action (Alexander *et al.*, 1999). The extent to which the wetting front moves through the concrete, as measured by the gain of mass with time, provides information on the general pore structure of the material.

The water sorptivity index (WSI) test measures the rate of movement of a water front through the concrete under capillary suction, normalised by porosity. It is particularly sensitive to the near-surface properties of concrete and therefore reflects the nature and effectiveness of curing (Ballim, 1993). The lower the sorptivity, the more resistant is the concrete to penetration of moisture. This is the case for the concrete made at w/b ratio of 0.40 compared to that made at w/b ratio of 0.55 regardless of the binder type. At a glance, the four concrete mixes can be ranked from the lowest to highest WSI value as SL-40 < PC-40 < SL-55 < PC-55. However, after a statistical analysis (at 95% confidence level) the PC-40 and SL-40 mixes were found to be virtually the same. The same was found for PC-55 and SL-55 mixes (see Appendix A for details).

The underlying phenomenon in the WSI test is still not clearly understood; making the interpretation of the WSI results difficult. For example, in a comparative testing programme

to determine the sensitivity of the test to changes in w/b ratio, binder type and curing condition, the WSI test failed to yield satisfactory results (Beushausen and Alexander, 2008).

(c) Chloride conductivity index

Chloride conductivity index (CCI) serves as a durability prediction parameter in two ways. Firstly, it is a direct measure of the resistance of the material to the movement of a charge. As corrosion is dependant upon ionic movement through concrete to complete the electrochemical circuit, a decrease in the conductivity can reduce or limit the corrosion rate. The second function of the CCI is to measure the susceptibility of the concrete to ingress of chlorides by diffusion and can therefore be correlated to corrosion rate. This will be explored in this section.

The concrete mixes can be arranged from the lowest to highest CCI values as SL-40 < SL-55 < PC-40 < PC-55. This trend applies for both the 28 and 90 day CCI values although the 90 day figures are lower than the 28 day ones. This is mainly due to continued binder hydration. It is clear from this that, contrary to the water sorptivity test, the CCI test is sensitive to binder type. From the chloride conductivity results obtained, it can be deduced that the concrete made at w/b ratio of 0.40 has a higher resistance to chloride conductivity than concrete made at w/b ratio of 0.55 (at 95% confidence level; see Appendix A for details). Another important observation is that the blended cement (50/50 OPC/Corex slag) performs better that the plain cement (100% OPC) with respect to chloride conductivity.

The relationship between 28 day CCI values and average corrosion rates between weeks 12 and 18 for the different binder types is presented in Figure 4.14. It is clear that irrespective of binder type, there exists a good correlation ($R^2 > 0.8$) between the CCI and corrosion rate for all the crack widths investigated.

For a given binder type, corrosion rate increases with increasing crack width irrespective of the CCI value i.e. in the presence of cracks, a low CCI value is not a guarantee for high chloride resistance (low corrosion rate). The CCI values are therefore not reliable when applied to cracked concrete. Theoretically, conductivity is the inverse of resistivity and the trends are therefore similar to those obtained between concrete resistivity and corrosion rate as will be seen in section 4.6. It can therefore be used as an alternative for concrete resistivity.

The chloride conductivity index has been used to predict corrosion rates using service life models such as the one by Scott (2004). However, these models apply the CCI determined from uncracked specimens. What is needed is to determine '*correction factors'* depending on the surface crack width. These correction factors can then be applied to the CCI obtained from

uncracked concrete specimens and subsequently be used to predict corrosion rate in cracked concrete.

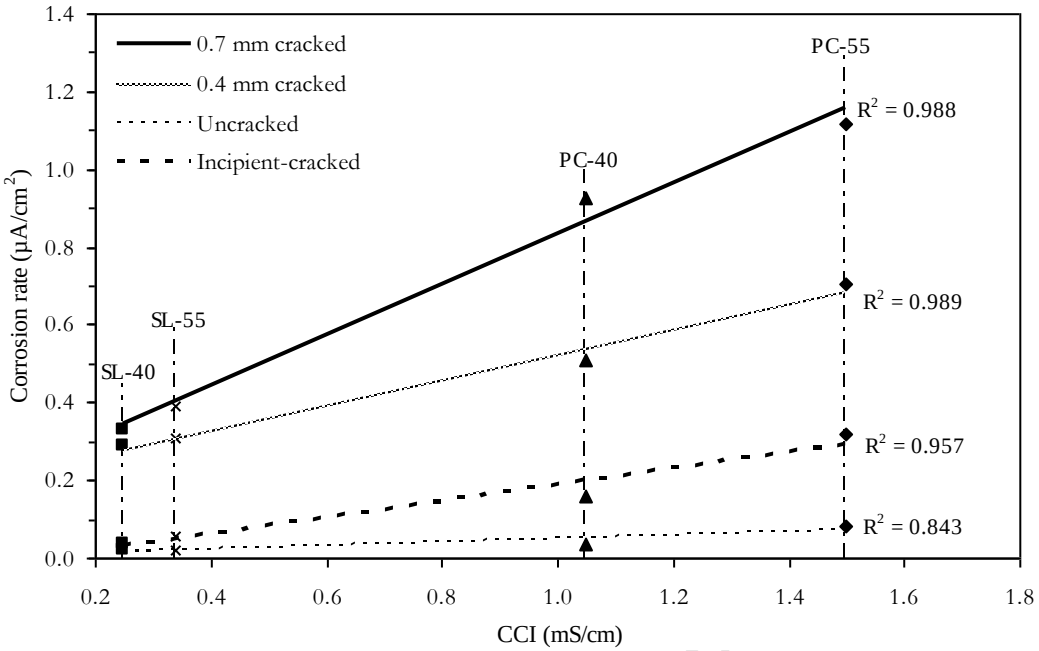

Figure 4.14: Relationship between 28 day CCI and corrosion rate (weeks 12-18)

Scott's model (2004) was developed in a similar study. An attempt will therefore be made to predict corrosion rates in the cracked concrete using the model (2004):

$$i_{corr} = \left(1.43\frac{C_c}{f} + 0.02\right) e^{\left[\left(\frac{40-x}{20}\right)1.2\left(\frac{C_c}{f}\right)^3\right]} \qquad (4.1)$$

where: i_{corr} = corrosion rate (µA/cm^2)

f = slag correction factor $= 10^{(|0.5-S|-0.5+S)}$

S is the slag concentration expressed as a decimal (e.g. 0.25 for 25%)

C_c = 90 day chloride conductivity index value (mS/cm)

x = depth of rebar i.e. concrete cover (mm)

The predicted corrosion rates using the above service life model are presented in Table 4.5. A constant cover of 40 mm and the corresponding 90 day chloride conductivity index values for the various binders (Table 4.3) are used.

It must be noted that inasmuch as the model was developed using experimental work on cracked concrete specimens, it does not explicitly incorporate crack width as an input parameter and has a limitation on the type of binder and cover thickness (< 40 mm) which are

within the requirements for marine structural concrete (Alexander and Beushausen, 2007, SANS 10100:2, 1994).

It is clear from the comparison of actual and predicted corrosion rates in Table 4.5 that the service life model seems to be more applicable to the 0.4 and 0.7 mm cracked Corex slag specimens (SL-40 and SL-55). Notably, the model is not applicable to the incipient-cracked specimens (and presumably uncracked specimens). This can be explained by the fact that the model was developed using ground granulated blastfurnace slag (GGBS) blend and 0.2 and 0.7 mm cracked specimens. The validity of this model therefore seems to be limited to the experimental variables and set-up used in its development i.e. crack widths between 0.2 and 0.7 mm, ground slag (both Corex slag and blastfurnace slag), and cover up to 40 mm.

Table 4.5: Predicted vs. actual corrosion rates for present study based on Scott's model (2004)

Mix Label	*Specimen condition*	*Corrosion rate ($\mu A/cm^2$)*		*% Deviation of actual from predicted*
		Actual (week 18)	*Predicted (cracked) (stable, 56 to 86 weeks)*	
PC-40	Incipient-cracked	0.16	1.25	-681
	0.4 mm cracked	0.51		-145
	0.7 mm cracked	0.92		-35
PC-55	Incipient-cracked	0.32	1.21	-280
	0.4 mm cracked	0.70		-71
	0.7 mm cracked	1.12		-8
SL-40	Incipient-cracked	0.04	0.25	-591
	0.4 mm cracked	0.29		14
	0.7 mm cracked	0.33		24
SL-55	Incipient-cracked	0.06	0.35	-523
	0.4 mm cracked	0.31		-13
	0.7 mm cracked	0.39		11

However, the differences between the actual and predicted corrosion rates in Table 4.5 may be due to significant differences in the experimental set up as shown in Table 4.6:

Table 4.6: Differences in experimental set up between Scott's study (2004) and present study

Experimental parameter	*Scott's study (2004)*	*Present study*
Type of reinforcing steel	High yield, plain (smooth)	High yield, deformed (ribbed)
Crack inducement mechanism	By bar slipping	By 3-point flexural loading
Type of binder used	GGBS (Blastfurnace slag)	GGCS (Corex slag)

It must also be appreciated that the predicted corrosion rates are long term stable corrosion rates (up to 86 weeks) while the actual values from this study are relatively early corrosion rates (25 weeks) and unstable.

(d) Comment on the use of durability index tests for cracked concrete

The three durability index tests measure different transport mechanisms in concrete to predict its potential durability performance. However, inasmuch as these tests provide very important indications of the expected durability performance of concrete in the service environment, they may not similarly predict the durability performance of cracked concrete, which occurs in most practical cases. However, these indexes are a powerful tool for performance-based RC durability design. They can be improved by finding correlations between the predicted uncracked concrete performance and actual long term performance of the cracked RC structure.

4.5 ***Effect of reloading on corrosion rate***

Reloading of the cracked beam specimens (incipient-cracked, 0.4 mm and 0.7 mm cracked) was done by opening the cracks to 0.2 mm, 0.6 mm and 1.0 mm respectively. The aim of reloading was to re-activate the cracks (especially self-healed cracks, if any) and consequently increase the corrosion rates. The first reloading was done between the 9^{th} and 10^{th} weeks while the second was done between the 18^{th} and 19^{th} weeks.

From Figure 4.1 to Figure 4.8, it is noticeable that after the 1^{st} reloading, there was no noticeable increase in corrosion rates, contrary to what might have been expected. Conceivably, the reloading was done somewhat too early for the effects of crack healing, if any, to be counteracted. However, the effect of the 2^{nd} reloading was quite evident, resulting in noticeable increases in corrosion rates which later reduced over a 5 week period. This can be attributed to accumulation of corrosion products in the crack and crack self-healing, although these were not verified. Table 4.7 gives the percentage increases in corrosion rates for the 2^{nd} reloading.

According to the corrosion rate results, the incipient-cracked specimens (except the PC-55 specimens) were still passively corroding (below 0.1 $\mu A/cm^2$) before and after the 2^{nd} reloading.

The minimal 2% increase in corrosion rate for the 0.7 mm cracked PC-55 specimens means that even before reloading, corrosion agents could easily penetrate to the steel and promote corrosion. Reloading therefore did not affect the concrete penetrability (with respect to corrosion rate) to a great extent.

Table 4.7 : Percentage increases in corrosion rates after 2nd reloading

Mix label	*Specimen condition*	*% increase*
PC - 40	Incipient-cracked	3
	0.4 mm cracked	13
	0.7 mm cracked	11
PC - 55	Incipient-cracked	16
	0.4 mm cracked	7
	0.7 mm cracked	2
SL - 40	Incipient-cracked	8
	0.4 mm cracked	10
	0.7 mm cracked	28
SL - 55	Incipient-cracked	9
	0.4 mm cracked	30
	0.7 mm cracked	12

Generally the highest increases in corrosion rate due to reloading were experienced in the 0.4 mm cracked specimens although the 0.7 mm cracked specimens also showed significant increments in some cases e.g. for SL-40. These specimens were actively corroding before the reloading process. A viable explanation to this observation is the reactivation of self-healed cracks, which increases the penetrability of concrete. For example Jacobsen *et al*. (1996) reported that crack self healing resulted in about 1/3 reduction in chloride ion migration. The same phenomenon of self-healing is expected to have taken place in the incipient-cracked specimens but the passive nature of the corrosion did not allow corrosion rate to increase substantially. As was mentioned earlier, smaller cracks (incipient cracks) are more prone to self-healing than wider ones (0.4 and 0.7 mm cracks). Corrosion agents may only be expected to increase corrosion rate once the passive protective layer on the steel surface is partially or fully destroyed due to chloride ingress. Reloading will therefore increase the corrosion rate substantially only if the steel is actively corroding. For passively corroding RC members, the effect of reloading will allow chlorides to reach the embedded steel and start (or accelerate) destroying the passive protective layer.

For an actively corroding RC structure, it can therefore be deduced that reloading may accelerate the corrosion process by:

(i) Widening the existing cracks
(ii) Re-activating (re-opening) the self-healed cracks
(iii) Increasing the loading level i.e. stress in the steel
(iv) All or a combination of the above

One important observation was made in the incipient-cracked beam specimens during the 2nd reloading process; the cracks did not completely close after load removal as occurred after the first reloading process i.e. there was permanent crack opening. This may be attributed to the accumulation of crack debris. The respective average residual crack widths along the specimen's top surface (Figure 4.15) for the different binder types are given in Table 4.8. A statistical analysis of the crack widths at a 95% confidence level showed that the crack widths can be grouped as ranging from 0.01 to 0.29 mm. However, they were still referred to as '*incipient-cracked*'.

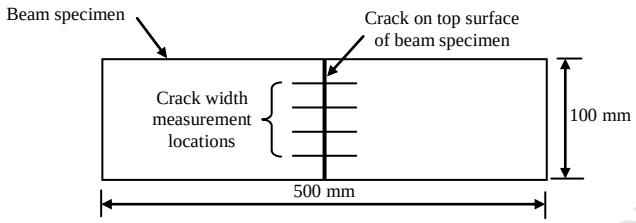

Figure 4.15: Plan of beam specimen showing crack width measurement locations (Incipient-cracked specimens)

Table 4.8: Residual crack widths in the incipient-cracked specimens after 2nd reloading

	Average residual*	*Standard*	*Range (95% confidence level)*	
Mix label	*crack width (mm)*	*deviation*	*Min*	*Max*
PC-40	0.14	0.04	0.01	0.28
PC-55	0.19	0.03	0.08	0.29
SL-40	0.14	0.03	0.05	0.23
SL-55	0.18	0.03	0.07	0.29

* Average of 4 readings

4.6 ***Relationship between corrosion rate, resistivity and half-cell potentials***

Chloride-induced corrosion of steel is dependent not only upon the chemical characteristics of the pore solution and ingress of chlorides but also on concrete resistivity. Concrete resistivity limits the ionic flow between the anode and cathode (Marta and Jezierski, 2005). However, Scott (2004) noted that the corrosion rate of the steel under passive conditions is sufficiently low as to not be governed by resistivity, or oxygen availability. At high active corrosion rates these factors become significant.

Three-point moving average resistivity measurements are given in Figure 4.16, which shows that GGCS specimens have higher resistivities than corresponding OPC specimens. Generally, the resistivity of all the concretes increased with time. This is attributed to ongoing hydration resulting in a reduction in pore solution conductivity, and with time, additional

microstructure densification (Hope *et al.*, 1985). Similar results have been obtained by Baweja (1996) and Scott (2004). Slag creates a finer pore size distribution (Malhotra, 1987) and lower ionic concentration, (Whiting and Nagi, 2003), which leads to higher electrical resistivity than in normal Portland cement concrete.

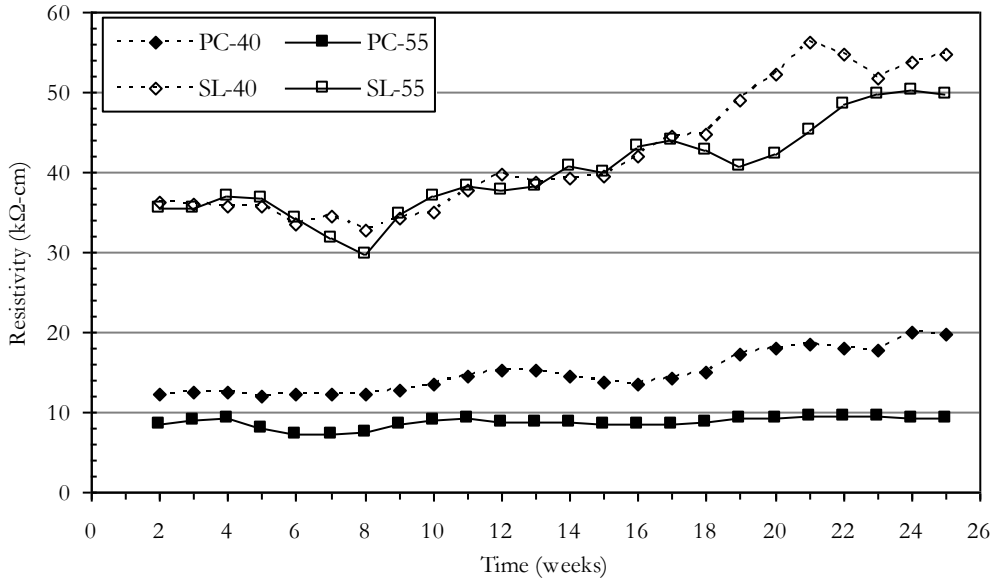

Figure 4.16: Moving average resistivity for the different binder types
(For both cracked and uncracked specimens)

The effect of w/b ratio also plays an important role in modifying the microstructure of cement paste and the ionic concentration of the pore solution (Shi, 2004). From the results obtained, it must however be realized that the effect of w/b ratio on concrete resistivity takes a secondary role after the binder type particularly for Corex slag concretes. It can therefore be deduced that binder type is more influential in this case than the w/b ratio in modifying the overall concrete resistivity.

The GGCS and OPC concretes show resistivities > 20 kΩ-cm and < 20 kΩ-cm respectively which according to Vienna (2002) should result in relatively low and moderate corrosion rates respectively. The resistivity is related to the ease with which ions can migrate through the concrete under the action of the potential field surrounding the anodes and cathodes. Comparing the corrosion rates and resistivity measurements, it is notable that corrosion rates for Corex slag specimens (having higher concrete resistivities) are lower than the corresponding OPC (having lower concrete resistivities) specimens. However, for a given binder corrosion rate increases with increasing crack width but the resistivity across the cracked specimens remained unchanged i.e. for a given binder there was no notable difference between the resistivity value of both the uncracked and cracked specimens. Similar results have been reported by Scott (2004). However, a study by Lataste *et al*. (2003) showed the

ability of concrete electrical resistivity to detect and locate cracks. The tests involved both on-site measurements on a damaged slab and laboratory measurements on a RC beam to confirm the results.

It must be noted that in this study, the resistivity measurements were taken at the end of the 4 days wetting (with 5% NaCl) period. This, to some extent, served as a pre-conditioning (pre-saturation) of the specimens and may have eliminated the sensitivity of the resistivity measurements to cracks because they were filled with the salt solution. This ensured a continuous electrical connectivity across the crack.

From Figure 4.16 and Figure 4.17, it can be seen that there is a significantly large difference in the resistivities of the OPC specimens than in the Corex slag specimens. This consequently suggests that the resistivity of Corex slag concretes is less sensitive to changes in w/b ratio i.e. 0.40 to 0.55.

Corrosion rates for the specimens were found to be inversely proportional to concrete resistivity (inverse of conductivity) as shown in Figure 4.17. It is notable that corrosion rates for Corex slag specimens (having higher concrete resistivities) are lower than the corresponding OPC (having lower concrete resistivities) specimens regardless of whether cra

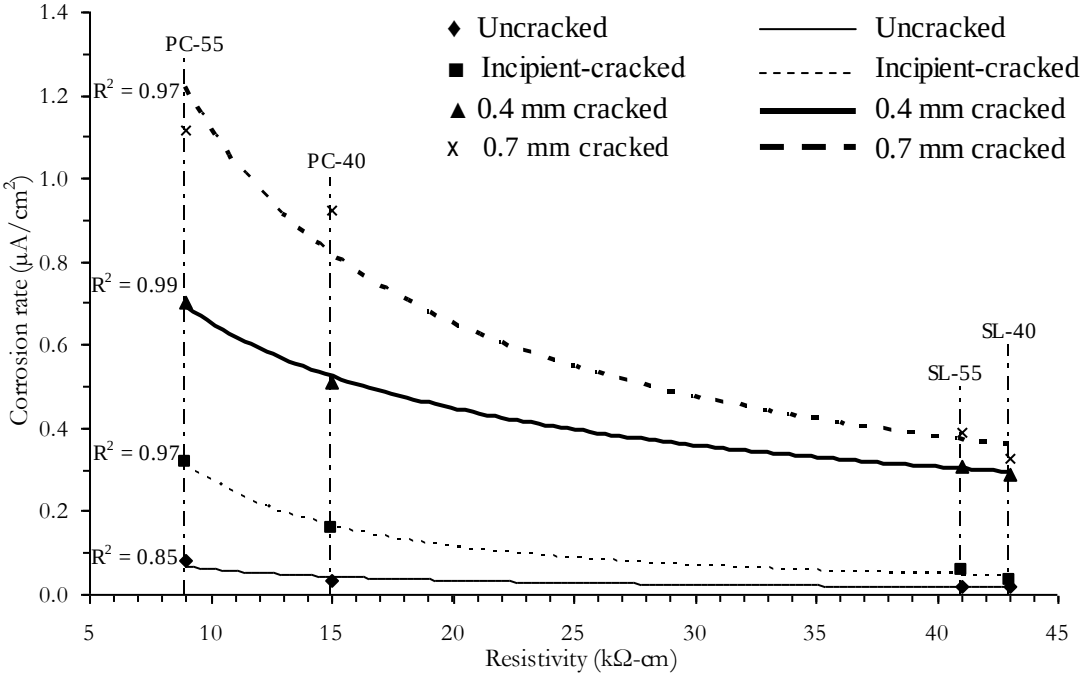

Figure 4.17: Relationship between average corrosion rate and concrete resistivity (weeks 12-18)

For clarity, the relationship between stable corrosion rates for the uncracked specimens and the respective concrete resistivities is reproduced separately in Figure 4.18.

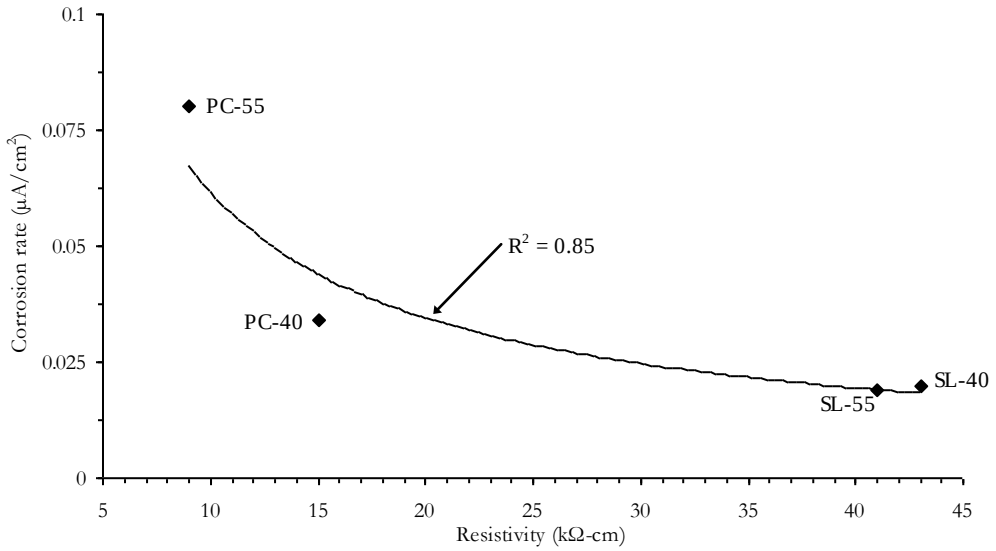

Figure 4.18: Relationship between average corrosion rate and concrete resistivity for uncracked specimens

The results also reveal that the effect of concrete resistivity is more influential than the crack width especially for the Corex slag specimens. For example, a 0.7 mm cracked specimen made using SL-55 mix had a lower corrosion rate that the 0.4 mm cracked specimen made using PC-40 mix. This clearly shows the dominating nature of high concrete resistivity in controlling corrosion rate even in the presence of cracks. A similar conclusion was reached by Scott (2004). Contrary to varying both the binder type and w/b ratio, only binder type was varied while the w/b ratio was kept constant at 0.58 in the study by Scott. Nevertheless, for comparison purposes only, the cause of the resultant concrete resistivity is not of importance if the testing criteria are the same.

The high correlation coefficient ($R^2 > 0.8$) between corrosion rate and concrete resistivity may therefore not give a true picture of the actual expected corrosion rates in cracked concrete. Resistivity values are therefore more reliable as corrosion performance indicators for uncracked concrete than for cracked concrete and should not be recommended as a corrosion assessment technique for the latter.

On the contrary, it seems that resistivity can serve as a good first indicator for corrosion activity in RC structures. What is required is a means of also allowing for the effects of cracking. With sufficient data from long term studies, a relationship between corrosion rate and resistivity for both uncracked and cracked concrete (of various crack widths) can be established.

In this study, resistivity values were more reliable as corrosion performance indicators for uncracked concrete than for cracked concrete mainly due to the specimen preconditioning already mentioned. However, a study by Scott (2004) revealed that the lower corrosion rates are not simply a function of resistivity alone. The reduction in corrosion rates is also dependant upon limiting the availability of oxygen at low rates of corrosion and the enhanced chloride binding effects of slag concrete. Concrete cover is also an important factor for low resistivity concrete. Scott and Alexander (2007) schematically presented this phenomenon as presented in Figure 4.19. The simultaneous interaction between these factors (cover, resistivity and oxygen availability) may govern the resulting corrosion rate depending on the dominating factor(s).

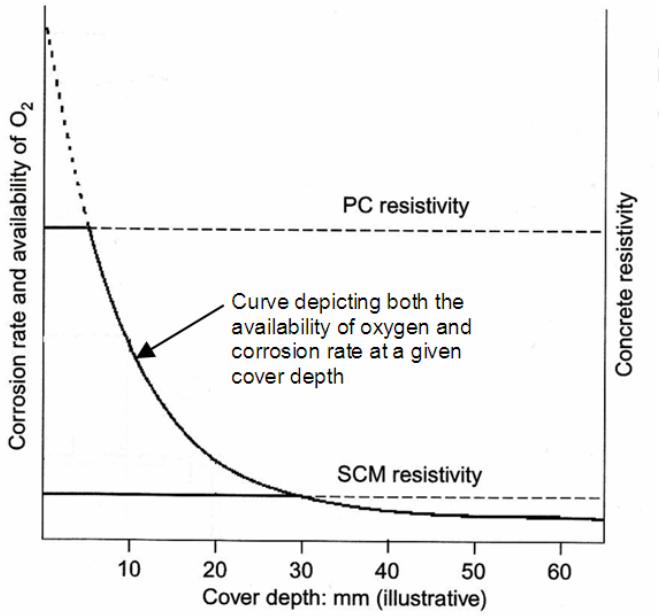

Figure 4.19: Schematic of the relationship between corrosion rate, O_2 availability and resistivity (PC: ordinary Portland cement, SCM: supplementary cementitious materials) (Scott and Alexander, 2007)

Therefore, corrosion rates of blended cements are mainly controlled by the resistivity of the concrete while rates in OPC are mainly governed by availability of oxygen and consequently, cover depth.

However, the results may be used to predict the corrosion rates for cracked concrete based on resistivity measurements on sound uncracked specimens (similar to the chloride conductivity index) in the laboratory. From long term studies (sufficient data), a relationship between corrosion rate and resistivity for uncracked concrete can be established. The model may take the form:

$$i_{corr} = f(concrete\ resistivity) \quad (4.2)$$

Concrete resistivity may be replaced by the chloride conductivity index which is basically a form of resistivity measurement procedure. This is because the chloride conductivity test, as opposed to the concrete electrical resistivity measurement, has been well developed/standardised for use as a potential durability performance indicator. Furthermore, it was seen in section 4.4(c) that there exists a high correlation between corrosion rate and the chloride conductivity index.

On the other hand, half-cell potential (HCP) measurements (see Figure A.4 to Figure A.11, Appendix A) are more reliable than the resistivity measurements. Generally, the trends in the half-cell potentials (HCP) for all the binder types and crack widths correspond to those for corrosion rates over the same period. According to ASTM C876-91, if the HCP measured is lower (more negative) than -256 mV (Ag/AgCl), there is a 90% probability that the reinforcement is actively corroding. For a given binder, the cracked specimens show more negative corrosion potentials (E_{corr}) than the uncracked specimens indicating correspondingly higher corrosion rates (Figure 4.20 to Figure 4.23). However, the HCP trends do not clearly show changes in corrosion rates due to effects of reloading (Figure A.4 to Figure A.11). Furthermore, there is not much significant difference in the HCP values for both uncracked and incipient-cracked Corex slag specimens as was observed in the corrosion rate results.

It must be noted that there is no general correlation between corrosion rate and half-cell corrosion potentials (Andrade *et al*., 2003). This lack of a clear correlation can be attributed to the fact that both parameters respond differently to the same variables, particularly moisture (or oxygen availability), temperature and concrete resistivity values. The relationship between corrosion rate and half-cell potentials obtained in this study may therefore only be applicable to the experimental set-up used. Half-cell potential measurements must be complemented by other methods, because although reliable relationships between potential and corrosion rate can be found in the laboratory for well established conditions as in this study; such relationships cannot be generalised, since wide variations in the corrosion rate are possible in a narrow range of potentials.

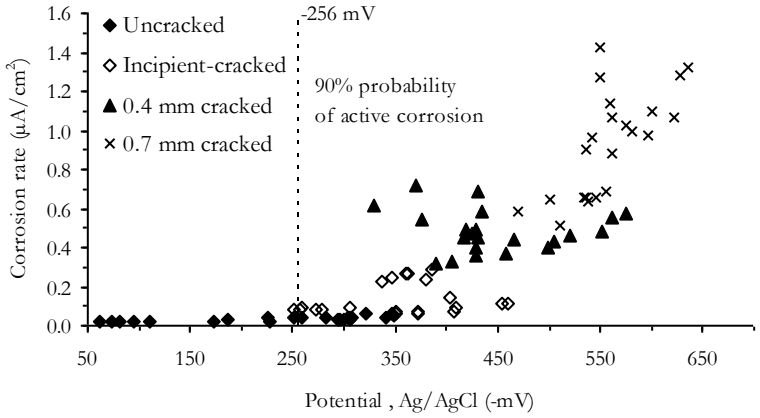

Figure 4.20: Corrosion rate vs. half-cell potentials - PC-40 mix

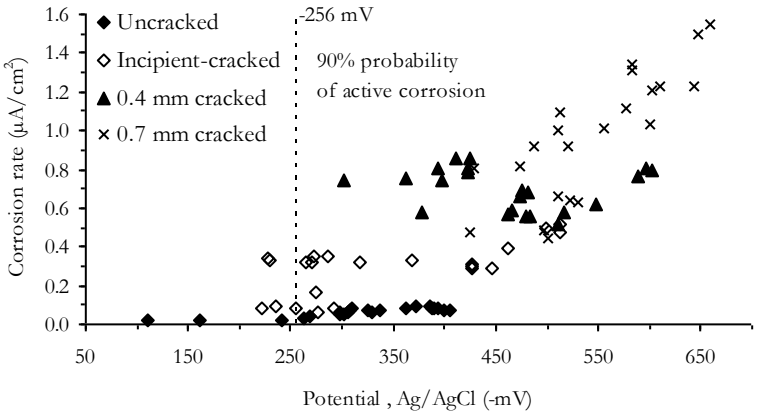

Figure 4.21: Corrosion rate vs. half-cell potentials - PC-55 mix

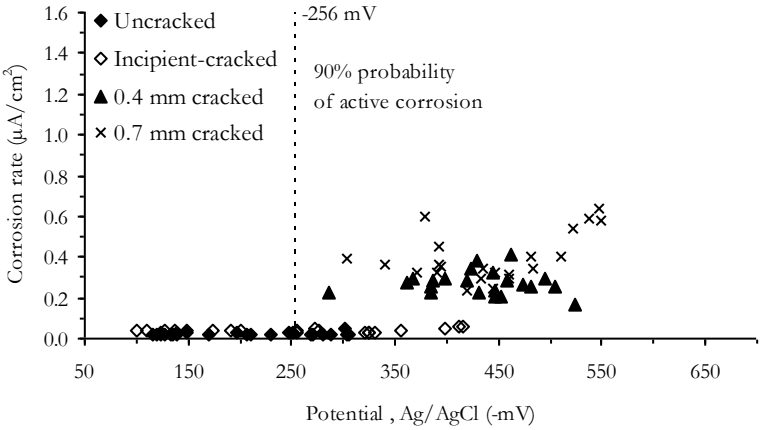

Figure 4.22: Corrosion rate vs. half-cell potentials - SL-40 mix

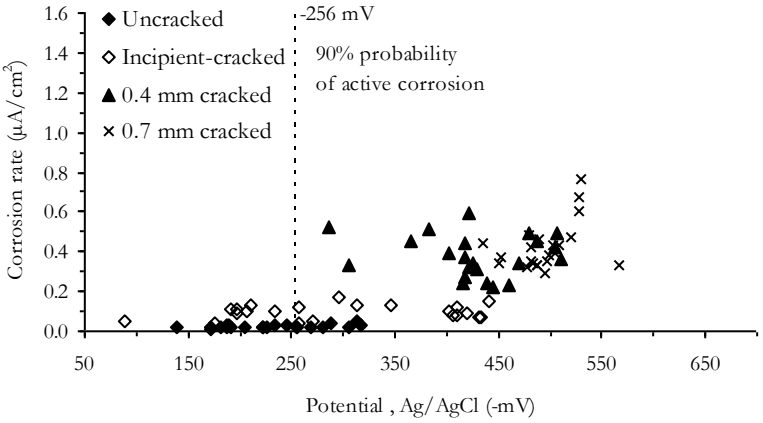

Figure 4.23: Corrosion rate vs. half-cell potentials - SL-55 mix

From Figure 4.20 to Figure 4.23, it is clear that the spread in corrosion rates for the different crack widths is more significant in the OPC specimens (PC-40 and PC-55) than in the Corex slag specimens (SL-40 and SL-55) (Figure 4.20 to Figure 4.23). This is in agreement with the corrosion rate results.

These observations stress the fact that HCP measurements need to be supplemented with other corrosion assessment techniques such as linear polarisation resistance (LPR) as was done in this study. It must be remembered that the link between HCP and corrosion rate is concrete resistivity. Both depend on the ease of ion movement in the concrete which is governed by resistivity. However, as mentioned earlier, both respond differently to changes in the same variables.

*4.7 **General discussion and closure***

The increase of crack width has been noted to have a significant influence on the corrosion rate for both Corex slag and OPC specimens. However, the difference in corrosion rates between uncracked and incipient-cracked, and 0.4 and 0.7 mm cracked Corex slag specimens were not large compared to that in the respective OPC specimens for the same crack widths. This consequently leads to the conclusion that the Corex slag concrete is less sensitive to the effects of cracking. The cause of this is mainly the high concrete resistivity exhibited by the Corex slag concrete relative to OPC concrete. In general, corrosion rate in Corex slag concrete is governed by the (high) concrete resistivity while in OPC concrete, the governing factor in oxygen availability.

Corex slag concretes have proven to be less sensitive to changes in w/b ratio than OPC concretes. This can be advantageous (and even economical) if a careful trade-off between, for example, strength and durability (penetrability) is sought during concrete mix design process. For example, it may not be necessary to use a low w/b ratio to attain low penetrability at the

expense of unnecessarily high strength. This is because the negative impact of high penetrability in the resultant Corex slag concrete can be overrun by the high concrete resistivity exhibited by Corex slag concretes. This phenomenon is however not applicable to OPC concretes.

These results also help to justify, to some extent, the idea of w/b ≤ 0.55 as being a useful limit for structural marine concrete. Furthermore the relatively high corrosion rates in the OPC concretes at relatively high w/b ratios (in this case 0.55) also strengthen the fact that OPC concrete is not good for structural concrete applications in the marine environment.

The impact of occasional flexural re-loading has been shown to depend on the nature of the corrosion (i.e. passive or active) prior to re-loading. In general the highest increases in corrosion rates were observed in specimens that were actively corroding prior to re-loading. Specifically, this was noted in the '*real*' cracked (0.4 and 0.7 mm) Corex slag specimens (at both 0.40 and 0.55 w/b ratios) and only in OPC specimens at low w/b ratio (0.40).

A good correlation has been found to exist between corrosion rate and concrete resistivity (or its inverse conductivity, as was seen in the chloride conductivity index results) for both cracked and uncracked concrete. However, this was found to be unreliable as the corrosion rates observed were higher for the cracked specimens. The resistivity (or its inverse conductivity) was therefore only reliable for the uncracked concrete. Nevertheless, both the concrete resistivity and chloride conductivity index values are still important first indicators of the potential durability of concrete. What is needed is to determine correction factors to be applied to the resistivity (or chloride conductivity index) values to account for the crack widths. On the contrary, the half-cell potentials correlated well with the corrosion rates for both the cracked and uncracked specimens. However, previous studies have shown that there is no general relationship between corrosion rate ad half-cell potential. The good correlation obtained in this study may therefore only be applicable to the experimental set up used in this study.

The phenomenon of crack self-healing was dealt with in this study by inference form previous studies and therefore no direct conclusions can be drawn from it. One aspect that has come up is the importance of the knowledge of limiting crack width above which crack self-healing cannot occur. This is important for RC durability design and can be incorporated in building codes. However, apart from just knowing this limiting crack width, another important question is how long it takes for the crack to heal. This is vital when the aggressiveness of the RC service environment is taken into consideration. It is therefore important to consider both the limiting crack width and time for the self-healing to take place in RC durability design.

Therefore inasmuch as it is useful to understand how crack self-healing works, it is also important to know when it works (limiting crack width), how to promote it, how long it takes and how to take advantage of it.

The next chapter will give the conclusions based on a critical evaluation and discussion of the experimental results of this study and recommendations for future study.

4.8 ***References***

Alexander M. G., Ballim Y. and Mackechnie J. R. (1999), Concrete durability index testing manual, *Research Monograph No. 4*, University of Cape Town, Department of Civil Engineering

Andrade, C., Gulikers, J., Polder, R. and Raupach, M., (2003), Half-cell potential measurements-Potential mapping on reinforced concrete structures, *Materials and Structures*, 36, pp 461-471.

ASTM C876-91, (1999), Standard test method for half cell potentials of uncoated reinforcing steel in Concrete.

Bakker, R.F.M., (1983), Permeability of blended cement concretes, Proceedings of the *CANMET/ACI First international conference on the use of Fly ash, Silica fume, Slag and other mineral by-products in concrete*, pp. 589-605.

Baweja D., Roper H. and Sirivivatnanon, V., (1996), Corrosion of Steel in Marine Concrete: Long-Term Half-Cell Potential and Resistivity Data, *Proceedings, Third CANMET/ACI International Conference on Concrete in Marine Environment*, SP-163, American Concrete Institute, Farmington Hills, MI, pp 89-110

Ballim, Y., (1993), Towards an early-age index for the durability performance of concrete, proceedings of the international conference, *Economic and durable construction through excellence*, Dundee, London, E&FN Spon, pp. 1003-1012.

Beushausen, H.-D. and Alexander, M. G., (2008), The South African durability index tests in an international comparison, *Journal of the South African institution of civil engineering*, 50(1), pp. 25-31.

Clear, C. A., (1985), The effects of autogenous healing upon the leakage of water through cracks in concrete, *Cement and Concrete Association report No. 559*.

Glass, G. K., Hassanein, N. M. and Buenfeld, N. R., (1997), Neural network modelling of chloride binding, *Magazine of Concrete Research*, 49, pp. 323-335.

Gautefall, O. and Vennesland, O., (1983), Effect of cracks in the corrosion of embedded steel in silica-concrete compared to Ordinary concrete, *Nordic Concrete Research*, No. 2, pp. 17-28.

Hearn, N. and Morley, C. T., (1997), Self-sealing property of concrete – experimental evidence, *Materials and Structures*, 30, pp. 404-411.

Hearn, N. (1998), Self-sealing, autogenous healing and continued hydration: what is the difference?, *Materials and Structures*, 31, pp. 563-567.

Hope, B. B., Ip, A. K. and Manning, D. G., (1985), Corrosion and electrical impedance in concrete, *Cement and Concrete Research*, 15(3), pp. 525 to 534.

Jacobsen, S., Marchand, J. and Boisvert, L., (1996), Effect of cracking and healing on chloride transport in OPC concrete, *Cement and Concrete research*, 26(6), pp. 869-881.

Lataste, J. F., Sirieix, C., Breysse, D. and Frappa, M., (2003), Electrical resistivity measurement applied to cracking assessment on reinforced concrete structures in civil engineering , *NDT & E international*, 36(6), pp. 383-394.

Malhotra, V. M., (1987), Properties of fresh and hardened concrete incorporating ground granulated blastfurnace slag, *Supplementary Cementing Materials for Concrete*, ed. Malhotra V.M., Ottawa: Canadian Government Publishing Centre, pp. 291-331.

Marta, K.-K. and Jezierski, W., (2005), Evaluation of concrete resistance to chloride ion penetration by means of electrical resistivity monitoring, *Journal of Engineering Management*, 11(2), pp. 109-114.

Mohamed, B., Sakai, K., Banthia, N., and Yoshida, H., (2003), Prediction of chloride ions ingress in uncracked and cracked concrete, *ACI Materials Journal*, 100(1), pp. 38-48.

SANS 10100-2, (1994), *South African Standard Code of practice*, The structural use of concrete, Part 2: Materials and execution of work (as amended, 1994).

Shi, C., (2004), Effect of mixing proportions of concrete on its electrical conductivity and the rapid chloride permeability test (ASTM C1202 or ASSHTO T277) results, *Cement and Concrete Research*, (34), pp. 537-545.

Scott, A. N., (2004), The influence of binder type and cracking on reinforcing steel corrosion in concrete, *PhD Thesis*, University of Cape town.

Scott, A. N. and Alexander, M. G., (2007), The influence of binder type, cracking and cover on corrosion rates of steel in chloride-contaminated concrete, *Magazine of Concrete Research*, 59(7), pp. 495-505.

Vennesland and Gjorv, (1981), cited by Neville, A. M., (2002), Autogenous healing - A concrete miracle?, *Concrete International*, November issue, pp. 76-82.

Vienna, (2002), *Guidebook on non-destructive testing of concrete structures*, International Atomic Energy Agency.

Wang, K., Daniel, C. J. and Surendra, P. S., (1997), Permeability study of cracked concrete, *Cement and Concrete Research*, 27(3), pp. 381-393.

Whiting, D. A. and Nagi, M. A., (2003), Electrical resistivity of concrete - A literature review, *Portland Cement Association*, Illinois, pp. 56.

Yoon, S., Wang, K., Weis, W. J., and Shah, S. P., (2000), Interaction between loading, corrosion, and serviceability of reinforced concrete, *ACI Materials Journal*, 97(6), pp. 637-644.

Chapter 5

5 CONCLUSIONS AND RECOMMENDATIONS

5.1 CONCLUSIONS

The objective of this study was to investigate the influence of crack width and crack re-opening on corrosion propagation. The results indicate that these factors affect corrosion rate. Other factors being constant, an increase in surface crack width will lead to increased corrosion rates although to a lesser extent in the blended cement specimens. Re-opening of cracks also results in increased corrosion rates. These factors will be critically evaluated in this chapter in a more general sense based on the results and discussion presented in Chapter 4.

5.1.1 Effect of crack width and binder type on corrosion rate

The results show that corrosion rate increases with increasing crack width but is sensitive to concrete quality. For a given binder type and w/b ratio, corrosion rate increased with increasing crack width while for a given crack width, corrosion rate increased in the following order: SL-40 < SL-55 < PC-40 < PC-55. These observations can be summarised as two distinct scenarios as follows:

(i) For a given crack width, corrosion rate is sensitive to binder type.
(ii) For a given binder type and w/b ratio, corrosion rate is sensitive to crack width.

However, a comparison of the corrosion rates of all the specimens showed that the high concrete resistivity was more influential than crack width for the Corex slag specimens. Moreover, the increase in corrosion rates with increasing crack width was less significant in the Corex slag specimens (SL-40 and SL-55). For example, at the end of the 18th week, increase in crack width from 0.4 mm to 0.7 mm in an SL-40 specimen resulted in 13% increase (from 0.29 to 0.33 µA/cm^2) in corrosion rate while for a PC-40 specimen, over 80% increase (from 0.51 to 0.92 µA/cm^2) was noted for increase in crack width from 0.4 mm to 0.7 mm. In general, corrosion rates in Corex slag concretes are governed by the concrete resistivity as opposed to OPC concretes which are governed by the availability of oxygen.

There was little difference in corrosion rates for both uncracked and incipient-cracked Corex slag specimens compared to OPC specimens. Significant differences in Corex slag specimens were only noticed in the '*real*' cracked specimens (0.4 and 0.7 mm). Corex slag concretes were less sensitive to changes in w/b ratio (from 0.40 to 0.55). This was also exhibited in the concrete resistivity and chloride conductivity index test results. In RC

durability design, advantage can be taken of this, together with the fact that Corex slag concretes generally have high resistivities. In particular, a balance can be struck between the achievement of the required strength and durability performances of RC structures in the marine environment. This can subsequently lead to significant economic savings, both in the short term and in the long term. It is not mandatory to have unnecessarily high strengths (low w/b ratio) in order to attain the required low concrete penetrability i.e. durable concrete. The same can be achieved by the high concrete resistivities in Corex slag concretes without having to greatly lower the w/b ratio.

The use of a blended cement (50/50 OPC/Corex slag) was also found to not only lengthen the passive corrosion state of the uncracked RC but also had a significant influence on the corrosion rates of cracked RC. This can be explained using Scott and Alexander's (2007) schematic diagram (Figure 5.1). In blended cements, concrete resistivity may be the dominating factor that governs the corrosion rate. For OPC concrete, oxygen availability (and hence cover depth) is the governing factor. The results of this study follow this trend although the influence of cover cannot be verified as this was kept constant (at 40 mm).

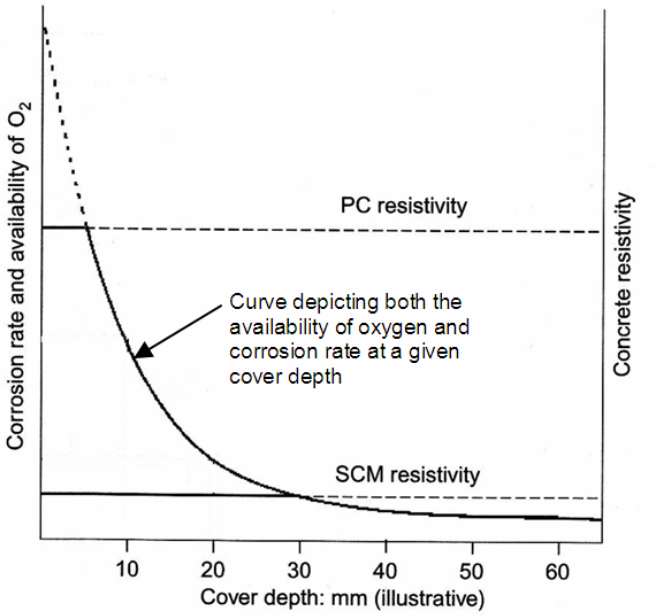

Figure 5.1 : Schematic of the relationship between corrosion rate, O_2 availability and resistivity (PC: ordinary Portland cement, SCM: supplementary cementitious materials) (Scott and Alexander, 2007)

*5.1.2 **Effect of crack re-opening on corrosion rate***

Crack re-opening (reloading) increased corrosion rate but only if the steel was actively corroding (i.e. corrosion rate was greater than 0.1 µA/cm^2) prior to reloading. In the presence of cracks, reloading may serve to widen the cracks, re-activate (re-open) self-healed cracks,

increase the loading level (i.e. stress in the steel) or all or a combination thereof. The maximum increase in corrosion rate was noted in the 0.4 mm cracked specimens where corrosion rate was decreasing before the reloading; a trend that was (by inference from previous studies) attributed to crack self-healing. Further study is required to verify this.

In practice, RC structures (e.g. bridges) are usually subjected to sustained, cyclic, occasional or fatigue loads, or a combination of these. The degradation of these structures by corrosion is therefore expected to be faster depending on the loading level and the frequency of the cyclic or occasional load.

This study dealt with only occasional reloading; a study by Yoon *et al*. (2000) showed that sustained loading also increases corrosion rate but this is also dependent on the loading level, with higher corrosion rates being experienced due to higher loading levels. Wide flexural cracks require higher loading levels than smaller ones and will therefore be subjected to higher stress levels. This was experienced in this study by the fact that the wider cracks required higher flexural cracking loads than the smaller ones. These loading levels were sustained in the specimens as corrosion proceeded. Therefore, the observed increases in corrosion rate cannot only be attributed to wider crack widths, binder type and reloading. The influence of sustained loading and loading level are also suspected to have contributed to the high corrosion rates.

5.1.3 ***General conclusions***

This study has made a stride towards understanding the combined influence of cracking, crack width, crack re-opening (re-loading), binder type and w/b ratio on chloride-induced corrosion in reinforced concrete structures. The following general conclusions can therefore be drawn from this study:

(i) Cracks accelerate chloride-induced corrosion by increasing concrete penetrability. The wider the crack width, the higher the corrosion rate. However, the effect of cracks on corrosion rate is modified by the concrete quality (this was mainly governed by the both binder type and w/b ratio).
   - In general, concrete quality (as depicted by penetrability and resistivity) may be used to control corrosion of steel in cracked concrete, especially for slag blended concrete.
   - In particular, Corex slag concretes (where corrosion rate is governed by the (high) concrete resistivity) have shown to be less sensitive to the effects of cracking compared to OPC concretes (with low concrete resistivities). Furthermore, Corex slag concretes are less sensitive to small changes in w/b ratio compared to OPC concretes.

(ii) Reloading of corroding RC structures/members accelerates corrosion by re-activating (re-opening) self-healed cracks, widening the existing ones, increase the loading level (i.e.

stress in the steel) or all or a combination thereof. However, the effect of reloading is more significant if the RC structure was actively corroding prior to reloading.

Based on the above premises, it is therefore important that these factors be quantified and incorporated in (corrosion propagation) service life prediction models to improve on their accuracy.

5.2 RECOMMENDATIONS

The following recommendations for further work are put forward based on this study:

(a) Quantification of crack self-healing

In this study, crack self-healing was assumed to have occurred in the cracked specimens but was not quantified. It would be interesting to carry out an assessment of the crack using a scanning electron microscope (SEM), an optical microscope or methods such as X-ray diffraction (a method used in the identification of fine-grained, crystalline compounds such as calcite, $CaCO_3$). The quantification of crack self-healing will enable its incorporation into service life models.

(b) Controlled laboratory environment

The corrosion rate monitoring should be carried out in a controlled environment of temperature and relative humidity. This can minimise the fluctuation in the actual corrosion rate due to variability of these parameters.

(c) Correlation with on-site corrosion rate measurements

The corrosion rates obtained in the laboratory especially for the cracked concrete should be correlated with on-site measurements. If necessary, correction factors may be applied in order to reliably predict corrosion rates.

(d) Concrete resistivity as potential durability indicator

Concrete resistivity measurement can be developed to become a potential durability indicator both in the laboratory and on site. This however requires more research to find out its sensitivity to different binder types, sample conditioning and, at what age it can be reliable when measured.

(e) Further laboratory experiments

This study can be extended by carrying out long term laboratory experiments, introducing more variables (binder types, crack widths, w/b ratios). The ultimate focus should be to develop a service life prediction model for corrosion propagation taking into account the effects cracks. This would mean establishing what criteria to use to precisely define 'end of service life'.

(f) Chloride distribution in cracked concrete

In order to establish quantitative data for service life prediction, the chloride content distribution at different depths of the cracked concrete and in the vicinity of the cracks is vital. Some data is available from Scott's study (2004) but more is needed.

(g) Limiting crack width vs. cover depth

The limitation of the surface crack width for RC durability purposes should be related to the cover depth. Further work should be done to establish the relationship between corrosion rate and different surface crack widths and concrete covers for various binder types.

5.3 ***References***

Alexander, M. G. and Beushausen H.-D, (2007), Performance-based durability design and specification in South Africa, *Proceedings of International Concrete Conference and Exhibition* (ICCX - Concrete Awareness), 14-16 February 2007, Cape Town, South Africa, pp. 12-15.

SANS 10100-2, (1994), *South African Standard Code of practice*, The structural use of concrete, Part 2: Materials and execution of work (as amended, 1994).

Scott, A. N., (2004), The influence of binder type and cracking on reinforcing steel corrosion in concrete, *PhD Thesis*, University of Cape town.

Scott, A. N. and Alexander, M. G., (2007), The influence of binder type, cracking and cover on corrosion rates of steel in chloride-contaminated concrete, *Magazine of Concrete Research*, 59(7), pp. 495-505.

Yoon, S., Wang, K., Weis, W. J., and Shah, S. P., (2000), Interaction between loading, corrosion, and serviceability of reinforced concrete, *ACI Materials Journal*, 97(6), pp. 637-644.

Appendix A

EXPERIMENTAL RESULTS

A1 *Compressive strength and density results*

Table A.1: Compressive strength results

Mix label	*Age (days)*	*Average**		*Std. Dev.*
		Density (kg/m^3)	*Strength (MPa)*	
PC-40	*7*	2433	42.3	0.3
	28	2432	49.5	1.3
	90	2460	56.8	2.1
PC-55	*7*	2365	26.8	1.6
	28	2372	32.5	2.1
	90	2363	36.2	1.3
SL-40	*7*	2428	46.9	0.5
	28	2433	51.9	0.5
	90	2428	61.5	1.0
SL-55	*7*	2388	28.8	2.8
	28	2403	33.0	2.1
	90	2383	40.9	1.4

* Average of 3 readings

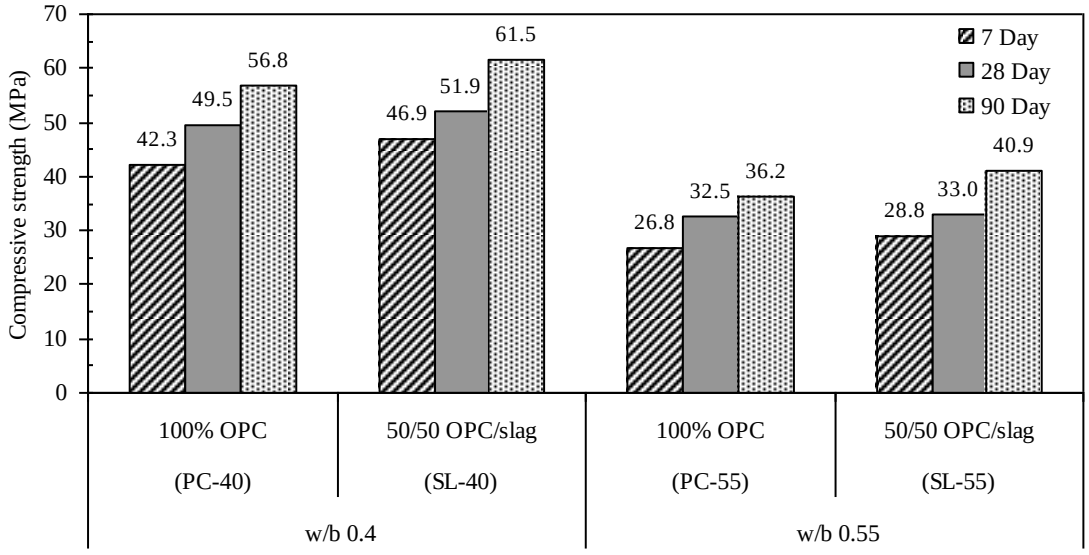

Figure A.1: 7, 28 and 90 day compressive strengths for the different mixes

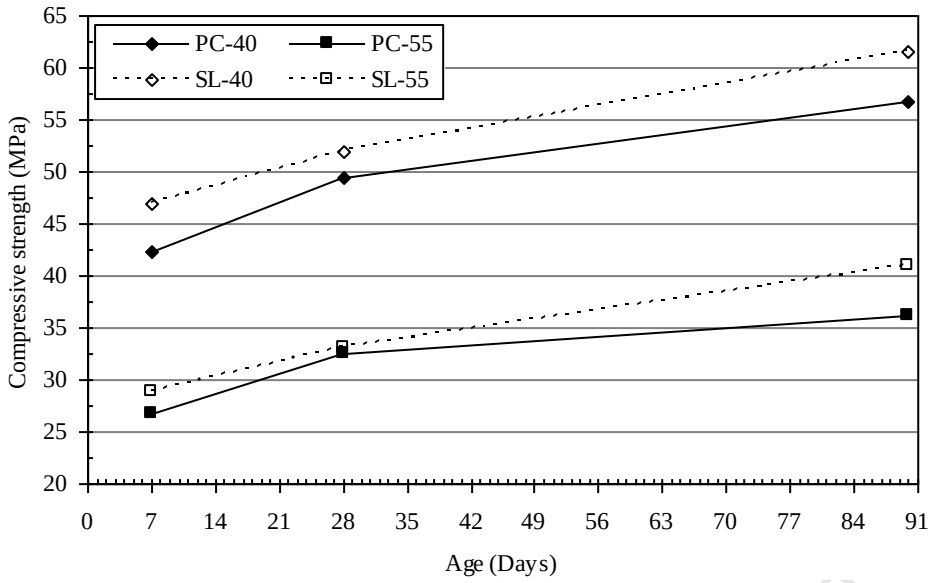

Figure A.2: Compressive strength development

A2 ***Durability index (DI) test results***

Table A.2: Durability index test results

Durability Index test			*PC-40*	*SL-40*	*PC-55*	*SL-55*
Oxygen Permeability Index	*Average** ($\bar{X}$)		**10.16**	**10.42**	**10.19**	**10.25**
	Standard deviation (σ)		0.05	0.11	0.07	0.04
	Coeff. of variation (%)		0.44	1.03	0.67	0.35
	Deviation (t-value=3.182) (d)		0.14	0.34	0.22	0.12
	Range	*Min.*	10.01	10.08	9.97	10.13
		Max.	10.30	10.77	10.40	10.37
Water Sorptivity Index	*Average** ($\bar{X}$)		**6.9**	**6.5**	**7.6**	**7.4**
	Standard deviation (σ)		0.2	0.3	0.1	0.1
	Coeff. of variation (%)		2.5	3.9	2.0	1.9
	Deviation (t-value=3.182) (d)		0.54	0.80	0.48	0.45
	Range	*Min.*	6.3	5.7	7.1	6.9
		Max.	7.4	7.3	8.1	7.9
Chloride Conductivity Index	*Average** ($\bar{X}$)		**1.05**	**0.25**	**1.50**	**0.34**
	Standard deviation (σ)		0.08	0.02	0.21	0.04
	Coeff. of variation (%)		7.3	9.7	14.3	11.4
	Deviation (t-value=3.182) (d)		0.24	0.08	0.68	0.12
	Range	*Min.*	0.81	0.17	0.82	0.22
		Max.	1.29	0.33	2.18	0.47

* Average of 4 readings

where: *Range* = $\bar{X} \pm$ d

d = $t\ \sigma$, The *t*-value is selected for a 95% confidence level

Table A.3: Corresponding oxygen permeability coefficients (*k*)

		Coeff. of oxygen permeability, k (m/s) x 10^{-11}			
		PC-40	*SL-40*	*PC-55*	*SL-55*
*Average** ($\bar{x}$)		**6.92**	**3.80**	**6.46**	**5.62**
Standard deviation (σ)		3.66	1.28	1.12	1.19
Coeff. of variation (%)		5.29	3.38	1.73	2.12
Deviation (t-value=3.182) (d)		1.16	4.08	3.57	3.79
Range	*Min.*	6.80	3.39	6.11	5.24
	Max.	7.03	4.21	6.82	6.00

* Average of 4 readings

A3 *Beam flexural cracking loads*

Table A.4: Average flexural cracking loads

Mix label	*Average* cracking load (kN)*		
	Incipient crack	*0.4 mm crack*	*0.7 mm crack*
PC-40	7.0	14.5	15.1
PC-55	6.6	12.8	13.4
SL-40	6.7	14.0	14.2
SL-55	6.0	12.8	13.1

* Average of 3 readings

A4 *Aggregate sieve analysis*

Table A.5: Fine aggregate (Pilippi dune sand) sieve analysis

Sieve size (µm)	*Mass retained (g)*	*% Mass retained*	*Cumulative % mass retained*	*Cumulative % mass passing*
2360	0	0	0	100.0
1180	2.78	0.6	0.6	99.4
600	62.5	12.5	13.1	86.9
300	212.73	42.5	55.6	44.4
150	212.73	42.5	98.1	1.9
75	8.75	1.8	99.9	0.1
<75	0.51	0.1	100.0	0
Sample size: **500 g**				

Table A.6: Coarse aggregate (Greywacke) sieve analysis

Sieve size (mm)	*Mass retained (g)*	*% Mass retained*	*Cumulative % mass retained*	*Cumulative % mass passing*
26.5	0	0	0	100.0
19.0	118.1	11.8	11.8	88.2
13.2	716.0	71.6	83.4	16.6
9.5	162.3	16.2	99.6	0.4
6.7	3.6	0.4	100.0	0
Sample size: **1000** g				

A5 *Corrosion rate results for all specimens*

The 3-point moving average corrosion rate results for all the specimens presented in Figure A.3. The calculation of 3-point moving average was done as follows:

A5.1 *Calculation of moving average*

An *n*-point moving average (also referred to as *running mean*) represents the average of the respective sample and the *n*-1 number of preceding samples (Chambers *et al*., 1983). A moving average smoothes data by replacing each data point with the average of the neighbouring data points defined within the range of data points. The following expression is used (Cleveland and Devlin, 1988):

$$y_s(i) = \frac{1}{2\mathrm{N}+1}\left[y(i+\mathrm{N}) + y(i+\mathrm{N}-1) + ... + y(i-\mathrm{N})\right] \qquad \text{(A.1)}$$

where: $y_s(i)$ = Moving averaged value for the i^{th} data point

N = Number of neighbouring data points on either side of $y_s(i)$

In this study, a 3-point moving average was adopted for the analysis of corrosion rate, resistivity and half-cell potential results. For example: take corrosion rate averaged values for weeks 1-5 i.e. i_1, i_2, i_3, i_4 and i_5. According to equation (A.1):

The 1st moving averaged data point is: $\left(\frac{i_1 + i_2 + i_3}{3}\right)$ and is plotted on the 2nd week;

The 2nd moving averaged data point is: $\left(\frac{i_2 + i_3 + i_4}{3}\right)$ and is plotted on the 3rd week;

and so on.

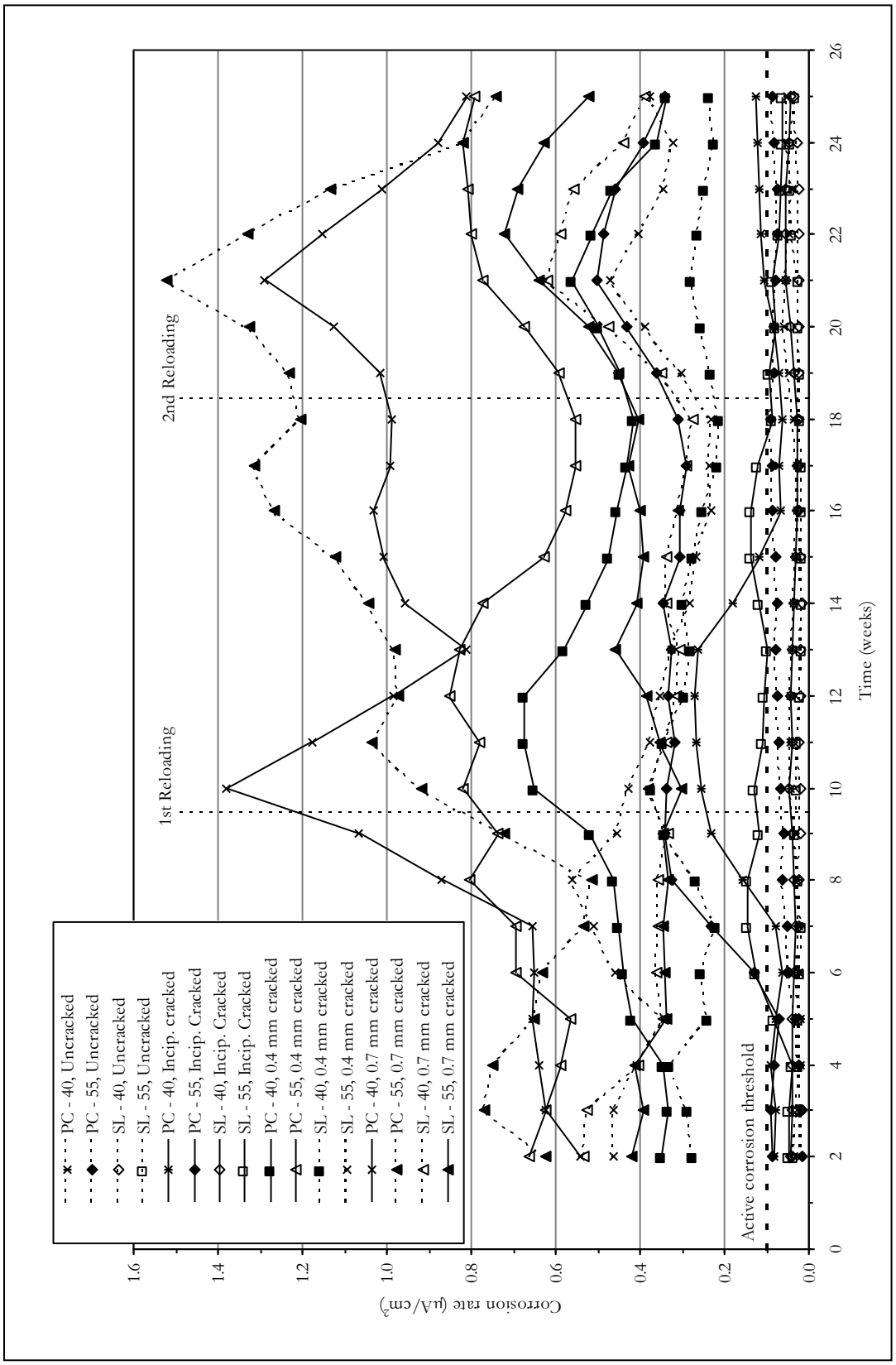

Figure A.3: Corrosion rate results for all specimens

A6 ***Half-cell potentials results***

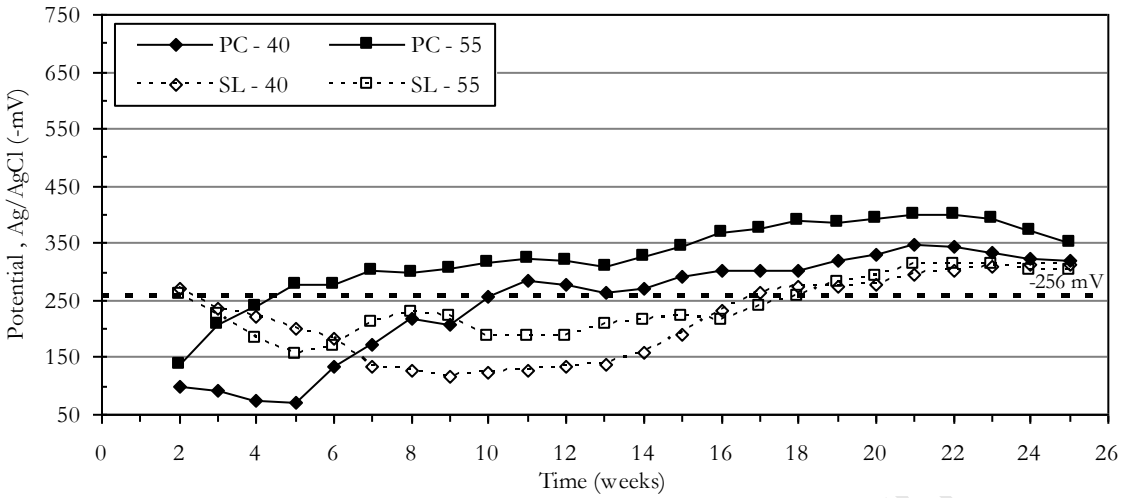

Figure A.4: 3-point moving average half-cell potentials – uncracked

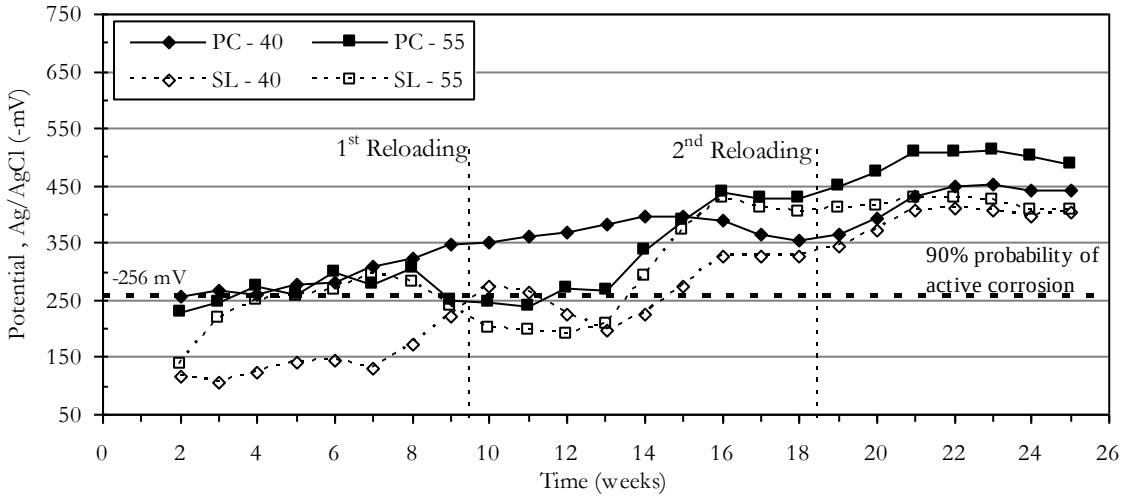

0.4 mm cracked

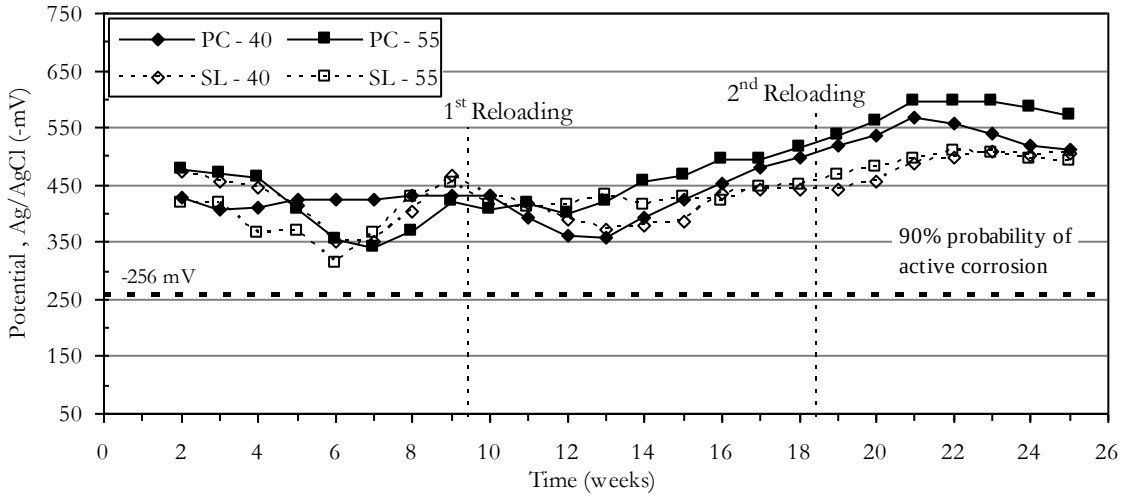

Figure A.6: 3-point moving average half-cell potentials - 0.4 mm crack width

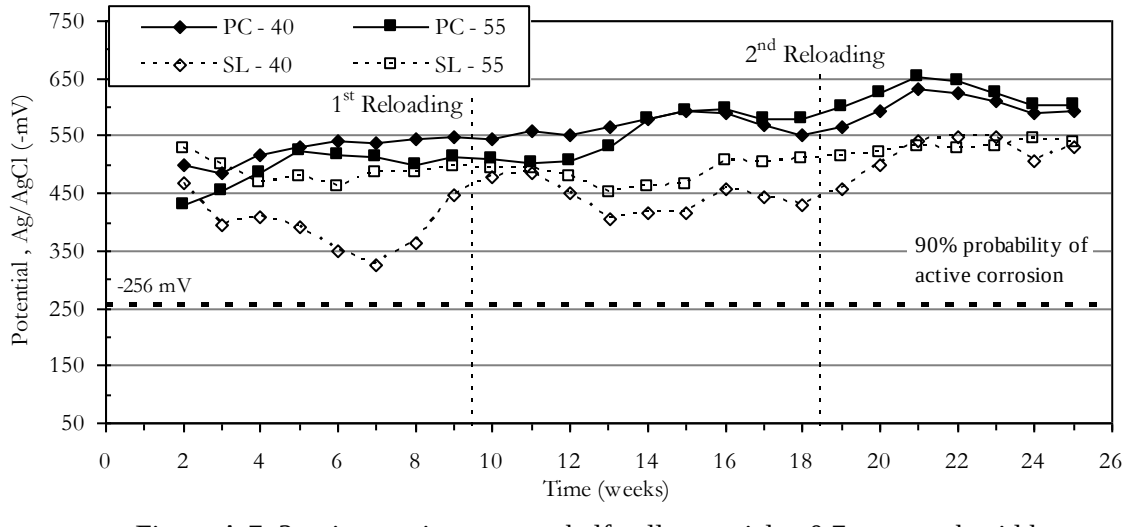

PC-40

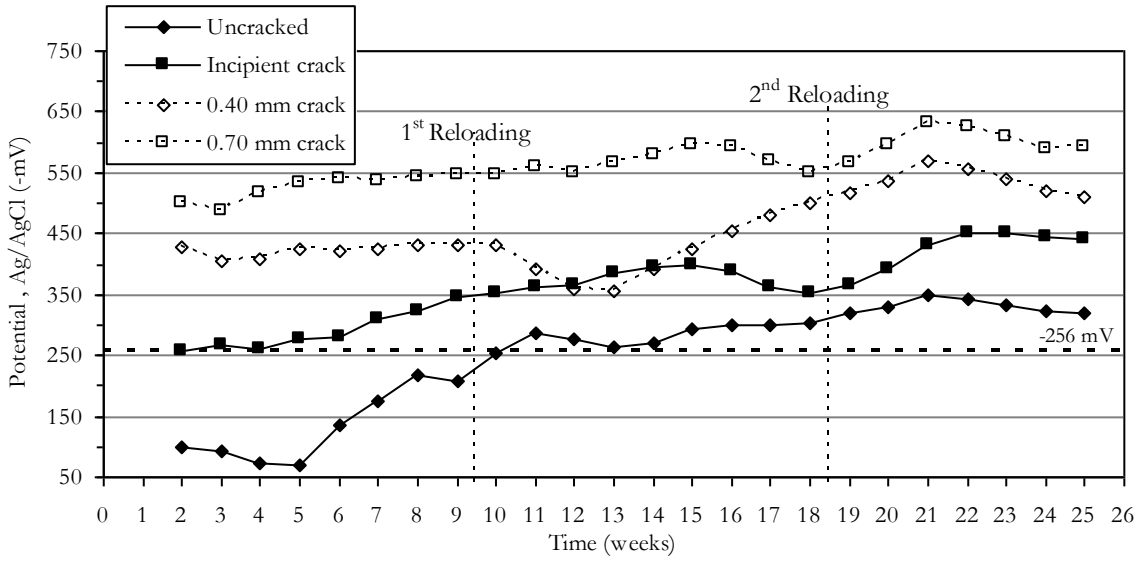

Figure A.8: 3-point moving average half-cell potentials - PC-40 mix

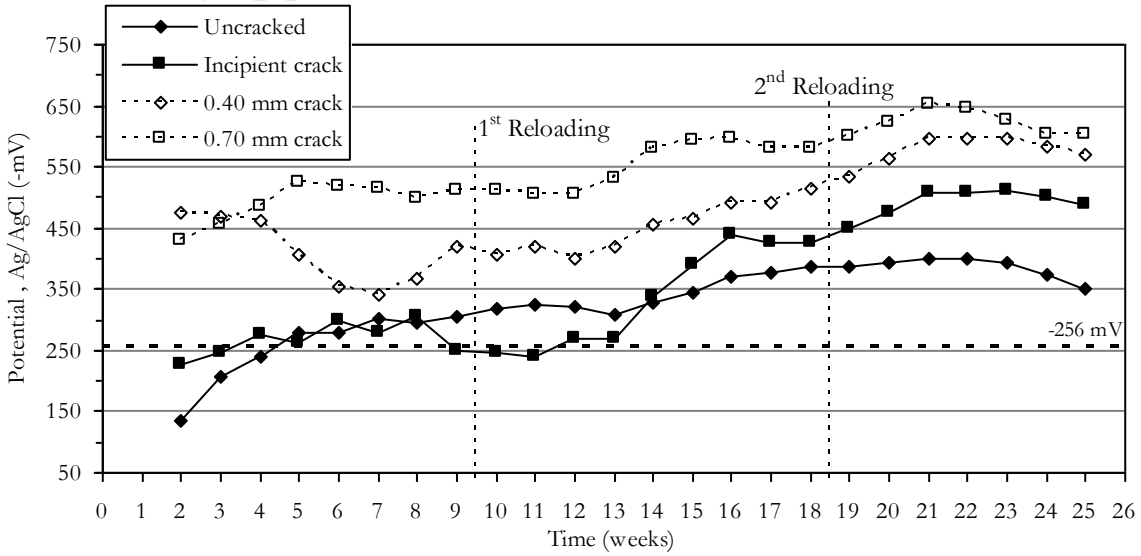

Figure A.9: 3-point moving average half-cell potentials - PC-55 mix

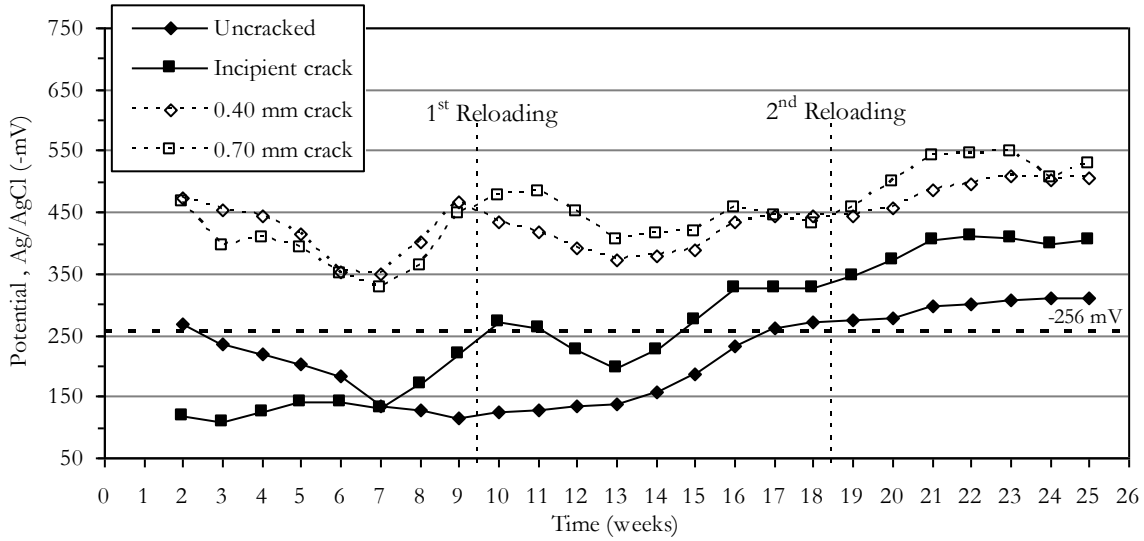

Figure A.10: 3-point moving average half-cell potentials - SL-40 mix

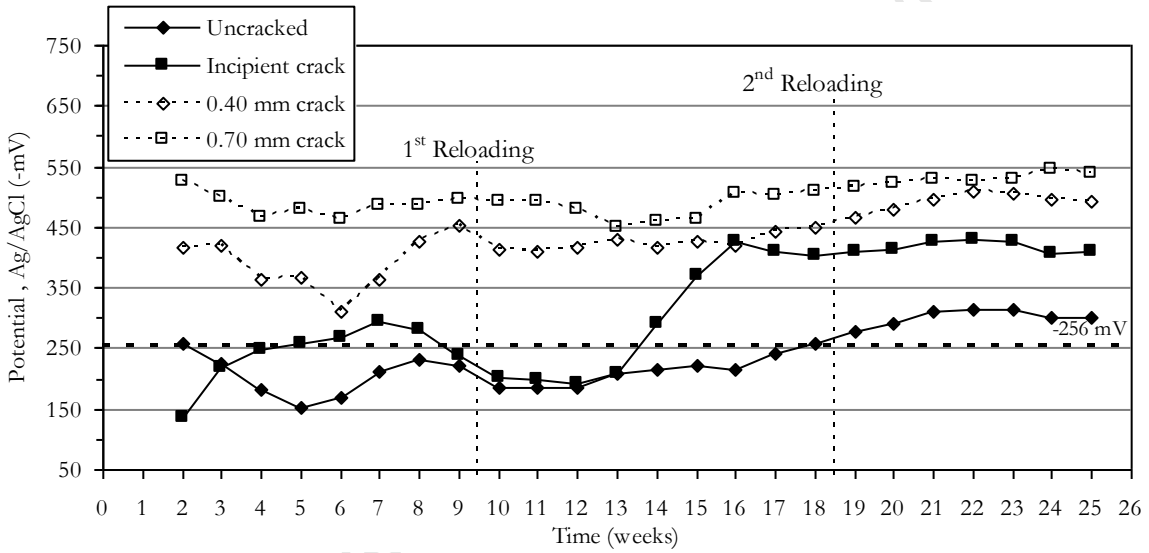

Figure A.11: 3-point moving average half-cell potentials - SL-55 mix

Appendix B

DURABILITY INDEX TESTS

The South African durability index tests comprise of oxygen permeability, chloride conductivity and water sorptivity. These are briefly covered in the following sections.

B1 *Oxygen permeability index (OPI) test*

This test involves the determination of the OPI of a concrete specimen from the rate of pressure decay through the sample when placed in a falling head permeameter (Figure B.1). The rate of pressure decay of a falling head permeameter is governed by the Darcy equation, allowing the coefficient of permeability (k) to be determined (Ballim, 1993).

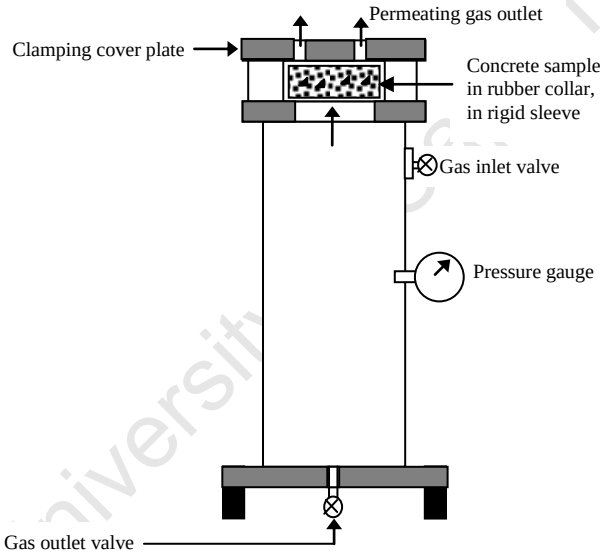

Figure B.1: Oxygen Permeability Index test cell set-up

The falling head permeameter (Figure B.1), developed at the University of Witwatersrand, applies an initial pressure to one side of a concrete specimen with the other side at normal atmospheric pressure. As permeation occurs, the decrease in pressure with time is measured. From the slope of the log of pressure head versus time, the oxygen permeability coefficient may be determined as follows (Alexander *et al*., 1999):

$$k = \frac{\omega V g d}{R A \theta t} \ln \frac{P_o}{p} \qquad \text{(B.1)}$$

where: k = coefficient of permeability (m/s)

ω = molecular mass of permeating gas (kg/mol)

V = volume of the pressure cylinder (m^3)

g = acceleration due to gravity (m/s^2)

d = sample thickness (m)

R = universal gas constant (Nm/Kmol)

A = cross sectional area of specimen (m^2)

θ = absolute temperature (K)

P_o, P = pressure at start of test and at time t (sec) respectively (kPa)

To obtain a less cumbersome number, the negative log of k is used, and termed the 'oxygen permeability index'.

$$OPI = -\log_{10} k \tag{B.2}$$

Oxygen permeability indices, expressed on a log scale, range from 8 to 11, i.e. three orders of magnitude. The higher the index, the less permeable is the concrete. The test therefore gives an indication of the gas permeation properties of the concrete and a rapid estimation of the resistance of a particular concrete to the transport of gas, especially with respect to carbon dioxide diffusion into the concrete (Alexander *et al.*, 1999). The OPI is more dependent on the amount and continuity of larger pores where most of the flow will occur and which are likely to have been caused by poor compaction and/or bleeding (Mackechnie, 1996).

The OPI values obtained for the various concretes can provide a basis of comparison and a means of estimating the degree of influence on the microstructure of the binders under consideration. The movement of oxygen through concrete is also one of the fundamental parameters governing the rate of corrosion and is therefore indispensable in any attempt to meaningfully study the corrosion of steel in concrete.

B2 *Water sorptivity index (WSI) test*

An important parameter of the pore structure of concrete, including its dimensional effects, is the degree to which it absorbs water. Sorptivity is the rate of movement of a water front through a porous material under capillary action. The dominant mechanism controlling rate of water ingress into unsaturated or partially saturated concrete is absorption, where fluid is drawn by capillary suction. Capillary suction depends significantly on the orientation and connectivity of the pores. It is significant near the surface of the concrete but tends to decrease with depth. The test is therefore a useful measure of the near surface characteristics of the

material (Alexander *et al*. 1999). The lower the water sorptivity index, the better is the potential durability of the concrete.

After pre-conditioning the concrete disc samples (68 ± 2 mm diameter and 25 ± 2 mm thickness), in an oven at 50 ^{o}C for 7 days (to ensure uniform moisture content), the sides of the specimens are sealed using epoxy (to ensure unidirectional movement) and placed in a few millimetres depth of water and weighed at regular intervals to determine the mass of water absorbed (Figure B.2). Prior to saturation the test is stopped and the samples are vacuum saturated to determine the porosity (Alexander *et al.* 1999). The sorptivity, S, of the concrete is obtained from the slope of the straight line of mass of water absorbed versus the square root of time:

$$S = \frac{\Delta M_t}{t^{1/2}}\left(\frac{d}{M_{sat} - M_o}\right) \qquad \text{(B.3)}$$

where: ΔM_t = change in mass with respect to the oven dried mass (g)

M_o = mass of oven-dried concrete (g)

M_{sat} = mass of saturated surface dry concrete (g)

t = period of absorption (hr)

d = average thickness of sample (mm)

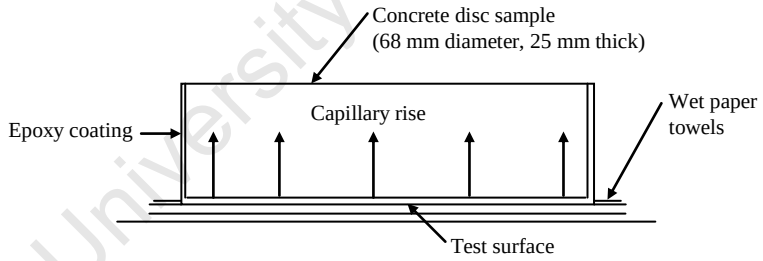

Figure B.2: Schematic of water sorptivity test
(Alexander *et al*., 2006)

B3 ***Chloride conductivity index (CCI) test***

The diffusion of gas, liquids or ions through concrete under a concentration gradient is one of the most useful pieces of information pertaining to the structure of the material under investigation. In particular, chlorides represent a big threat to the long term durability of concrete under numerous environmental conditions and their movement is often by means of diffusion as the steel is normally at depths greater than would be substantially affected by capillary suction. Diffusion rates in concrete are dependant upon temperature, moisture content, type of diffusant, and inherent diffusivity of the material with further complications

arising from chemical interactions (e.g. chloride binding), presence of cracks and possible presence of stray currents (Alexander *et al.*, 1999). The purpose of measuring conductivity is that (Streicher and Alexander, 1995):

(i) It is a relevant durability parameter and;

(ii) It can be used as an index which characterises the intrinsic potential of the concrete to resist chloride penetration.

The test (developed by Streicher, 1997) involves measuring the ionic flux (current) across a sample due to a 10 V potential difference as shown in Figure B.3. Pre-conditioning of the concrete disc samples (68 ± 2 mm diameter and 25 ± 2 mm thickness) involves oven drying at 50 ^{o}C for 7 days followed by vacuum saturation in a 5M NaCl solution for 24 hours.

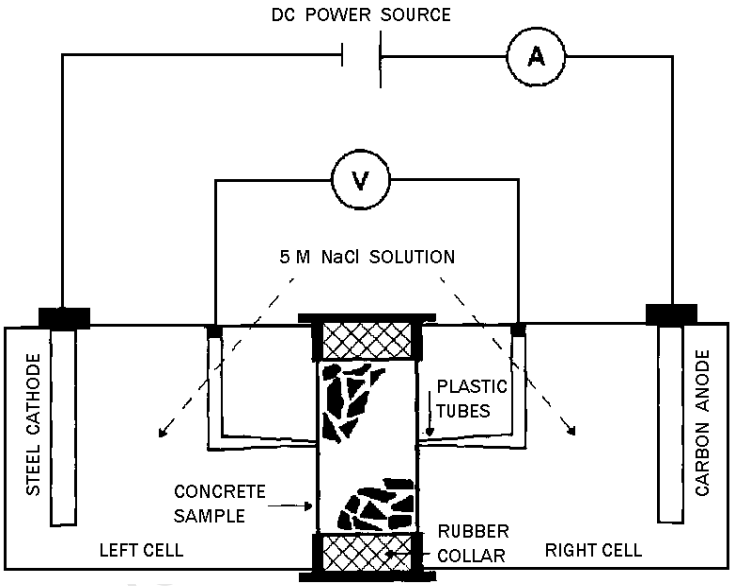

Figure B.3: Schematic of chloride conductivity test
(Alexander *et al*., 1992)

The test allows for a very rapid determination of the chloride conductivity value which can be defined as (Alexander *et al*., 1999):

$$\sigma = \frac{it}{VA} \tag{B.5}$$

where: σ = conductivity of the specimen (mS/cm)

i = electric current (mA)

V = voltage difference (V)

t = average thickness of specimen (cm)

A = cross-sectional area of the specimen (cm^2)

B4 ***References***

Alexander M. G., Ballim Y., Mackechnie J. R. (1999), Concrete durability index testing manual, *Research Monograph No. 4*, University of Cape Town, Department of Civil Engineering.

Alexander, M. G., Stanish, K. and Ballim, Y., (2006), Performance-based durability design and specification: Overview of the South African Approach, proceedings of the International RILEM workshop on *Performance based evaluation and indicators for concrete durability*, 19-21 March, Madrid, Spain.

Ballim Y. (1993), Towards an early age index for the durability of concrete, *proceedings of international conference, Concrete 2000 - Economic and durable construction through excellence*, London, pp. 1003-1012.

Mackechnie J. R., (1996), Predictions of reinforced concrete durability in the marine environment, *PhD Thesis*, University of Cape Town.

Streicher P. E., (1997), The development of a rapid chloride test for concrete and its use in engineering practice, *PhD Thesis*, Department of Civil Engineering, University of Cape Town.

Appendix C

DEALING WITH OUTLIERS IN EXPERIMENTAL MEASUREMENTS

C1 *Introduction*

An outlier is defined as an observation or data point which does not appear to fall within the expected distribution for a particular data set (Barnett *et al*., 1994). They can seriously affect the results of analyses. Outliers may be rejected outright if they are caused by a known or demonstrated physical reason, such as sample spillage, contamination, mechanical failure, or improper calibration. However, data points which appear to deviate from the expected sample distribution for no known physical reason must be verified as outliers using statistical criteria (Quinn and Keough, 2006).

The rejection of suspect observations must be based exclusively on an objective criterion and not on subjective or intuitive grounds. This can be achieved by using statistically sound tests for the detection of outliers. On such test, which was adopted in this study, is the Grubb's test.

C2 *Grubb's outlier test*

This method is used to determine single-sided outliers when both the population mean (μ) and the population standard deviation (s) are unknown. It was developed by Grubbs (Grubbs, 1979) and is included in standard methods:

$$T_u = \frac{X_n - \bar{x}}{\sigma} \quad \text{(for high-sided outliers)} \qquad \text{(C.1)}$$

$$T_l = \frac{\bar{x} - X_l}{\sigma} \quad \text{(for low-sided outliers)} \qquad \text{(C.2)}$$

where: X_n, X_l = data point in question (suspected outlier)

$\bar{x}$ = sample mean

σ = sample standard deviation

The value T_u or T_l is then compared against critical values depending on the number of replicates and significance (or confidence) level. If T_u or T_l is greater than the critical value for the appropriate number of replicates at the appropriate significance level, the questionable data point is an outlier, and may be rejected. The critical values for various numbers of replicates at the 1% and 5% significance levels are given in Table C.1.

Table C.1: Critical values for Grubb's outlier test

(Barnett *et al*., 1994)

No. of observations	*Significance level*	
	1%	*5%*
3	1.15	1.15
4	1.49	1.46
5	1.75	1.67
6	1.94	1.82
7	2.10	1.94
8	2.22	2.03
9	2.32	2.11

C3 ***References***

Barnett, V., Lewis, T. and Rothamsted, V., (1994), *Outliers in Statistical Data*, Wiley series in Probability and mathematical statistics, applied probability and statistics, John Wiley & Sons.

Grubbs, F. E., (1979), Procedures for detecting outlying observations, *Army Statistics Manual* DARCOM-P706-103, U.S. Army Research and Development Center, Aberdeen Proving Ground, MD 21005.

Quinn, G. P. and Keough, M. J., (2006), *Experimental Design and Data Analysis for Biologists*, Published by The Press Syndicate of the University of Cambridge.

EBE Faculty
Assessment of Ethics in Research Projects

EBE Faculty
Assessment of Ethics in Research Projects

Name of Principal Researcher/Student: **MIKE BENJAMIN OTIENO**

Supervisor: **PROF. MARK G. ALEXANDER**

Department: **CIVIL ENGINEERING**

If a Student: Degree: **MSc.(Eng)**

Research Project Title: **CORROSION PROPAGATION IN CRACKED AND UNCRACKED CONCRETE**

Overview of ethics issues in your research project:

Question 1: Is there a possibility that your research could cause harm to a third party (i.e. a person not involved in your project)?	YES	NO ✓
Question 2: Is your research making use of human subjects as sources of data? If your answer is YES, please complete Addendum 2.	YES	NO ✓
Question 3: Does your research involve the participation of or provision of services to communities? If your answer is YES, please complete Addendum 3.	YES	NO ✓
Question 4: If your research is sponsored, is there any potential for conflicts of interest? If your answer is YES, please complete Addendum 4.	YES	NO ✓

If you have answered YES to any of the above questions, please append a copy of your research proposal, as well as any interview schedules or questionnaires (Addendum 1) and please complete further addenda as appropriate.

I hereby undertake to carry out my research in such a way that

- there is no apparent legal objection to the nature or the method of research; and
- the research will not compromise staff or students or the other responsibilities of the University;
- the stated objective will be achieved, and the findings will have a high degree of validity;
- limitations and alternative interpretations will be considered;
- the findings could be subject to peer review and publicly available; and
- I will comply with the conventions of copyright and avoid any practice that would constitute plagiarism.

Signed by:

	Full name and signature	Date
Principal Researcher/Student:	**MR. MIKE BENJAMIN OTIENO**	**4th AUGUST, 2008**

This application is approved by:

Supervisor (if applicable):	**PROF. MARK G. ALEXANDER**	05/08/08
HOD (or delegated nominee): Final authority for all assessments with NO to all questions and for all undergraduate research.	**PROF. ALPHOSE ZINGONI**	06/08/08
Chair : Faculty EIR Committee For applicants other than undergraduate students who have answered YES to any of the above questions.	**NOT APPLICABLE**	